1-1-2015

Discovery of Alternative Artemisinin Binding Sites in Plasmodium falciparum ATPase-6

Shuneize Elizabeth Slater
University of Mississippi

THE DISCOVERY OF NOVEL INHIBITORS OF PLASMODIUM FALCIPARUM ATPASE-6 OBTAINED FROM A MECHANISTIC STUDY OF ARTEMISININ

A Dissertation
presented in partial fulfillment of requirements
for the degree of Doctor of Philosophy
in the Department of BioMolecular Sciences
Division of Medicinal Chemistry
The University of Mississippi

by

SHUNEIZE E. SLATER

December 2015

ABSTRACT

Malaria is a fatal yet preventable and treatable disease. It is commonly spread through the bite of an infected *Anopheles* mosquito. Malaria parasites belong to the *Plasmodium* genus and can be caused by the *falciparum, malariae, ovale, vivax,* and *knowlesi* species. Artemisinin is an endoperoxide lactone extracted from qinghaosu (*Artemisia annua* L. or sweet wormwood). It and its derivatives possess uncharacteristically rapid action against *Plasmodium falciparum*. Artemisinin is unique in its effectiveness in deadly cerebral malaria. The endoperoxide bridge is crucial for its antimalarial activity; however, how it aids in killing the parasite is unknown.

While there are multiple suggested modes of action (MOA) for artemisinin, none to date have a well-characterized protein target except for PfATP6, proposed by Krishna, *et al*. His work suggested that artemisinin binds to the homologous thapsigargin binding site of PfATP6. Herein, knowledge of the previously proposed mechanisms was utilized along with numerous computational techniques to determine a more detailed and plausible MOA for artemisinin against PfATP6. This led to the discovery of two new, putative PfATP6 binding sites for artemisinin.

None of the previous work has explained the co-dependence of antimalarial efficacy on the concentration of Fe(II). In our work, we searched for putative sites containing a cysteine residue, Fe(II) and artemisinin in a conformation allowing for the well-accepted ring-opened C4 primary artemisinin carbon radical to form a covalent bond with a cysteine thiol rather than undergoing an intramolecular self-emolative diradical ring closure. Clearly there are geometric

constraints for a transition state that side-steps the latter reaction and instead allows for interception by a cysteine thiol. We have suggested mechanistic possibilities for this capture by the artemisinin C4 radical and propose that PfATP6 is deactivated by blocking the Ca(II) channel by the modification of a cysteine at either C1031 or C92. It is alternatively possible that these modifications lead to alterations in the function of the protein, rendering it dysfunctional.

Structure-based virtual screening was then used to screen a commercial database of compounds to find novel inhibitors of PfATP6. Biological testing will be done to determine if targeting these new sites can produce potent antimalarials with less structural complexity than artemisinin itself.

DEDICATION

This dissertation is dedicated to everyone who encouraged me and helped me to stay the course throughout my years here at the University of Mississippi. A special dedication goes to my loving and supportive husband, Bernard Slater, Junior, who helped me to see the light at the end of the tunnel when it seemed so unreachable and for believing in me when I did not believe in myself.

ACKNOWLEDGMENTS

First and foremost, I would like to thank my advisors, Dr. Mitchell A. Avery and Dr. Robert J. Doerksen, for their support and guidance throughout every aspect of my research. It is because of the both of them that my skills, both in research and in critical thinking, have evolved from the preliminary level to a higher understanding of medicinal chemistry. I am forever grateful to them.

I would also like to thank the chairman of the Department of BioMolecular Sciences, Dr. Stephen J. Cutler, for the Department's many years of financial support which allowed me to focus on my research.

Many thanks also go to my committee members, Dr. John M. Rimoldi and Dr. Murrell Godfrey. They agreed to be a part of my committee and have offered me guidance when I asked for it. Again, many thanks.

A special thanks is also due to Dr. John S. Williamson, the past graduate coordinator for the department. His constant encouragement and friendship made my beginning years here at the University of Mississippi very enjoyable.

I would like to thank the two best postdoctoral associates that I have ever had the privilege of working with, Dr. Khaled Elokely and Dr. Kuldeep Roy. Neither of them ever hesitated to drop what they were doing to help me in any capacity. In person, through emails, or

over the phone, they were always there to help me. All of my computational modeling skills were taught to me by these two men, and I am forever grateful to them both.

Dr. Sanjeev Krishna and his associates at St. George's University of London also played a vital role in my dissertation work and continue to do so. I thank all of them for their collaborative efforts.

A special thanks goes to Jakub Kollar, our Fulbright fellow from Slovakia and his advisor, Dr. Vladimir Frecer. Many of the calculations in this work were performed by Jakub. Even after his return to Slovakia, if our servers here were not working, I could always send a file and instructions to him, and he would submit the job for me. I would not have made it this far without his help.

Thanks to Dr. Chih-Hao Lu at China Medical Center for helping me with the fragment transformation method that he developed. It was very essential to our work.

I cannot forget to thank my labmates/good friends, Manal Nael and Pankaj Pandey. The relationship that we share is so remarkable. We work together so well. There was no competition between us; we worked hard to help each other and build each other up. I will truly miss the comradery that we share, and I am thankful that I had the opportunity to experience it.

I would like to acknowledge partial financial support from the National Science Foundation, EPS-0903787 and EPS-1006883, as well as NSF MRI Award #1338056, and a Dissertation Fellowship from the UM Graduate School for the Spring 2015 semester.

I would also like to thank my many friends that I have made here at the University of Mississippi, both past and present. Each of them played a vital role in my life and will never be forgotten. Thanks goes to my best friend, Dr. Andrekeus (Missy) Lee, for sharing with me her own ‘special’ brand of encouragement. Finally, I need to thank my parents, my sister, my brother, my son, the rest of my family members, and last but definitely not least, my husband. Thank you all.

TABLE OF CONTENTS

LIST OF TABLES

LIST OF FIGURES

CHAPTER 1
INTRODUCTION

1.1 MALARIA

Malaria is one of the world's most fatal diseases, although it is preventable and treatable.[1] It is the world's third most deadly infectious disease, falling behind tuberculosis and pneumococcal respiratory infections. It is a mosquito-borne infectious disease that affects humans and other animals. The disease is commonly spread through the bite of an infected *Anopheles* mosquito.[2] As of 2013, 97 countries had ongoing malaria transmission. According to the World Health Organization (WHO), 3.4 billion people are at risk of malaria with 1.2 billion people being at high risk. In 2012 there was an estimated 207 million cases and an estimated 627,000 deaths from malaria with approximately 90 percent of the deaths occurring in sub-Saharan Africa. In the same year, malaria killed around 482,000 children under five years of age. This adds up to 1,300 children per day or one child almost every minute.[3]

Malaria parasites belong to the *Plasmodium* genus. Human malaria is caused by the *Plasmodium falciparum, Plasmodium malariae, Plasmodium ovale, Plasmodium vivax,* and *Plasmodium knowlesi* species.[5] Infection by all species of *Plasmodium* begins with the bite of an infected female *Anopheles* mosquito. After a silent infectious phase in the liver hepatocytes, exoerythrocytic merozoites pass into the bloodstream as merosomes that eventually rupture. This allows the parasite access to circulating erythrocytes. Merozoites rapidly invade erythrocytes, giving rise to poorly formed and rigid red blood cells as they grow and reproduce.[6] Infection leads to symptoms such as headache, fever, shivering, chills, vomiting, joint pain, and convulsions within 8 to 25 days.[7,8] *Plasmodium falciparum,* also called malignant malaria, is the most dangerous form of malaria with the highest rates of morbidity and mortality.[9]

Throughout history, there have been many therapeutics to manage and, in some cases, cure *Plasmodium falciparum* malaria. Quinine, shown in **Figure 1.1**, was the first Western treatment that was effective against *Plasmodium falciparum* malaria. Starting from the 17th century, it was the antimalarial of choice until the 1940s. Occurring naturally in the bark of the Cinchona tree, quinine is the only drug that has remained effective in the treatment of malaria. As of 2006, the World Health Organization (WHO) suspended quinine as the first-line treatment for malaria. It is now only used in the treatment of severe malaria or when artemisinins are not available. [10,11,12,13] The mechanism of action of quinine has not been fully resolved. It has been hypothesized that it, along with other quinolone antimalarials, act in inhibiting hemozoin bicrystallization in the heme detoxification pathway. This facilitates the aggregation of cytotoxic heme, causing heme to accumulate in the parasite which leads to its death.[14]

Chloroquine, shown in **Figure 1.1**, is a very effective drug for both the treatment and prevention of malaria. It was first used in the 1940s after World War II and was very good in curing all forms of malaria.[15] Unfortunately, most strains of *falciparum* malaria are resistant to chloroquine which may have come from the drug having been extensively used in mass drug administrations. Similarly to quinine, chloroquine acts by inhibiting hemozoin bicrystallization in the heme detoxification pathway. Other than acting as an antimalarial, chloroquine many other uses. It is used in the treatment of amoebic liver abscess, as an immune system suppressant, and is being investigated as a retroviral in human HIV-1/AIDS.[16,17,18]

Mepacrine, shown in **Figure 1.1** and also known as both quinacrine and Atabrine, was developed in the early 1930s and was used on a large scale during World War II. During this time, it was considered to be a very safe drug, but it is now considered to have too many

undesirable side effects and is no longer used.[15] Its mechanism of action is uncertain, but it is thought to act against the cell membrane.[19] Mepacrine has many medical applications. Not only is it an antimalarial, but it is also used to treat giardiasis, systemic lupus erythematosus, used as an intrapleural sclerosing agent, and is also used to treat tapeworm infections.[20] It has also been studied for use as a non-surgical sterilizing agent for women.[21]

Mefloquine, shown in **Figure 1.1**, was first introduced in the 1970s, shortly after the end of the Vietnam War, and is structurally related to quinine. Not only is it used to treat malaria, but it also is used as a prophylactic antimalarial because of its long half-life.[15] It is used to treat chloroquine-resistant *Plasmodium falciparum* malaria and is a reasonable alternative for uncomplicated chloroquine-resistant *Plasmodium vivax* malaria. However, mefloquine is not useful against severe malaria.[22,23] It is thought to act against malaria in the same way as quinine and chloroquine. Mefloquine is associated with numerous neuropsychiatric side effects such as anxiety, hallucinations, depression, dizziness, tinnitus, and suicidal thoughts.[24] It also is known to cause abnormalities in heart rhythms.[23,25]

Halofantrine, shown in **Figure 1.1**, was introduced in the 1980s, and it is not structurally related to quinine. It has a very short half-life, so it is not used as a prophylactic.[15] To date, its mechanism of action is unknown; however, a crystallographic study showed that this compound binds to hematin in vitro.[26] Unlike other antimalarials, halofantrine is only used to treat malaria and has no other uses. Similarly to mefloquine, halofantrine has many undesirable side effects. Several neuropsychiatric disturbances have been reported along with abdominal pain, diarrhea, vomiting, rash, headache, itching, and cardiac arrhythmias.[15,27]

Malarone is a drug combination of atovaquone and proguanil, which are shown in **Figure 1.1**. The combination has been commercially available in the US since 2000. Malarone is used for both the treatment of malaria and the prevention of malaria; however, proguanil is an antifolate so caution should be exercised regarding its use as a prophylactic. The drug combination has undergone many clinical trials, and it was found that this combination is more than 95% effective against drug resistant *falciparum* malaria. Although some adverse effects have occurred, malarone is largely free from undesirable side effects. To date, this drug is very expensive.[15]

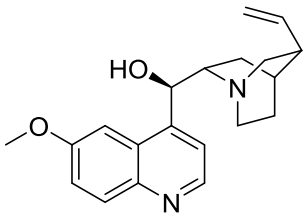

Quinine

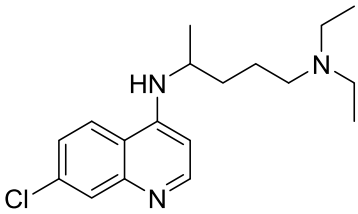

Chloroquine

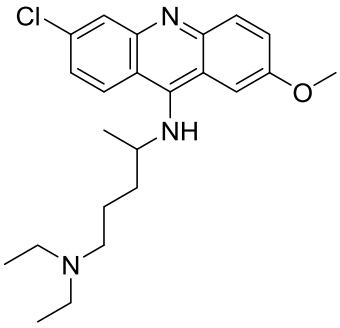

Mepacrine

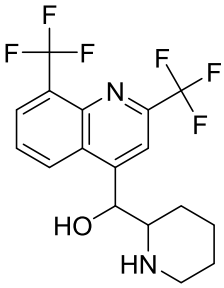

Mefloquine

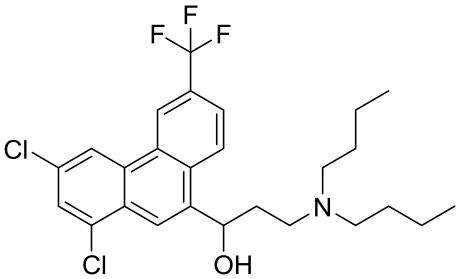

Halofantrine

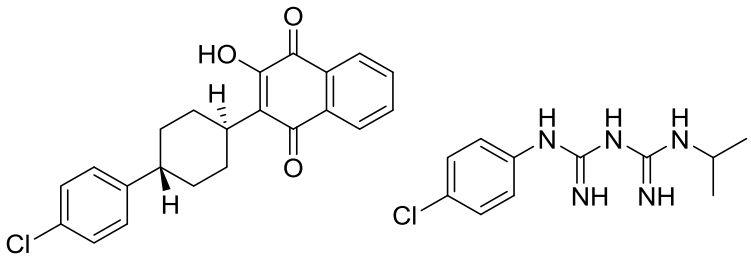

Malarone (atovaquone/proguanil)

Figure 1.1: Structures of antimalarials.

1.2. ARTEMISININ

Artemisinin is an endoperoxide antimalarial lactone that was derived from qinghao (Artemisia annua or sweet wormwood). This plant has been used medicinally for over 2,000 years, and in the late 1500s, Li Shizhen recommended qinghao tea to treat malaria symptoms.[28] The earliest record of artemisinin being used medicinally dates back to around 200 B.C. in an unearthed manuscript entitled "Fifty-two Prescriptions". Its antimalarial application was first described in "The Handbook of Prescriptions for Emergencies" in the fourth century.[29] In 1967, the Chinese army set up a plant screening research program, Project 523, to find a treatment for malaria to aid the malaria-stricken North Vietnamese army. Through the course of the research, artemisinin was discovered in the leaves of the *Artemisia annua* plant.[30, 31]

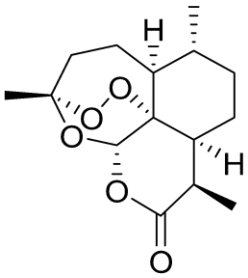

Figure 1.2: The chemical structure of artemisinin (**1**).

Artemisinin and its derivatives (artemether, artesunate, artemotil, dihydroartemisinin, etc.) possess the most rapid action of all drugs against *Plasmodium falciparum* malaria.[32] Use of the drug alone is highly discouraged by the World Health Organization (WHO) as this results in a high rate of parasite return. This could lead to a catastrophic resistance to artemisinin.[33] Instead, WHO recommends artemisinin combination therapies (ACTs) as the first line therapy against *Plasmodium falciparum* malaria. The artemisinin component kills the majority of the parasites quickly while the more slowly-eliminated portion clears the rest of the parasites.[34] Artemisinin has been found to be active against uncomplicated malaria, severe malaria, certain cancers, and helminth parasites.[35, 36, 37] It is also seeing an increase in use against *Plasmodium vivax* malaria.[38]

1.3. SERCA/PfATP6

Calcium pumps are calcium ATPases that transport calcium ions across a wide variety of cellular membranes by using the energy that is obtained from the hydrolysis of ATP. These pumps are members of the P-type family of ion pumps. The name, P-type, comes from the mechanism which involves the phosphorylation of a residue in the active site using the terminal phosphate in ATP. This results in conformational changes in both the ATP-binding domains and the calcium-binding transmembrane domain which is responsible for shuttling ions across the membrane.[39] Calcium P-type ATPases are categorized into one of two different classes: plasma membrane Ca^{2+} ATPases (PMCA) or sarcoplasmic/endoplasmic reticulum Ca^{2+} ATPases (SERCA).[40]

Calcium is used to signal many cellular functions such as muscle contraction and synaptic transmission. The release of a large amount of free calcium can cause a fertilized egg to

drop, skeletal muscles to contract, and many other events. Also an elevated calcium level is taken to signify cell death and triggers the mechanisms of apoptosis. Cells use calcium pumps, or SERCA pumps, to accumulate calcium in the lumen of the endoplasmic reticulum and simultaneously regulate cytosolic calcium levels.[41] For a cell to use calcium as a signaling molecule, the cell must first create calcium gradients across its membrane. When a stimulus signal opens the calcium channels, calcium ions rush into the cytosol signaling muscle contraction.[42] To construct differences in ion concentrations, calcium ions must be actively pumped across the membrane. These pumps are needed to force the calcium back out of the cytoplasm returning the cell to its pre-signal state and allowing muscle relaxation. If the calcium is not forced out of the cytoplasm, the level remains high, and apoptosis commences.[39]

The structure of SERCA consists of three main parts, which are the cytoplasmic headpiece, the stalk region, and the transmembrane domain. The cytoplasmic headpiece is composed of the nucleotide domain (N domain), the phosphorylation domain (P domain), the hinge region, and the actuator domain (A domain).[43] The headpiece is connected to the transmembrane domain which is comprised of ten alpha helices. While the ATPase is unphosphorylated, two of the helices form a cavity that is accessible from the cytosol and binds two calcium ions. ATP binds to a site in the N domain and phosphorylates an aspartate residue in the adjacent P domain. This causes a conformational change which brings the N and P domains closer together. This, in turn, results in a 90° rotation of the A domain, causing two of the transmembrane helices to rearrange. This rearrangement aids in the release of calcium into the lumen of the sarcoplasmic/endoplasmic reticulum.[39]

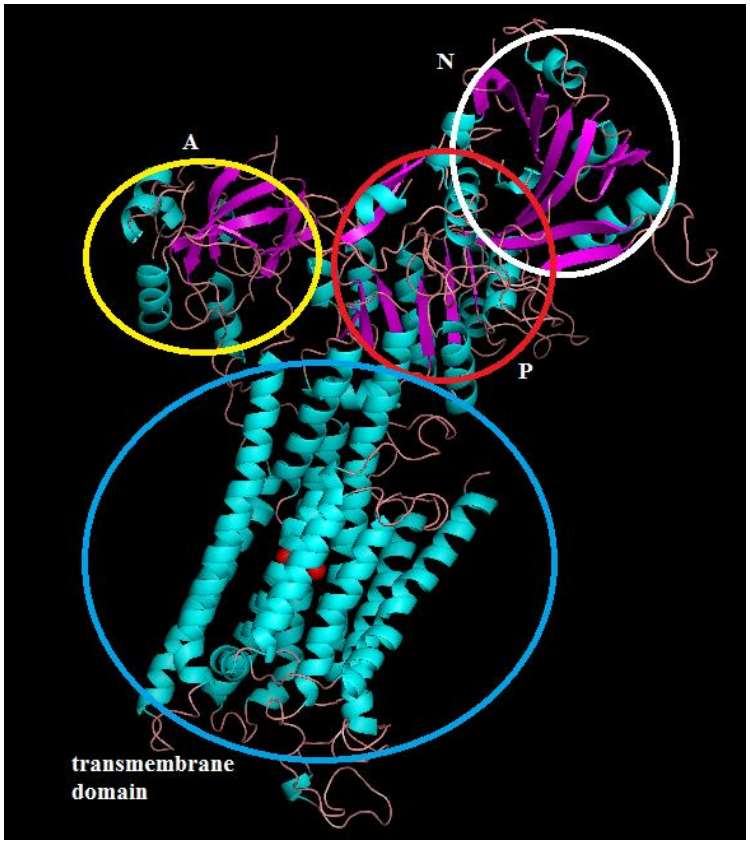

Figure 1.3: Representation of SERCA-like proteins showing the P domain, the N domain, the A domain and the transmembrane domain.

Years ago, a hypothesis was proposed that a SERCA from *Plasmodium falciparum*, PfATP6, may be an important target for artemisinin. This was based on biochemical assays performed on oocytes that heterologously express PfATP6 and on parasite cultures. This is also based on the fact that PfATP6 is the only SERCA-like protein in the parasite's genome and that artemisinins are structurally similar to thapsigargin, a selective, non-competitive inhibitor of mammalian SERCA.[44]

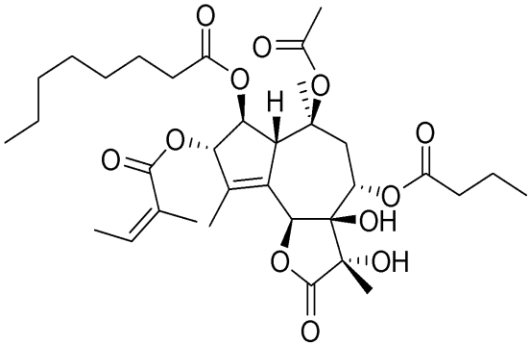

Figure 1.4: Structure of thapsigargin (**2**).

Thapsigargin, like artemisinin, is a sesquiterpene lactone extracted from a plant, *Thapsia garganica*. It works by raising the intracellular cytosolic calcium concentration by blocking the ability of SERCA to pump calcium out of the cytoplasm and back into the sarcoplasmic reticulum. This shut down of the pump results in a rapid calcium leak from calcium stores.[45] An antagonistic relationship was observed in the actions of artemisinin and thapsigargin from isobologram analysis and competition studies, indicating a common target. PfATP6 shares an overall 40% identity with human SERCA1 but an over 90% identity in the transmembrane domain. Also, mutation studies on PfATP6 suggested that certain mutations regulate its sensitivity to artemisinin. For example, in SERCA1, the thapsigargin binding site is near Phe-256, and SERCA1 is insensitive to artemisinin. When Leu-263 of PfATP6 was mutated to a glutamate residue, artemisinin sensitivity decreased, and conversely, when the homologous glutamate residue in SERCA1, Glu-255, was mutated to a leucine, SERCA1 became sensitive to artemisinin. These results suggest that PfATP6 is a target for artemisinin.[42, 46]

1.4 STUDIES OF PfATP6 AND ITS INHIBITORS

Although many research groups have been researching PfATP6, very few inhibitors of this protein have been reported. Batista, *et. al.* published the synthesis, cytotoxicity, and

antiplasmodial activity of *ent*-kaurane derivatives. When tested in a cell-based assay, these compounds exhibited IC_{50} values ranging from 5.4 to 10.4 µM and very good selectivity indices. Later, members of the same group took the three most active compounds, shown in Figure 1.6, and performed rigid and flexible docking studies and binding energy analyses. All three compounds showed good binding energies against PfATP6, shown in Table 1.1. These data suggest that PfATP6 is a potential target for diterpene epoxides derived from *ent*-kauranes, and further optimization of these lead compounds could provide a more potent and selective antimalarial.[47,48]

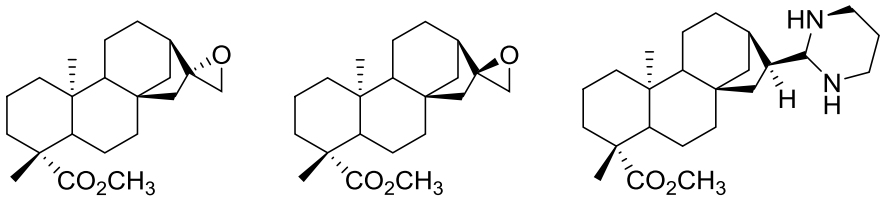

3 **4** **5**

Figure 1.5: Structures of the three most active diterpene *ent*-kaurane derivatives.

Table 1.1. Calculated binding energies (kcal/mol) of the three most active diterpene antiplasmodials.

Compound	Rigid Binding Energy	Flexible Binding Energy
3	-7.7	-6.6
4	-7.8	-6.3
5	-8.4	-6.8

Curcumin, a yellow spice found in the root of *Curcuma longa*, is a beta-diketone and has been used to cure diseases such as jaundice, indigestion, urinary tract diseases, rheumatoid arthritis, insect bites, and cancer. Curcumin was found to act synergistically with artemisinin against *Plasmodium berghei* and can also serve as a potent inhibitor against chloroquine-resistant *Plasmodium falciparum.* However, its mechanism is not fully elucidated yet. To examine the possibility of curcumin analogs as ligands for PfATP6, 351 curcumin derivatives from the ZINC database were docked into a homology model of PfATP6 using two different docking programs. Docking results showed that more than 50 curcumin analogs can bind to PfATP6 with similar, or better, affinity than curcumin itself. One compound, **ZINC05606394**, was predicted to bind better than curcumin by both docking programs.[49]

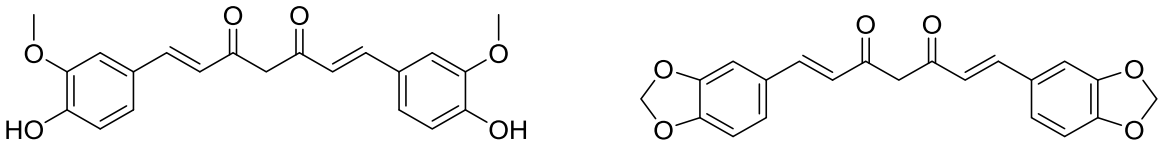

Figure 1.6: Structures of curcumin (**6**, left) and the curcumin analog, **ZINC05606394**.

Table 1.2: Glide docking scores and FlexX docking scores of curcumin and its analogs.[49]

Compound	Glide score	Compound	FlexX score
ZINC13781298	-7.890	**ZINC49111530**	-19.8003
ZINC49881409	-7.878	**ZINC05606394**	-19.2761
ZINC44281717	-7.796	**ZINC28955244**	-18.2869
ZINC05606394	-7.775	**ZINC35050563**	-15.8370
ZINC13781298	-7.755	**ZINC00899824**	-15.2578
ZINC49124982	-7.669	**ZINC28955244**	-13.9284
curcumin	-6.753	**curcumin**	-13.9685

Uhlemann, *et. al.* studied the possible mechanism of action of a fully synthetic peroxidic antimalarial, RBX11160 (OZ277). In this compound, the crucial peroxidic pharmacophore of the artemisinins is present within a 1,2,4-trioxane heterocycle. Since they have this feature in common, the group tested the idea that RBX11160 may also specifically inhibit PfATP6. Several experiments were performed including ATPase assays, *Plasmodium falciparum* hexose transporter (PfHT) glucose reuptake experiments, culturing of parasites and isobolograms, and immunofluorescence microscopy.[50]

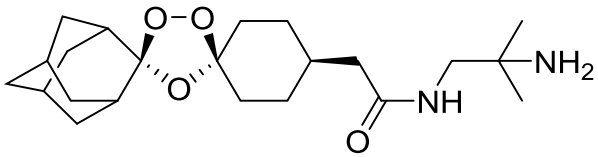

Figure 1.7: Structure of RBX11160. **(7)**

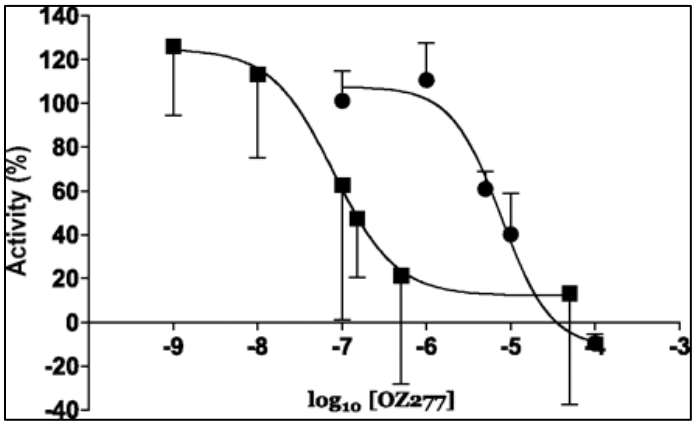

Figure 1.8: Apparent inhibitory constants for PfATP6 of RBX11160 and artemisinin. The apparent K_i values are 7,700 nM for RBX11160 (filled circles) (n = 3 for each value) and 79 nM for artemisinin (filled squares) (n = 5 for each value). (Figure duplicated with permission from Dr. Sanjeev Krishna of St. George's University of London.)[50]

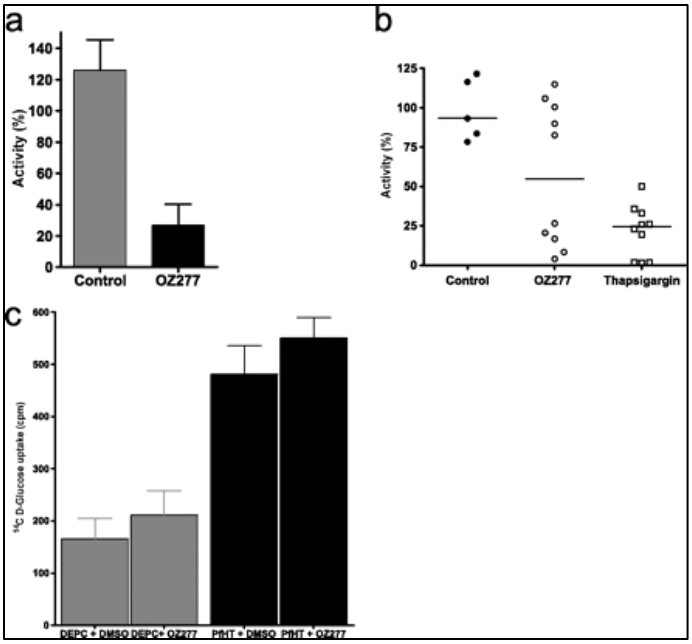

Figure 1.9: RBX11160 inhibition of transporter activities. (a) Inhibition of PfATP6 activity by RBX11160 (50 µM) compared with results for control preparations (n = 6 for both groups; P = 0.0018). (b) Inhibition of mammalian SERCA by RBX11160 (100 µM; P = 0.13) and thapsigargin (10 µM; P = 0.0007) compared with results for control experiments. (c) Uptake of D-glucose in water-injected (diethyl pyrocarbonate [DEPC]) and PfHT-expressing oocytes is shown. There is no inhibition of PfHT activity by RBX11160 (50 µM, n ≥ 9 per column; P > 0.5). DMSO, dimethyl sulfoxide. (Figure duplicated with permission from Dr. Sanjeev Krishna of St. George's University of London.)[50]

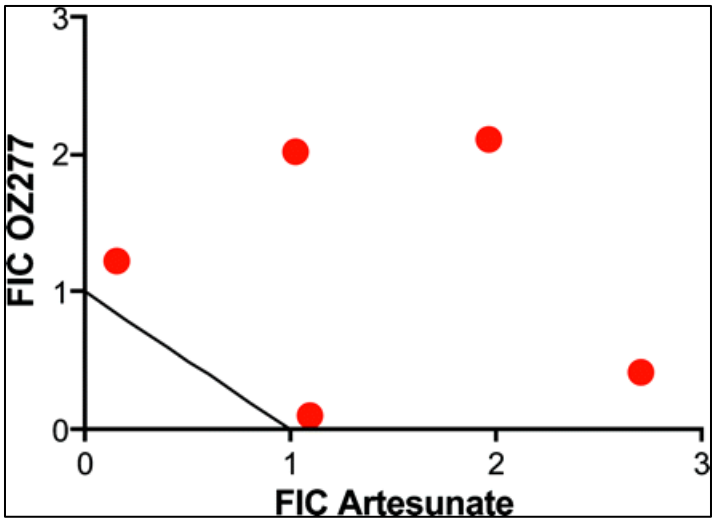

Figure 1.10: Isobologram of RBX11160 and artesunate. Points lying above the line of additivity indicate antagonistic effects. The summed fractional inhibitory concentration index (FIC) for this assay [geometric mean (range)] is 2.4 (1.85 to 4.2). (Figure duplicated with permission from Dr. Sanjeev Krishna of St. George's University of London.)[50]

RBX11160 inhibits PfATP6 with an IC_{50} of 7,700 nM, almost one hundred times less potently than artemisinin. However, all the data demonstrate that there are similarities and differences between RBX11160 and the semisynthetic antimalarials such as artemisinin and its derivatives.[50]

Bousejra-El Garah, *et. al.* divided antimalarial compounds into two groups based on their chemical structures and their reactivities towards iron. The two groups were peroxide-containing drugs and quinolone-based drugs. The peroxide-containing compounds used were artemisinin derivatives, 1,2,4-trioxane, 1,2,4-trioxolane, and 1,2,4,5-tetraoxane derivatives. The quinolone-based compounds used were chloroquine derivatives, quinine, and mefloquine. Trioxaquines, which are hybrid molecules with a dual mechanism of action, were also studied for comparison. The predicted binding affinities of these compounds with PfATP6 were evaluated using their binding free energies (E_{bind} kcal/mol) and inhibition constants (Ki, µM). The group concluded that the predicted binding affinities of these compounds for PfATP6 do not correlate with either their antimalarial activity or the reported inhibition of the protein.[51]

Artemisinin derivatives

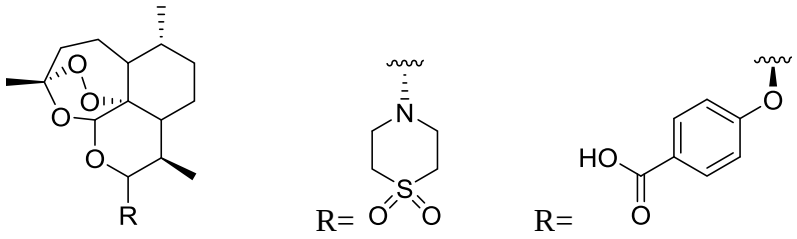

(8) Artemisinin R=O **(10)** Artemisone **(11)** MP118
(9) DHA R=OH

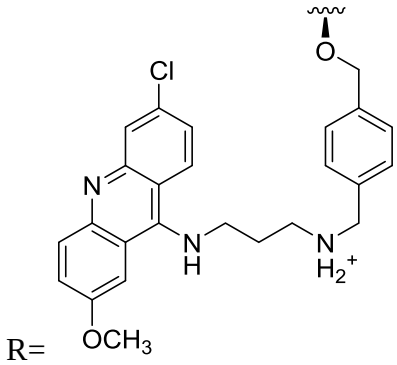

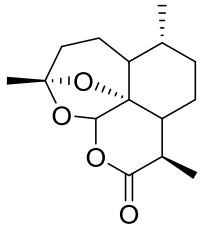

Artemisinin-acridine derivative **(12)** Deoxyartemisinin **(13)**

Figure 1.11: Artemisinin derivatives used in the study in reference #51.

Trioxolanes and Tetraoxane

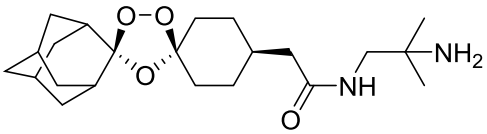

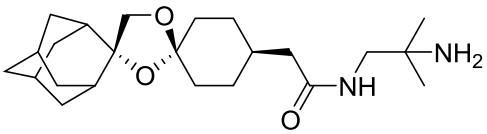

OZ277 **(14)** carba-OZ277 **(15)**

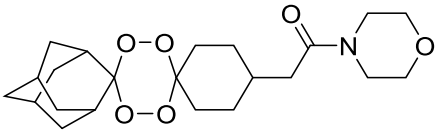

RKA216 **(16)**

Figure 1.12: Trioxolane derivatives used in the study in reference #51.

Trioxaquines

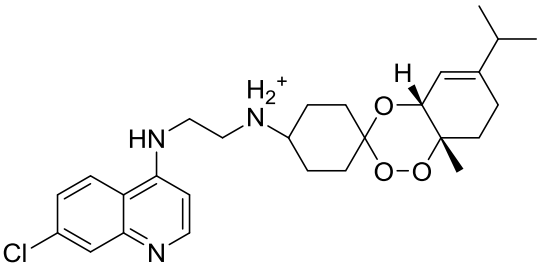

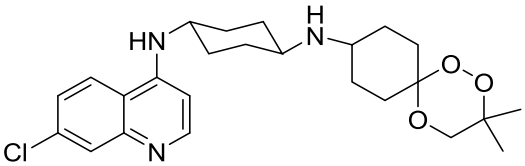

DU1301 **(17)** DU1302 **(18)**

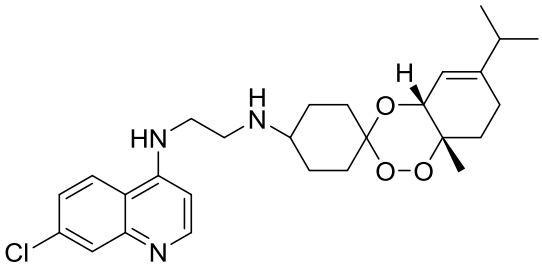

PA1103 **(19)**

Figure 1.13: Trioxaquines used in the study in reference #51.

Quinolines

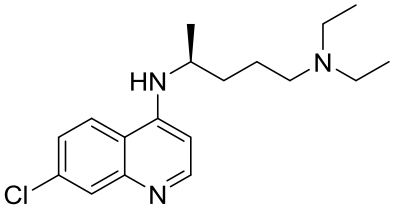

Chloroquine **(20)**

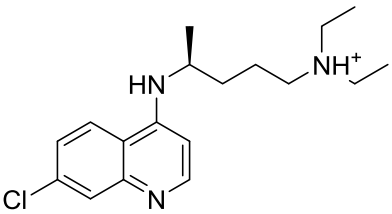

21

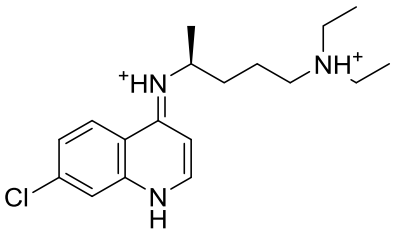

22

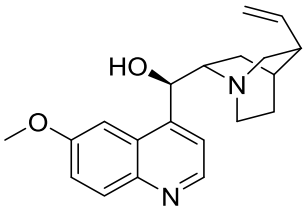

Quinine **(23)**

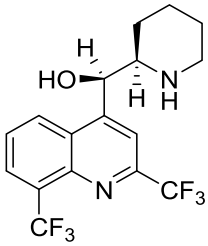

Mefloquine **(24)**

Figure 1.14: Quinoline-based compounds used in the study in reference #51.

David-Bosne, *et. al.* performed an investigation that focused on purifying PfATP6 on a large scale and maintaining its enzymatic activity. They then tested classical SERCA1a inhibitors such as cyclopiazonic acid (CPA) to determine their ability to inhibit parasite growth. They wanted to test whether there is a correlation between the enzymatic inhibition of PfATP6 and their antiplasmodial activity results. They then ran a test to measure inorganic phosphate

liberation to screen several compounds. The IC_{50} values for the inhibition of PfATP6 ATPase activity were determined for 1,680 compounds. Twenty of these compounds exhibited potent inhibitory effects with IC_{50} values less than 10 μM. Eight compounds were selected based on their ability to inhibit the growth of the FcB1 and 3D7 strains of *Plasmodium falciparum*. The group eventually concluded that there is no correlation between the inhibition of PfATP6 activity and the antiplasmodial activity of the compounds. They found that compounds can exhibit PfATP6 activity in vitro but possess limited antiplasmodial activity and vice versa.[52]

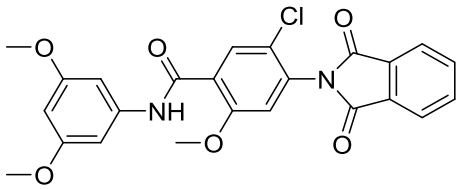

25

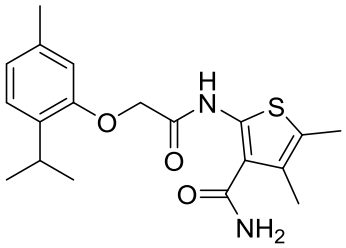

26

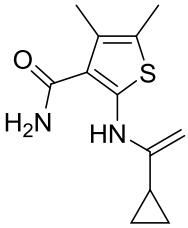

27

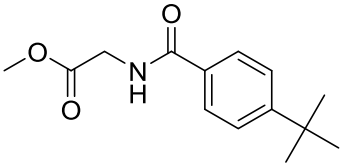

28

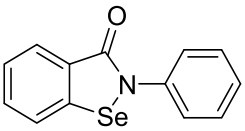

29

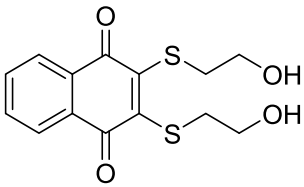

30

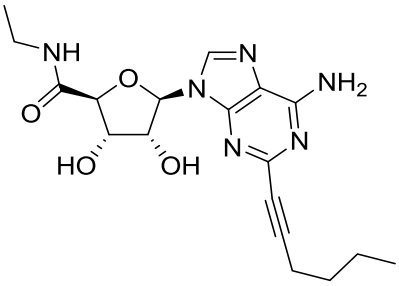

31

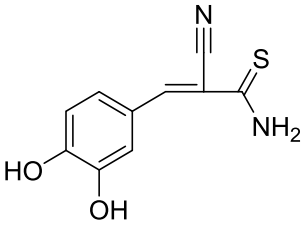

32

Figure 1.15: Structures of the compounds that were identified to be potent inhibitors of PfATP6.

Table 1.3: Effect of SERCA classical inhibitors upon *Plasmodium falciparum* growth *in vitro*. IC_{50} PfATP6: values of the inhibition of the ATPase activity determined on the purified PfATP6. Indication of the IC_{50} values for each drug on two *P. falciparum* laboratory strains differently resistant to chloroquine (3D7 and FcB1). Values (µM) correspond to at least three biological replicates. ND= not determined.[52]

Compound	**IC_{50} PfATP6**	**IC_{50} FcB1**	**IC_{50} 3D7**
Thapsigargin	150	6.1 ± 1.05	11.5 ± 5.7
BHQ	65	17.2 ± 11.3	30.6 ± 13.5
CPA	0.4	4.9 ± 0.9	8.8 ± 3.4
Chloroquine	ND	0.13 ± 0.02	0.012 ± 0.002

Table 1.4: IC_{50} of the compounds identified to be potent inhibitors of PfATP6 and chosen to be tested on *P. falciparum* cultures. IC_{50} PfATP6: values of the inhibition of the ATPase activity determined on the purified PfATP6; IC_{50} FcB1/IC_{50} 3D7: effect of the identified PfATP6 inhibitors on two *P. falciparum* strains differently resistant to chloroquine (3D7 and FcB1). Values (µM) correspond to at least three biological replicates.[52]

Compound	**IC_{50} PfATP6**	**IC_{50} FcB1**	**IC_{50} 3D7**
25	3.0 ± 2.2	71 ± 25	108 ± 8
26	1.1 ± 0.5	57 ± 15.8	53 ± 19
27	3.1 ± 1.0	88 ± 33	91.5± 16
28	1.2 ± 0.6	169 ± 17	241 ± 19
29	1.0 ± 0.6	6.2 ± 1.7	4.9 ± 2.1
30	1.0 ± 0.6	2.3 ± 1.2	3.1 ± 1.2
31	8.5 ± 1.6	14.3 ± 3.6	14.8 ± 7.7
32	7.0 ± 5.4	61 ± 26	62 ± 26

The topic of artemisinin is not an unfamiliar one to our research group. Previously in our group, Sun, *et. al.*, focused their attention on using the natural product sesquiterpene, thapsigargin, as a potential lead compound for drug discovery. Thapsigargin belongs to the

guaianolide class of sesquiterpenes, and as mentioned before, it is a highly potent and specific irreversible SERCA inhibitor. It also moderately inhibits PfATP6. While attempting to synthesize thapsigargin, a precursor, **33**, was designed and named thaperoxide. This compound showed striking similarities to both artemisinin and thapsigargin. Derivatives of thaperoxide were synthesized to derive a structure-activity relationship (SAR). The activities of these derivatives were evaluated and compared to the activities of both artemisinin and thapsigargin.[53]

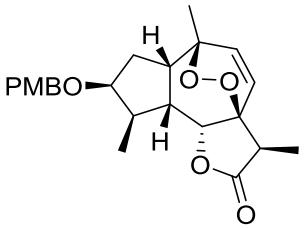

33

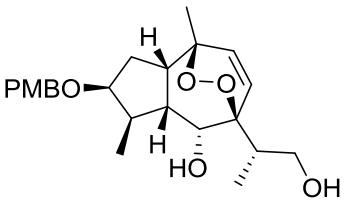

34

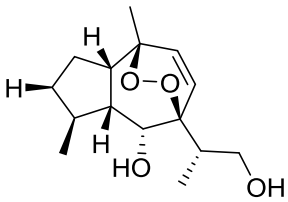

35

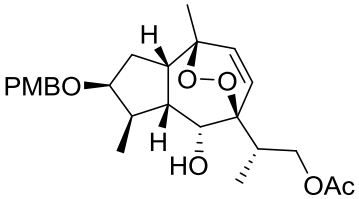

36

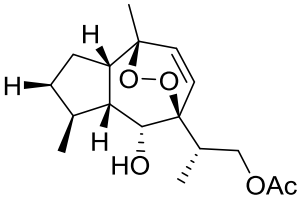

37

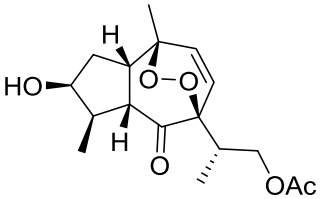

38

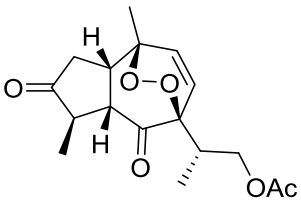

39

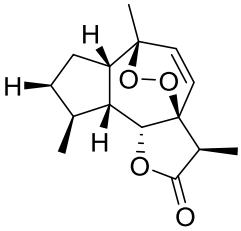

40

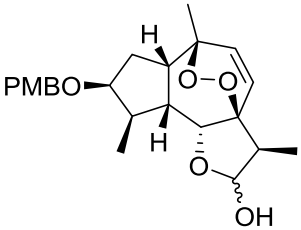

41

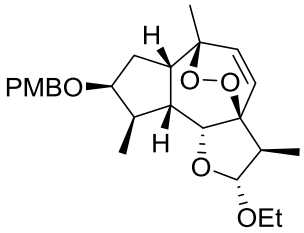

42

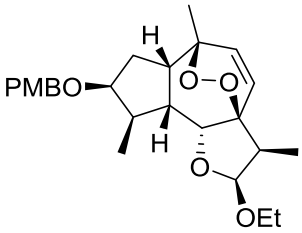

43

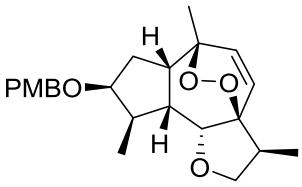

44

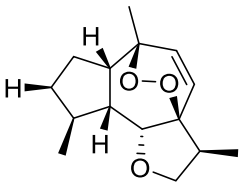

45

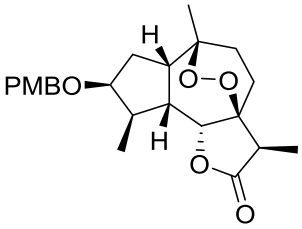

46

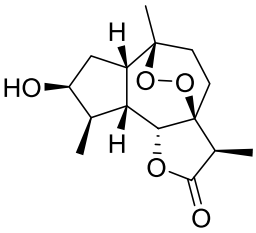

47

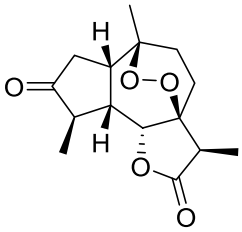

48

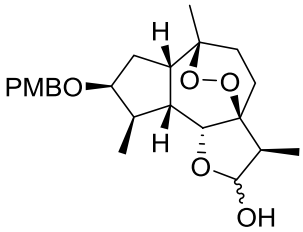

49

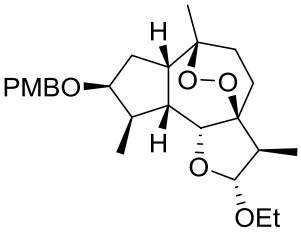

50

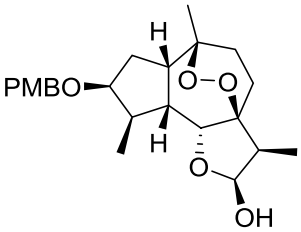

51

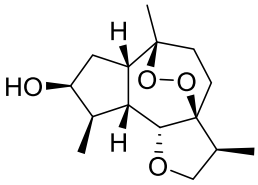

52

Figure 1.16: Structures of the guaianolide-endoperoxides that were synthesized and tested in reference #51.

Table 1.5: Antimalarial Activity against W2 Clones of *P. falciparum*

Compound no.	IC50 (µM)	Compound no.	IC50 (µM)
33	0.29 ± 0.01	**44**	0.23 ± 0.09
34	9.11 ± 0.21	**45**	0.57 ± 0.04
35	NA	**46**	0.37 ± 0.00
36	NA	**47**	0.61 ± 0.03
37	NA	**48**	0.27 ± 0.02
38	NA	**49**	NA
39	4.60 ± 0.10	**50**	3.40 ± 0.87
40	1.05 ± 0.00	**51**	0.024 ± 0.02
41	1.04 ± 0.01	**52**	7.50 ± 0.04
42	0.62 ± 0.02	artemisinin	0.005 ± 0.00
43	0.013 ± 0.000	thapsigargin	9.92 ± 0.10

NA = not active up to 10 µM

CHAPTER 2. PREVIOUSLY PROPOSED MECHANISMS

As previously mentioned, artemisinins contain an endoperoxide bridge that is absolutely crucial for their antimalarial activity. However, exactly how this endoperoxide bridge aids in killing the parasite is still a controversial subject. Theories have emerged over the years ranging from an artemisinin-heme interaction in the parasite that generates carbon-centered radicals to the inhibition of the sarcoplasmic/endoplasmic reticulum Ca^{2+} ATPase inside the parasite. All will be discussed.

2.1. HEME MECHANISM

A portion of the life cycle of *Plasmodium falciparum*, as stated earlier, occurs in the erythrocyte, or red blood cell, of a human host. It is during this stage that hemoglobin is utilized by the parasite as a food source. The hemoglobin is then taken into the food vacuole and broken down by proteolytic enzymes called plasmepsins. The broken down hemoglobin is further degraded into amino acids by food vacuole cysteine proteases known as falcipains.[54,55]

The proposed heme mechanism is that hematin, which is ferric protoporphyrin IX or Fe(III)PPIX, upon reduction to heme, or Fe(II)PPIX, is the source of ferrous iron that is responsible for bioactivation of the endoperoxide bridge of artemisinin to cytotoxic radical species. Artemisinin-mediated oxidative stress is the proposed mechanism of action based on in vitro experiments with infected red blood cells or parasite membranes. Heme catalyzes the reductive decomposition of artemisinin, and artemisinin was shown to increase the methemoglobin concentration and to slightly reduce the glutathione and membrane fatty acid concentrations which result in a dose-dependent increase of cell lysis.[55] The possible mechanism is depicted in **Scheme 2.1**. Further studies with Mn instead of Fe porphyrin led to isolable C4 adducts to the porphyrin ring system shown in **Figure 2.1**.[56]

Scheme 2.1: The possible mechanism for the artemisinin mediated lipid peroxidation of cell membranes.

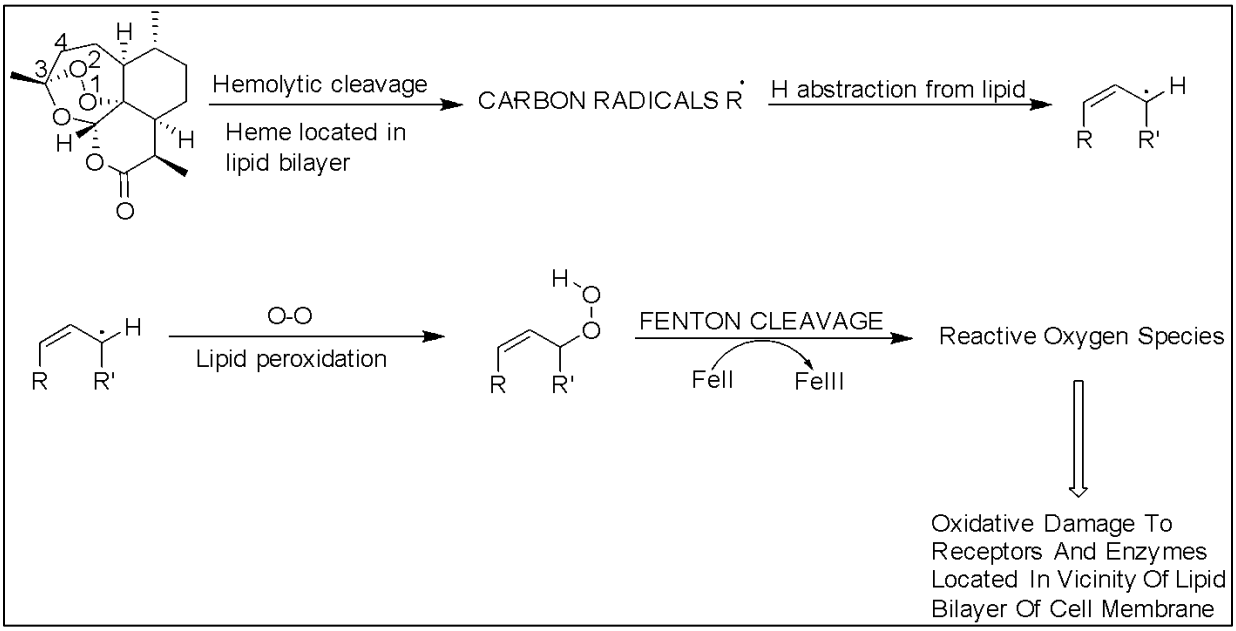

Lipid solubilized heme interacts with artemisinin followed by ferrous-mediated generation of oxygen and carbon radicals. These radicals are in the vicinity of target allylic hydrogens of unsaturated lipid bilayers. Hydrogen radical formation followed by oxygen capture results in the formation of lipid hydroperoxides. Fenton cleavage of the hydroperoxide forms reactive oxygen species such as hydroxyl radicals and superoxide which is thought to be the cause of damage to the food vacuole membrane. This damage leads to vacuolar rupture and parasite autodigestion. However, numerous workers in the field have proposed that parasite death is probably not caused by random cell damage from freely diffusing reactive oxygen species, but may involve specific radicals and targets.[55]

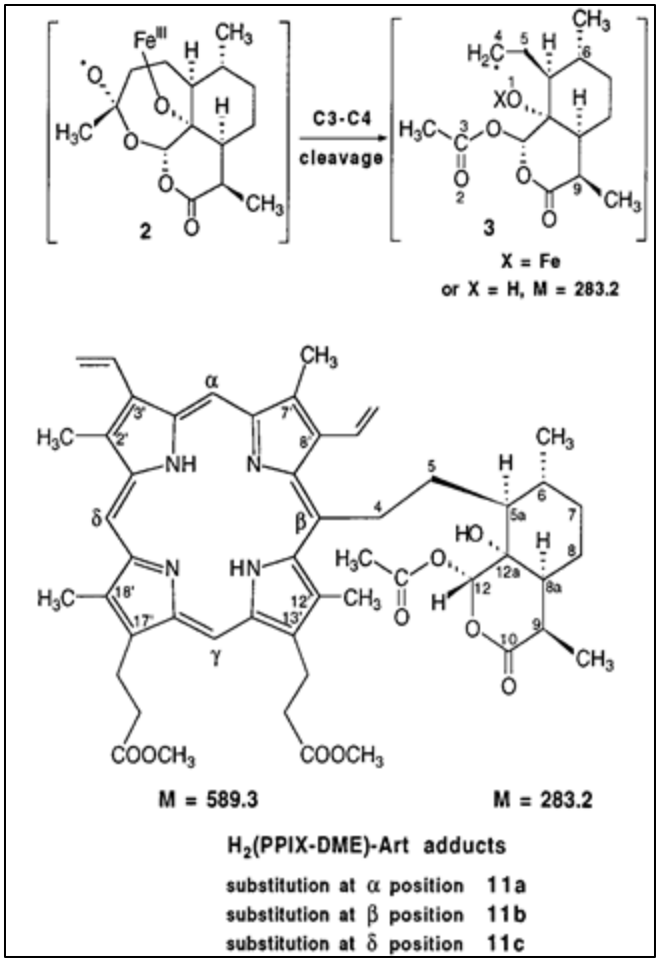

Figure 2.1: Isolated reaction products of artemisinin with manganoporphyrin.

2.2. CARBON RADICALS MECHANISM

The free radical chemistry of artemisinin is very well defined and has been shown to involve an initial chemical decomposition induced by ferrous ions within the malaria parasite. This produces an oxygen radical initially but subsequently rearranges into one or both of two distinctive carbon-centered radicals. **Scheme 2.2** shows the main radical pathways for artemisinin following endoperoxide-mediated bioactivation.[55]

Scheme 2.2: Proposed mechanism of the *in vitro* reaction of artemisinin with FeII.

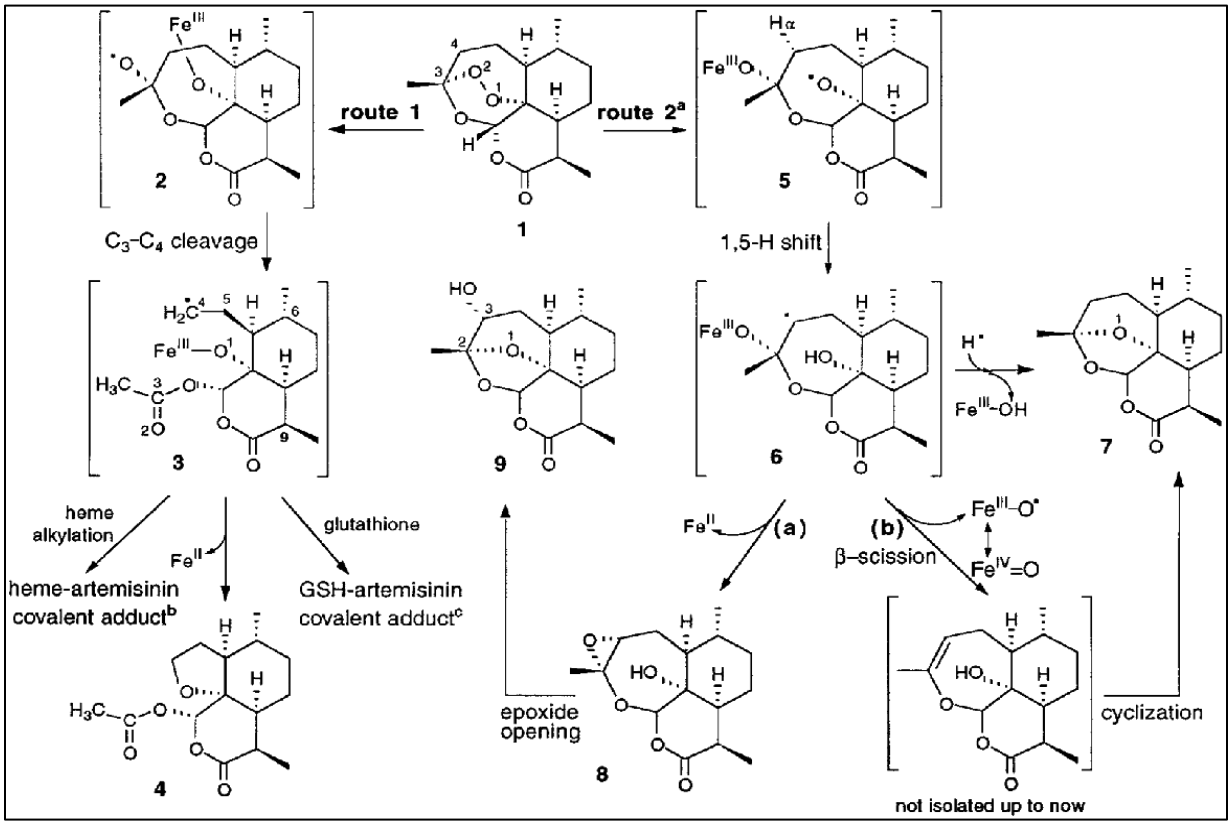

Since artemisinin **(1)** is an asymmetric endoperoxide, the peroxide oxygens can interact with ferrous ions in two ways: through O1 or through O2. Association through O1 produces an oxygen radical **2** that goes on to become a primary carbon radical **3**. This radical is then thought to be scavenged by molecules such as heme or gluthione to create the corresponding adducts. Association through O2 provides an oxygen radical **5** that produces a secondary carbon radical **6** via a 1,5-H shift. The final product is the stable hydroxydeoxoartemisinin **9**. It has been proposed that alkylation by the radical intermediates of biomacromolecules results in the death of the malarial parasite.[55] It has also been suggested that the non-isolable epoxide 8 was responsible for protein alkylation, but total synthesis of 13-carba-artemisinin by Avery, *et al* led to a stable

epoxide that was without activity, yet its peroxy precursor was of similar potency to artemisinin (cf. Figure 2.2).[57]

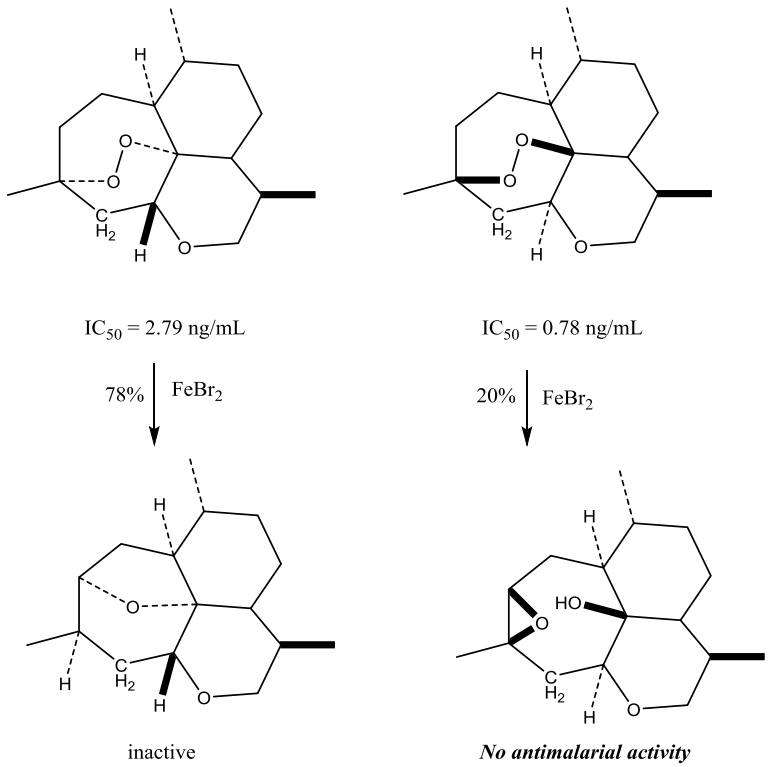

Figure 2.2: Activities of peroxidic and non-peroxidic derivatives of artemisinin.

These studies clearly show that the epoxide proposed by Posner, compound **8** (**Scheme 2.2**), is an unlikely intermediate that, even if it did form, would not be essential for activity.

2.3. CYSTEINE MECHANISM

Following the pioneering work of Meshnick and Posner, the cleavage theory could not be further developed because there was no logical link between the death of the parasite and the damage occurring to free heme since it is not essential to the life of the parasite. Wu *et.al.* reported that non-heme iron in the presence of cysteine can also cleave artemisinin efficiently,

and the transient carbon radical formed can covalently bind to the ligand at iron through a sulfur atom.[58]

Under near physiological conditions, FeII plays a negligible role. However, free FeII ions may form complexes with amino acids and be greatly activated. For instance, in the presence of cysteine, artemisinin can be degraded quite rapidly. It was believed that the catabolism of hemoglobin causes a higher concentration of free amino acids in infected erythrocytes than in uninfected erythrocytes, and the malaria parasite has a high concentration of reduced glutathione which is the main sulfhydryl-containing reducing agent in physiological systems. This was the first piece of established evidence for intermolecular interactions involving artemisinin.[58]

Scheme 2.3: Acetate elimination mediated by a thiol.

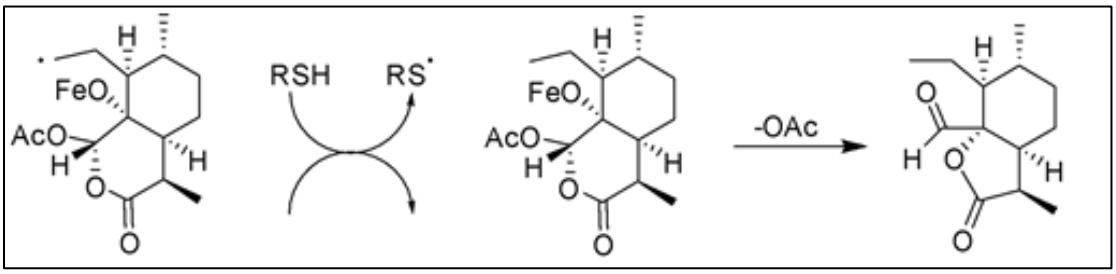

9 **10** **11**

Scheme 2.3 shows how the carbon radical formed from the FeII association with O1 interacts with a thiol such as in cysteine and then eliminates an acetate. The formation of **11** provides unequivocal evidence for the involvement of the highly reactive primary radical **9**. They envisaged that **9** may intramolecularly attack the cysteine sulfur atom complexed to the FeIII ion and release an FeII ion. The product resulting from such an attack after degradation leads to structure **13** as shown in **Scheme 2.4**.[58]

Scheme 2.4: Intramolecular attack of a cysteine sulfur to form a complex.

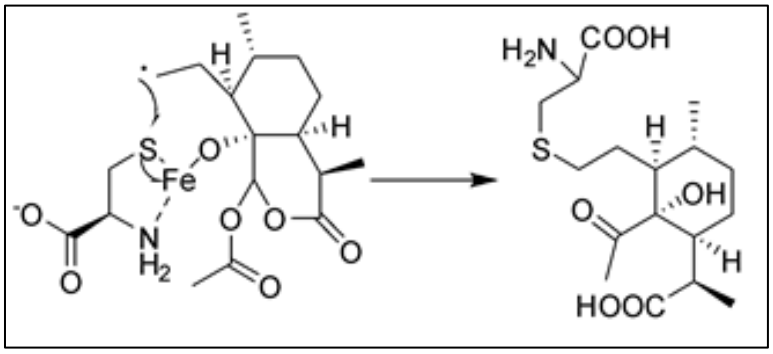

12 **13**

The importance of the concatenation of artemisinin and cysteine observed here in this simple chemical model system lies in the precise mechanistic basis it offered at the molecular level for the radical-mediated alkylation of proteins. Such a basis had been missing in all documented investigations to date.[58] Although mechanistically pleasing, the difficulty with this mechanism is that a covalent adduct of cysteine to Fe(II) is required. Under physiological conditions, formation of Fe(II)-SR compounds are implausible thermodynamically and even intuitively; if cysteine thiols or other biological thiols were susceptible to formation of covalent bonds, mammals would act as Fe(II) scavengers shutting down biochemical pathways, and the food we eat would be a deadly poison. A more complicated mechanism is therefore more likely to be involved that we will discuss shortly.

2.4. COFACTOR MECHANISM

Haynes *et.al.* conducted many experiments to point to the unlikelihood of carbon radicals or heme triggering the antimalarial activity of artemisinin and adopted a rather different approach to the consideration of the mechanism of action. The antimalarial methylene blue works by affecting the redox behavior of parasite flavin-dependent disulfide reductases such as glutathione reductase that control oxidative stress in the parasite. The synergism observed

between methylene blue and the artemisinin derivative artesunate suggests a complementary mode of action.[59]

Scheme 2.5: The ascorbic acid and methylene blue transformation of artemisinin.

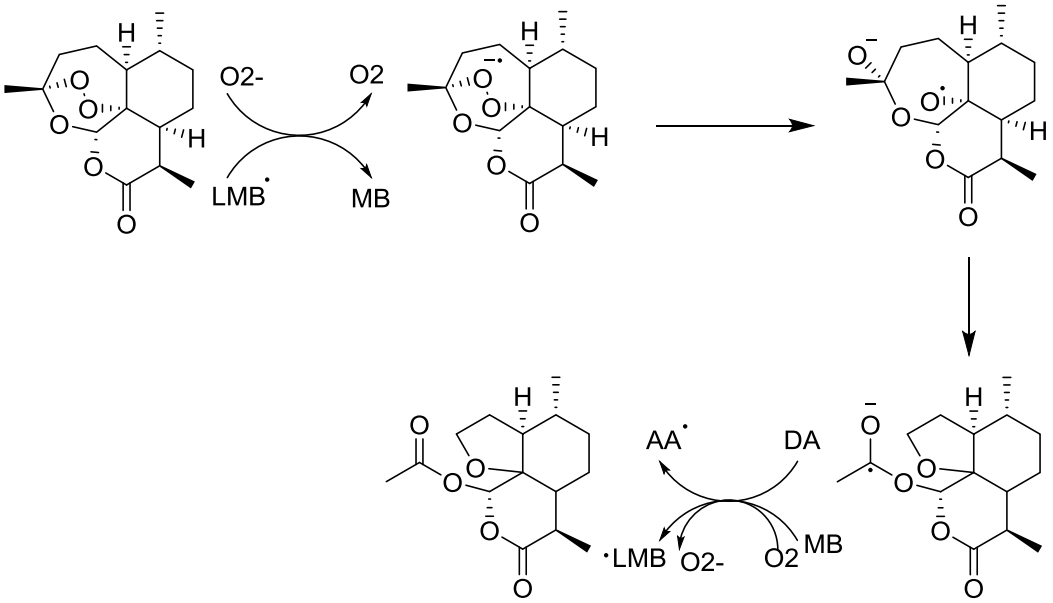

From the proposed scheme, we see that Haynes found that artemisinins are transformed by leucomethylene blue which is generated from methylene blue and ascorbic acid in situ in aqueous buffer at physiological pH into single electron transfer (SET) or two electron reduction rearrangement products. A ketyl arose that was oxidized to the carbonyl. Since artemisinins generate reactive oxygen species and behave synergistically with methylene blue and doxorubicin, they concluded that artemisinins act as electron acceptors and are likely to interfere with redox-active cofactors such as flavoenzymes.[59]

2.5. SERCA/PfATP6 MECHANISM

As discussed under preceding hypotheses, studies have suggested that artemisinin acts by heme-dependent activation of the endoperoxide bridge occurring within the food vacuole. However, localization of artemisinin to parasite and not food vacuole membranes and the fact that artemisinin can effectively kill the ring stage of the parasite even though it lacks hemazoin argue against the food vacuole being a major site for drug action. Krishna *et.al.* discovered that artemisinin shows structural similarities to thapsigargin, a highly specific inhibitor of sarco/endoplasmic reticulum Ca^{2+}-ATPase (SERCA). They proceeded to hypothesize that when activated, artemisinin acts by specifically and selectively inhibiting PfATP6, the only SERCA-type CA^{2+}-ATPase sequence in *Plasmodium falciparum*.[44]

PfATP6 was expressed in *Xenopus laevis* oocytes. It was found to be inhibited not only by artemisinin, but also by thapsigargin and another mammalian SERCA inhibitor, cyclopiazonic acid. They then assessed the inhibitory properties of chloroquine, quinine, and artemisinin on transporter proteins encoded by *P. falciparum* as well as their effects on SERCA1a. None of these structurally diverse compounds interferes non-specifically with the function of integral membrane proteins of *P. falciparum*. SERCA1a activity was also not affected by these compounds.[44]

PfATP4 is the only other Ca^{2+}-ATPase-like sequence identified in the *P. falciparum* genome and defines a non-SERCA subclass of Ca^{2+}-ATPase unique to apicomplexan organisms. The antimalarials tested also did not inhibit the activity of PfATP4. The Ca^{2+}-ATPase activity of PfATP6 was inhibited by artemisinin but not by chloroquine or quinine. Even at relatively high concentrations, artemisinin inhibits PfATP6 with high specificity. Endogenous Ca^{2+}-ATPase

activity is also resistant to the action of artemisinin, which demonstrates the unique specificity of artemisinin for PfATP6.[44]

The interactions of artemisinin and thapsigargin with PfATP6 were compared by measuring their inhibitory constants. Thapsigargin irreversibly inhibited Ca^{2+}-ATPase activity with 1:1 stoichiometry, and the inhibitory profile of artemisinin was directly superimposable over that of thapsigargin, showing that they inhibit PfATP6 with the same potency and stoichiometry *in vitro*.[44]

Since both thapsigargin and artemisinin specifically inhibit PfATP6, Krishna *et.al*. went on to predict that they would exhibit mutual antagonism in cultured parasites. They were administered simultaneously in varying concentrations. As predicted, thapsigargin antagonized the parasiticidal activity of artemisinin. The two drugs show significant antagonism indicating that artemisinin specifically inhibits PfATP6 in intact parasites. To confirm that PfATP6 is the target for artemisinins, they compared inhibitory constants of a range of artemisinin derivatives such as dihydroartemisinin, artesunate, artemether, artemotil, and arteflene against PfATP6 in oocytes with their ability to kill parasites *in vitro*. Almost perfect correlations existed between the inhibitory potencies and the IC_{50} values from cultured parasites. To confirm that ferrous ions are indeed necessary for artemisinin's antimalarial activity, desoxyartemisinin, artemisinin without the endoperoxide bridge, was assayed and found to be inactive against PfATP6. Chelation of iron by desferrioxamine abrogates the antiparasitic activity of artemisinins. These studies support PfATP6 as a target of artemisinin, and it likely operates via an Fe^{2+}-dependent activation mechanism. This allowed, for the first time, rational biological target-guided drug design efforts to be carried out.[44]

CHAPTER 3. DEVELOPMENT OF A HYBRID MECHANISM

***Shuneize E. Slater, Jakub Kollar, Kuldeep K. Roy, Khaled M. Elokely, Sanjeev Krishna,**

Robert J. Doerksen, Mitchell A. Avery, Unpublished.

3.1 INTRODUCTION

After studying all of the previously proposed mechanisms of action, we began sifting through them to determine which was more feasible. However, we discovered that each mechanism was flawed for various reasons. The alkylation of heme was not acceptable as heme is not important to the survival of the parasite, and carbon radicals did not completely answer the question as random alkylation of biomolecules seemed far-fetched. The SERCA and cysteine hypotheses finally gave a specific target for artemisinin, but they give no further explanation of what happens after radical extraction. The two that caught our attention the most were the SERCA and the cysteine hypotheses, so we developed the PfATP6/ferrous ion/cysteine hypothesis, otherwise known as the Hybrid SERCA hypothesis.

Our current hypothesis was not our first, however. Our first hypothesis suggested that a cysteine thiol moiety in the protein is able to recruit a ferrous ion as it is “passing by”. The ferrous ion then ligates the endoperoxide bridge of artemisinin. This would be possible in any of ten different locations. This hypothesis relieves us of finding a ferrous ion binding site and also of finding an artemisinin binding site as both are recruited when in the vicinity of the cysteine thiol. We abandoned that hypothesis as it would not be computationally efficient to examine every cysteine in the protein. We then hypothesized that a ferrous ion finds a binding site near a cysteine residue. The ion then ligates the endoperoxide bridge of artemisinin as it approaches. We looked, particularly, at the two calcium ions in the channel. Thinking that the calcium ions could exchange for the ferrous ions, we examined the pocket. We found that there are no cysteine residues near the calcium ion binding sites, and also the ferrous ions are not able to be coordinated by the same residues as the calcium ions. So this hypothesis, too, was discarded.

In our third hypothesis, we predicted that artemisinin would bind in its binding site somewhere near a cysteine residue. The endoperoxide bridge of artemisinin would then ligate the ferrous ion as it approaches. In this scenario, only artemisinin is required to have a binding site. In the final hypothesis, both artemisinin and the ferrous ion bind in their respective binding sites near a cysteine residue. Since the last two hypotheses seem more feasible, these are the two that we decided to investigate further.

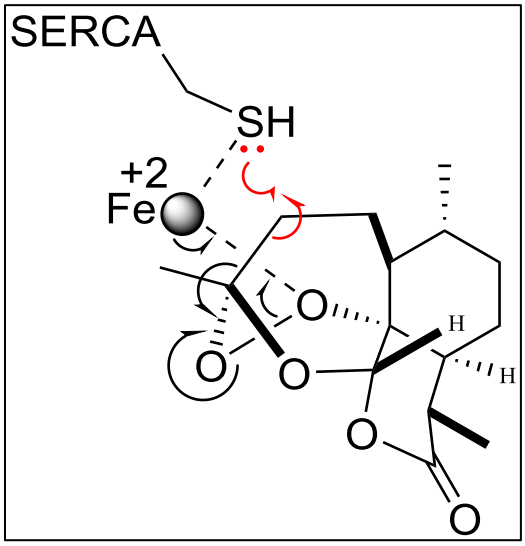

Figure 3.1: The optimal synchronous reaction that occurs between iron, artemisinin, and the cysteine residue of PfATP6.

Figure 3.1 shows the importance of the orientation of the iron atom, the cysteine residue, and the peroxide bridge of artemisinin. The reaction that occurs between artemisinin and PfATP6 is more than likely a synchronous reaction; however, it may occur in 2 steps. Either way, there are certain distances between the three components that need to be obtained. Once Fe^{2+} cleaves the peroxide bridge of artemisinin, a short-lived oxygen radical forms and quickly rearranges to a carbon radical. Carbon radicals are also extremely short-lived. Intramolecular destruction will

commence, and this leads to neutral products. Therefore, the geometry and the distances between the atoms are so significant.

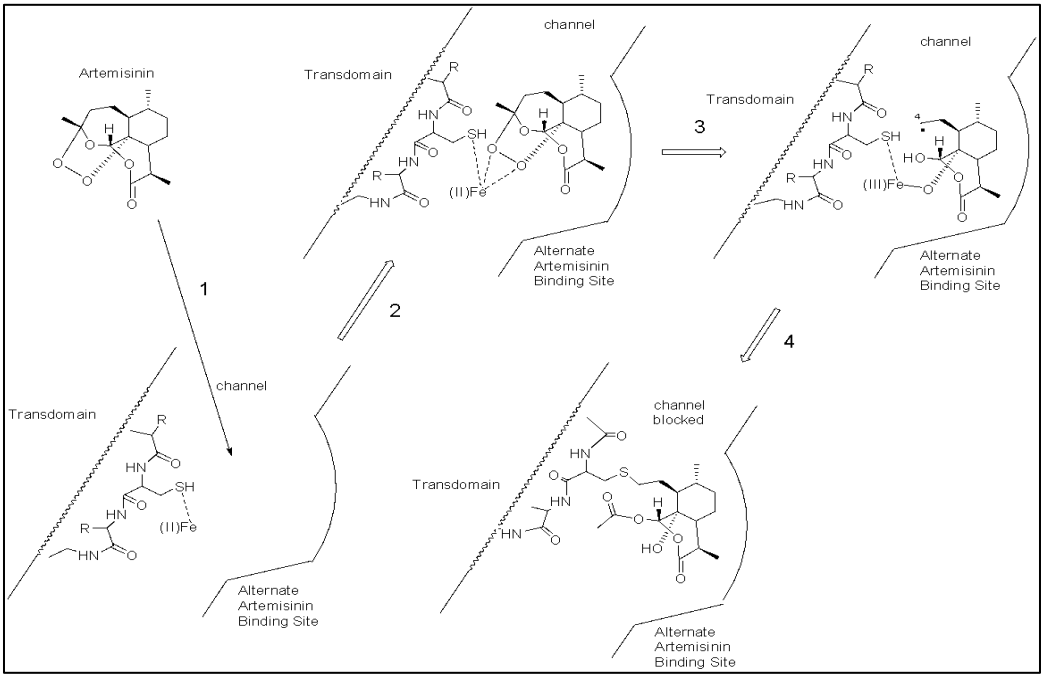

Figure 3.2: Mechanism of action of our third hypothesis.

Figure 3.2 represents our third hypothesis. Artemisinin comes in and binds in its binding site near a cysteine residue. The ferrous ion is recruited and then ligates the endoperoxide bridge of artemisinin. Cleavage of the bridge effects an oxygen radical that rearranges to a carbon centered radical. This radical is in close proximity to the cysteine thiol moiety and is captured. A covalent sulfide bond is formed between the protein and artemisinin thus shutting down the calcium pump and leading to the death of the parasite.

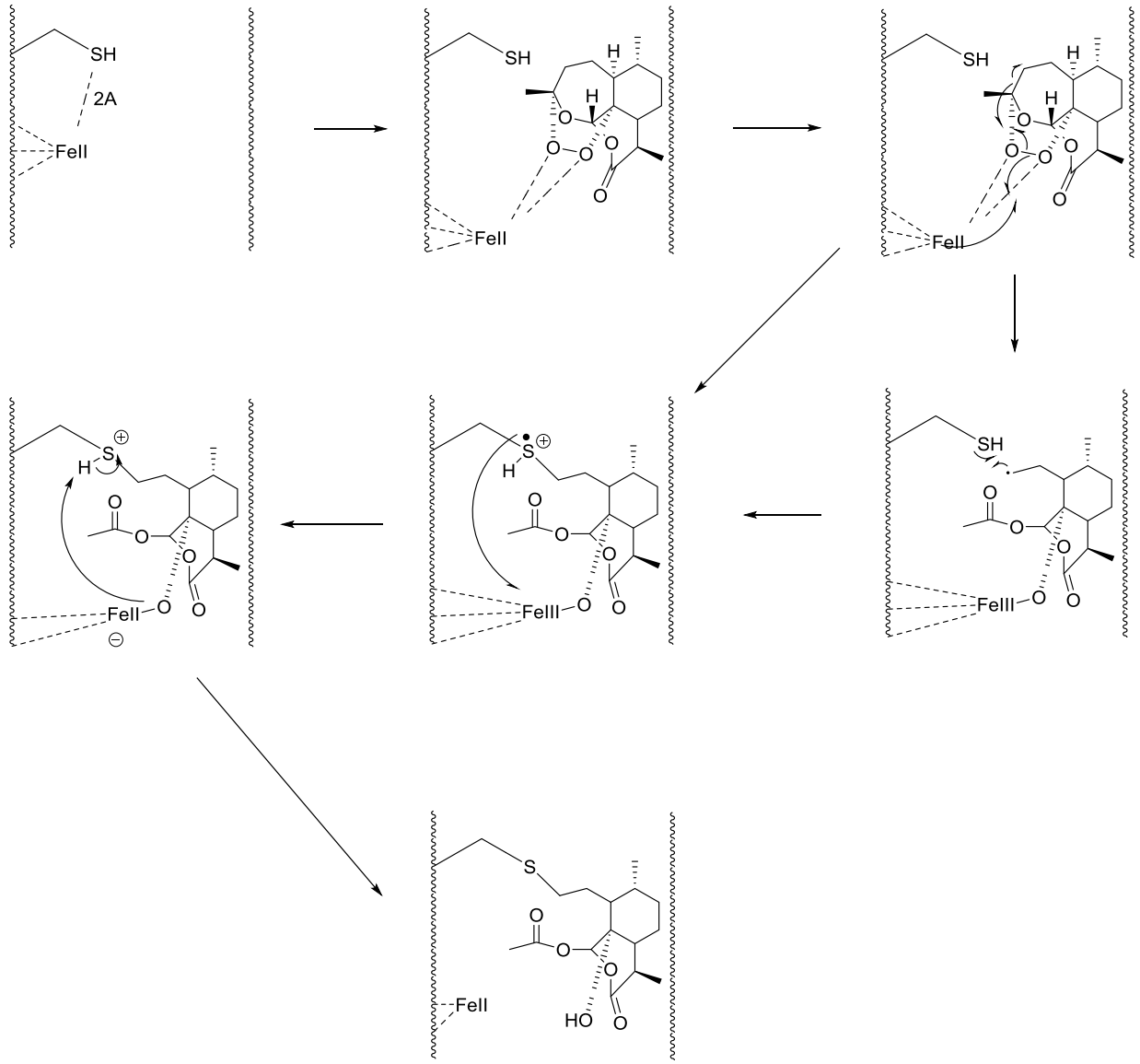

Figure 3.3: Details of Putative Mechanism of our fourth hypothesis.

Figure 3.3 represents our fourth hypothesis. The ferrous ion binds in its binding site near a cysteine residue. Artemisinin comes in and binds in its binding site nearby. The ferrous ion then ligates the endoperoxide bridge. Cleavage of the bridge effects an oxygen radical that rearranges to a carbon centered radical. This radical is in close proximity to the cysteine thiol moiety and is captured. A covalent sulfide bond is formed between the protein and artemisinin

thus shutting down the calcium pump and leading to the death of the parasite. We have exhausted many computational tools to test the likelihood of our hypotheses, and they will all be discussed thoroughly.

3.2 STRUCTURE MODELING AND VALIDATION

Protein structure modeling, or protein structure prediction, is the prediction of a protein's folding and its secondary, tertiary, and quaternary structure from its primary structure or amino acid sequence. Structure modeling is one of the most important goals pursued by bioinformatics and is very important in drug design. Protein structure prediction is now more significant than ever. There is a huge amount of protein sequence data produced by modern large-scale DNA sequencing efforts such as the Human Genome Project. X-ray crystallography and NMR spectroscopy produce protein structures but are typically time-consuming and expensive and lag far behind the output of protein sequences.[60]

The two major problems facing protein structure prediction are the calculation of protein free energy and finding the global energy minimum. Comparative protein modeling can partially bypass these issues. Although the number of proteins is vast, there is only a limited set of tertiary structural motifs to which most proteins belong. Comparative modeling uses previously solved protein structures as starting points, or templates.[61]

Homology modeling, which is a type of comparative modeling, is based on the fact that a protein's fold is more evolutionarily conserved than its amino acid sequence. This allows a target sequence to be modeled with reasonable accuracy from a very distantly related template; however, homology modeling is most accurate when the target and template have similar sequences.[61]

The 1,228 amino acid sequence of *Plasmodium falciparum* ATPase 6 (PfATP6) was obtained from the Plasmo Database (PlasmoDB) website and is as follows:

MEEVIKNAHTYDVEDVLKFLDVNKDNGLKNEELDDRRLKYGLNELEVEKKKSIFELILN
QFDDLLVKILLLAAFISFVLTLLDMKHKKIEICDFIEPLVIVLILILNAAVGVWQECNAEKS
LEALKELQPTKAKVLRDGKWEIIDSKYLYVGDIIELSVGNKTPADARIIKIYSTSLKVEQS
MLTGESCSVDKYAEKMEDSYKNCEIQLKKNILFSSTAIVCGRCIAVVINIGMKTEIGHIQH
AVIESNSEDTQTPLQIKIDLFGQQLSKIIFVICVTVWIINFKHFSDPIHGSFLYGCLYYFKIS
VALAVAAIPEGLPAVITTCLALGTRRMVKKNAIVRKLQSVETLGCTTVICSDKTGTLTTN
QMTTTVFHLFRESDSLTEYQLCQKGDTYYFYESSNLTNDIYAGESSFFNKLKDEGNVEA
LTDDGEEGSIDEADPYSDYFSSDSKKMKNDLNNNNNNNNNSSRSGAKRNIPLKEMKSN
ENTIISRGSKILEDKINKYCYSEYDYNFYMCLVNCNEANIFCNDNSQIVKKFGDSTELALL
HFVHNFDILPTFSKNNKMPAEYEKNTTPVQSSNKKDKSPRGINKFFSSKNDNSHITSTLN
ENDKNLKNANHSNYTTAQATTNGYEAIGENTFEHGTSFENCFHSKLGNKINTTSTHNNN
NNNNNNSNSVPSECISSWRNECKQIKIIEFTRERKLMSVIVENKKKEIILYCKGAPENIIKN
CKYYLTKNDIRPLNETLKNEIHNKIQNMGKRALRTLSFAYKKLSSKDLNIKNTDDYYKL
EQDLIYLGGLGIIDPPRKYVGRAIRLCHMAGIRVFMITGDNINTARAIAKEINILNKNEGD
DEKDNYTNNKNTQICCYNGREFEDFSLEKQKHILKNTPRIVFCRTEPKHKKQIVKVLKDL
GETVAMTGDGVNDAPALKSADIGIAMGINGTEVAKEASDIVLADDNFNTIVEAIKEGRCI
YNNMKAFIRYLISSNIGEVASIFITALLGIPDSLAPVQLLWVNLVTDGLPATALGFNPPEH
DVMKCKPRHKNDNLINGLTLLRYIIIGTYVGIATVSIFVYWFLFYPDSDMHTLINFYQLSH
YNQCKAWNNFRVNKVYDMSEDHCSYFSAGKIKASTLSLSVLVLIEMFNALNALSEYNS
LFEIPPWRNMYLVLATIGSLLLHVLILYIPPLARIFGVVPLSAYDWFLVFLWSFPVIILDEII
KFYAKRKLKEEQRTKKIKID

The sequence was then aligned with a 2.4 Ångstrom resolution crystal structure of human calcium ATPase (PDBID: 2AGV) using ClustalW. The alignment was then visually inspected and manually altered to match the alignment obtained by Prime[62], which is the protein structure prediction module of Schrödinger. The final alignment was used as an input for the building of 100 homology models of PfATP6 using Modeller version 9.12 software. After the 100 models were generated they underwent loop refinement, and their Ramachandran plots were analyzed to find the models with the least number of outliers. Six models (Model 3, Model 4, Model 10, Model 11, Model 13, and Model 44) were chosen to be saved as pdb files, uploaded into the Maestro[62] workspace, which is the visual interface for all of Schrödinger's applications, and prepared and minimized using the Protein Preparation Wizard[62] default procedure which is as follows: the bond orders were assigned, hydrogens were added, zero-order bonds were created to metals, disulfide bridges were formed, waters beyond 5 Å from het groups were deleted, non-coordinated water molecules and all het groups other than thapsigargin were deleted, and finally the protein was minimized.

Figure 3.4: Sequence alignment of PfATP6 and 2AGV.

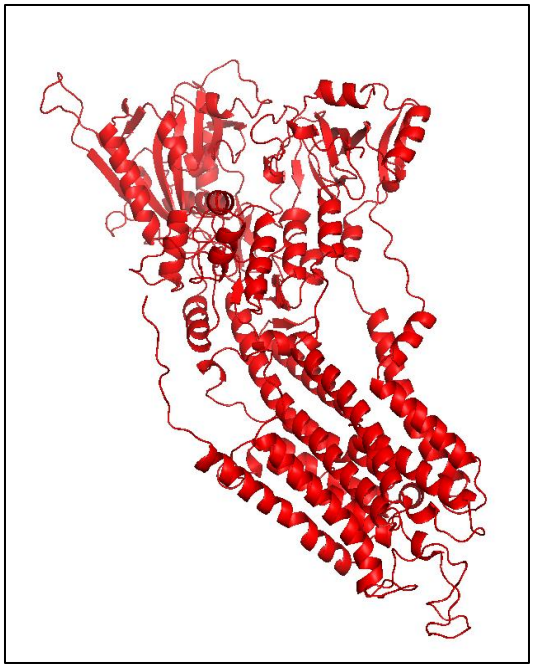

Figure 3.5: After Modeller homology modeling and loop refinement, the complete structure of Model 3 emerged as is shown here in red.

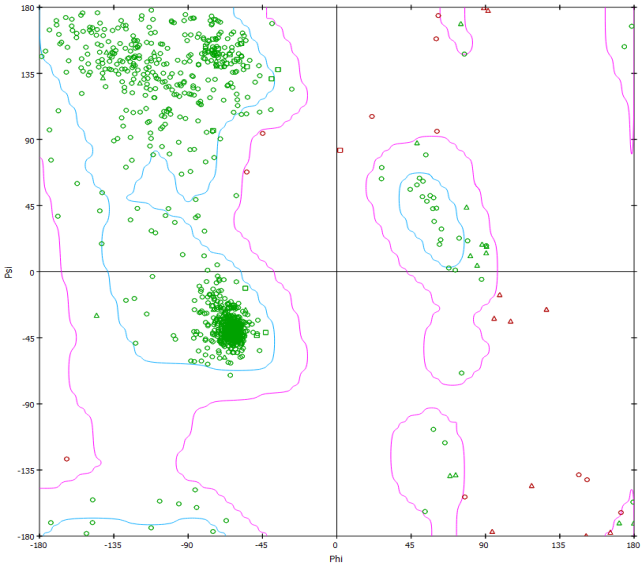

Figure 3.6: The Ramachandran plot for Model 3 shows that 93.7% of the residues are in the favored region, 4.8% of the residues are in the allowed region, and only 1.6% of the residues are in the outlier region.

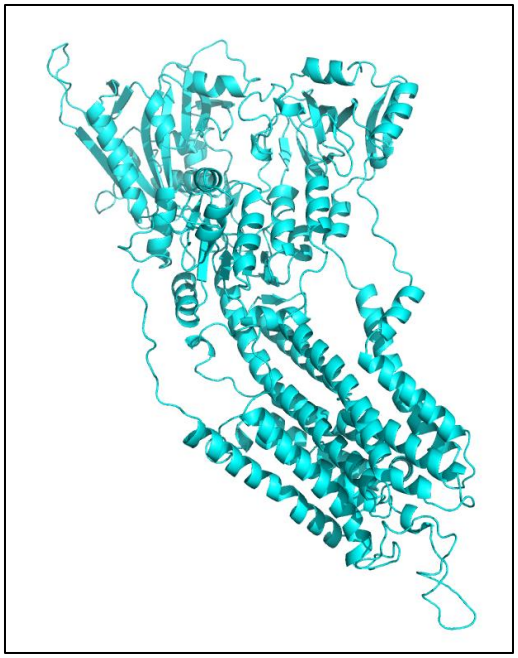

Figure 3.7: After Modeller homology modeling and loop refinement, the complete structure of Model 4 emerged as is shown here in aquamarine.

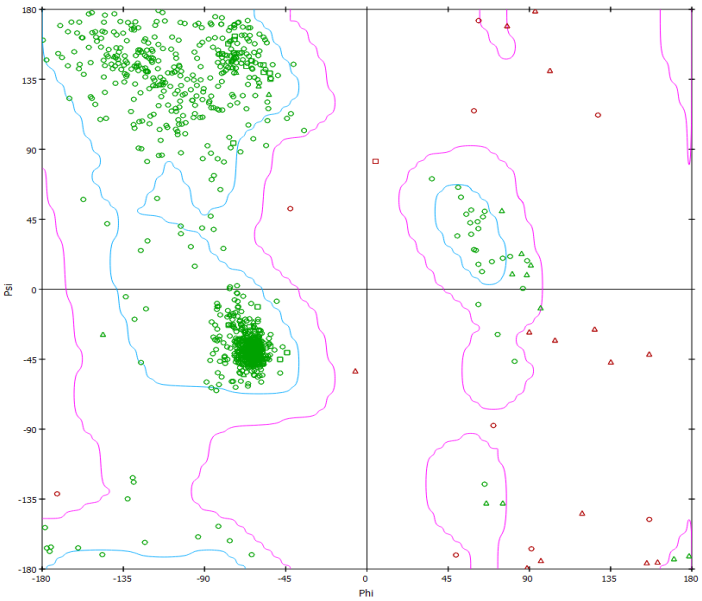

Figure 3.8: The Ramachandran plot for Model 4 shows that 94.1% of the residues are in the favored region, 4.6% of the residues are in the allowed region, and only 1.4% of the residues are in the outlier region.

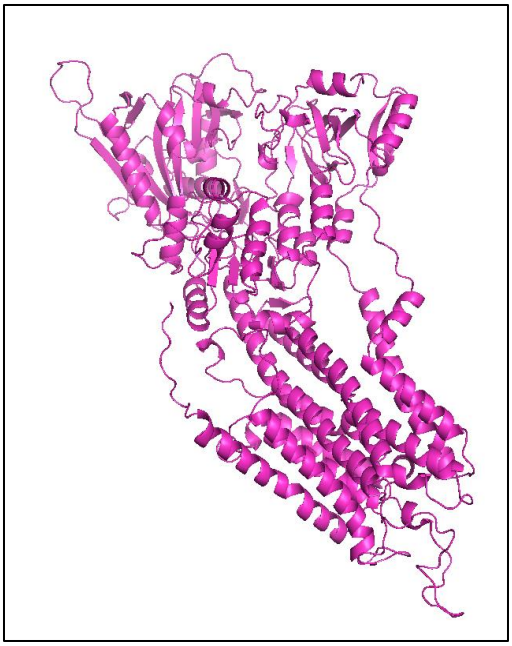

Figure 3.9: After Modeller homology modeling and loop refinement, the complete structure of Model 10 emerged as is shown here in magenta.

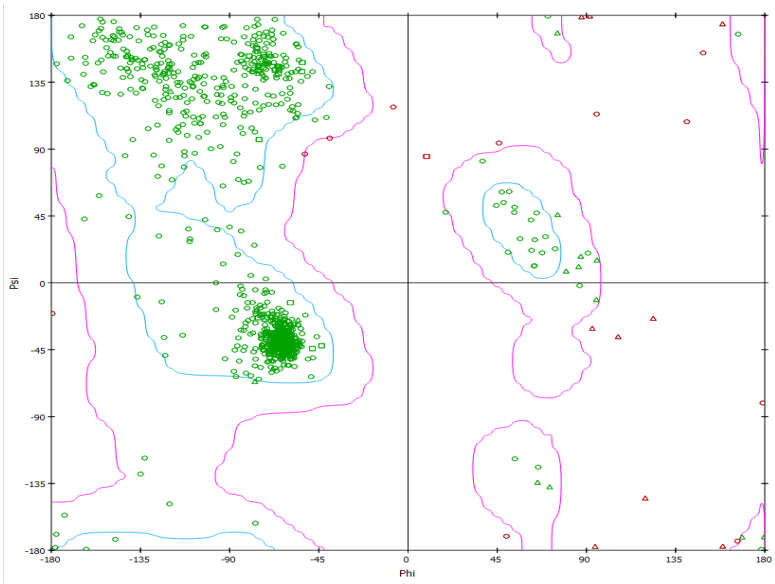

Figure 3.10: The Ramachandran plot for Model 10 shows that 94.9% of the residues are in the favored region, 3.6% of the residues are in the allowed region, and only 1.6% of the residues are in the outlier region.

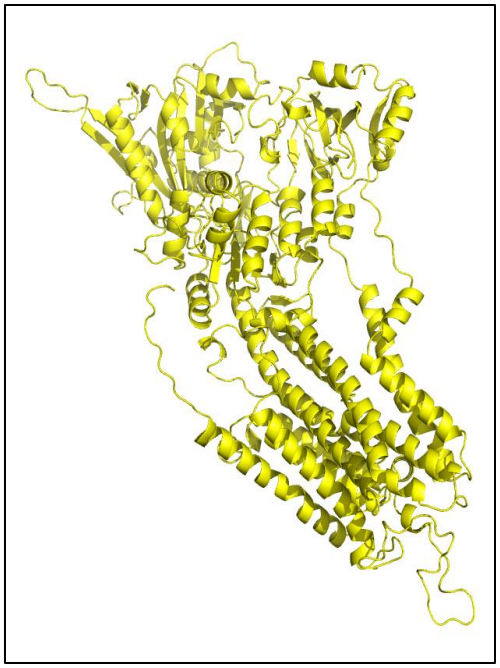

Figure 3.11: After Modeller homology modeling and loop refinement, the complete structure of Model 11 emerged as is shown here in yellow.

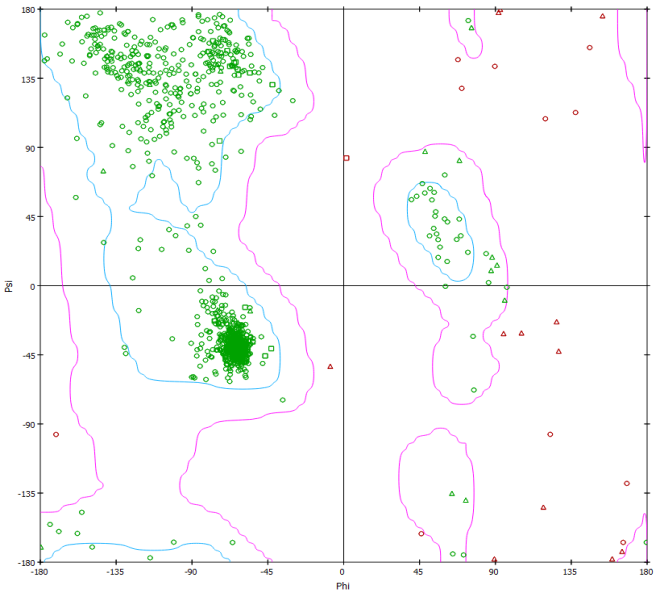

Figure 3.12: The Ramachandran plot for Model 11 shows that 94.2% of the residues are in the favored region, 4.3% of the residues are in the allowed region, and only 1.6% of the residues are in the outlier region.

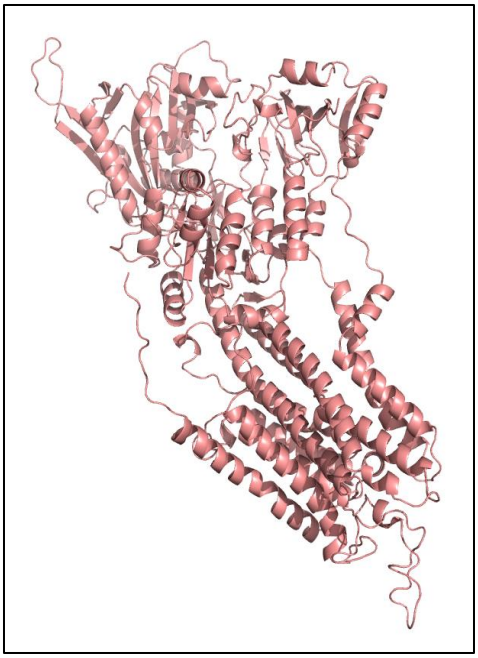

Figure 3.13: After Modeller homology modeling and loop refinement, the complete structure of Model 13 emerged as is shown here in peach.

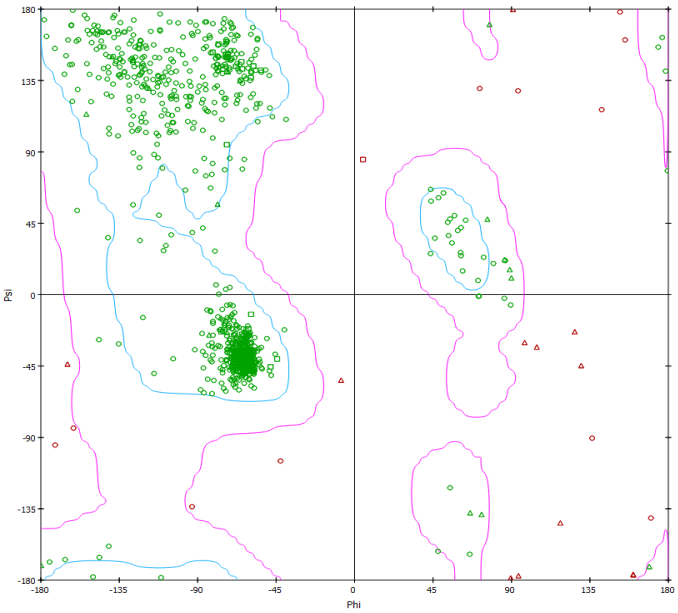

Figure 3.14: The Ramachandran plot for Model 13 shows that 94.5% of the residues are in the favored region, 3.9% of the residues are in the allowed region, and only 1.7% of the residues are in the outlier region.

Figure 3.15: After Modeller homology modeling and loop refinement, the complete structure of Model 44 emerged as is shown here in gray.

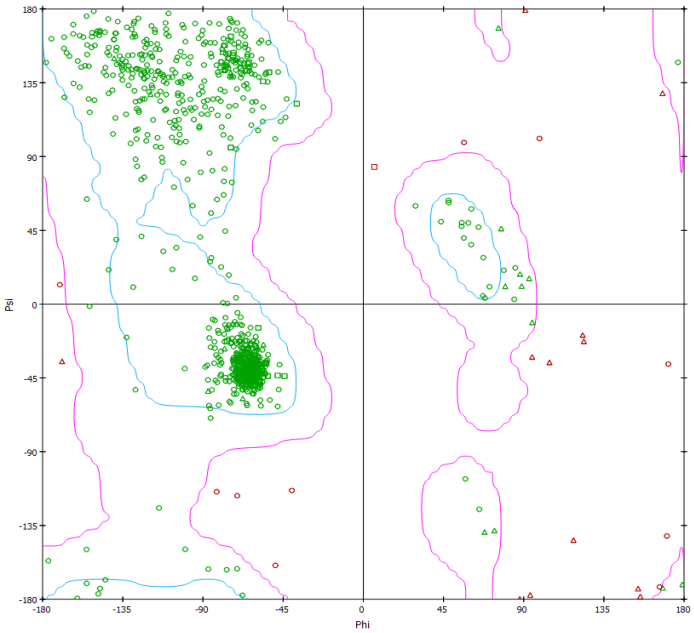

Figure 3.16: The Ramachandran plot for Model 44 shows that 94.6% of the residues are in the favored region, 4.2% of the residues are in the allowed region, and only 1.3% of the residues are in the outlier region.

To determine the validity of the Modeller models, the six prepared and minimized models were used to generate receptor grids of the active sites using the default options available in Glide[62], which is a docking program in the Schrödinger suite. The co-crystallized ligand, thapsigargin, was used to indicate the active site. After the grids were generated, artemisinin, thapsigargin, and the thaperoxides were drawn in the Maestro workspace, then submitted to MacroModel[62] for conformational searches. MacroModel is a module of the Schrödinger suite. It combines force fields, solvation models, and an advanced conformational searching method to comprise an advanced and complete molecular modeling package. A total of 855 conformers were created and then docked both flexibly and rigidly into the active site of all of the models using Glide. After many tries including using positional constraints to bias the tricyclic core to the phenylalanine in the active site, no correlation could be detected between the biological activities and docking scores. We drew an assumption that using the extremely large ligand, thapsigargin, to indicate the active site was causing all the small molecules to fit into the active site posing an inability to properly rank the compounds. So the six models were again prepared and minimized, but this time all co-crystallized ligands were deleted. Receptor grids of the active sites were then generated by specifying residues Leu263, Phe264, Gln267, Ile977, Ile981, Asn1039, Leu1040, Ile1041, and Asn1042. Also realizing that the thaperoxide compounds had only undergone a cell-based assay and not a PfATP6 target-based assay, we decided to use the eight compounds assayed by David-Bosne *et.al*. that were proven to have PfATP6 inhibitory activity in a target-based assay as test compounds. These eight compounds were drawn and minimized in the Maestro workspace for visualization. The compounds were then submitted to MacroModel conformational search. 1,488 conformers were generated and then docked into the

active sites using Glide. However, no significant correlation could be found between the docking scores and the reported biological activities.

Prime was also used to construct a homology model of PfATP6. In the homology model building panel, the PfATP6 sequence was pasted into the text box, and a BLAST homology search was initiated to find homologous proteins. PDBID 1SU4, having an overall 44% identity with the input sequence, was selected as the template. ClustalW was then used to align the two sequences. An energy-based building method was selected because it is more accurate than the knowledge-based method. The two bound calcium ions in the channel were chosen to be included in the model. Loop refinement was not performed. This procedure produced four models. To determine their validity, the Prime models were prepared and minimized in the same manner as the Modeller predicted models. Receptor grids were made of the active sites of the models by specifying Leu263, Phe264, Gln267, Ile977, Ile981, Asn1039, Leu1040, Ile1041, and Asn1042. The 1,488 conformers of the eight PfATP6 inhibitors were then docked into the grids using Glide docking. The fourth model was able to identify the four most active compounds and the least active compound and ranked them accordingly. So this was the model chosen for further studies and experimentation.

Figure 3.17: The fourth and best model predicted by Prime shown in green, also showing the bound calcium ions in the channel.

3.3 PROTEIN POCKET DETECTION

Predicting functional sites in protein structures such as ligand binding sites or catalytic sites is very important. It largely relies on the identification and characterization of clefts and cavities in the protein structure, and it can guide the design of small molecules that could interact with a protein and modulate its activity and function. Many online services have been proposed for pocket detection. The fpocket protein pocket detection program was introduced a few years

ago and was found to be able to correctly identify more than 90% of known binding sites in both holo and apo proteins. It also ranks the sites found in the protein based on their "druggability".[63]

The validated PfATP6 model was uploaded, and fpocket was executed. After concluding, 51 pockets were found in the protein.

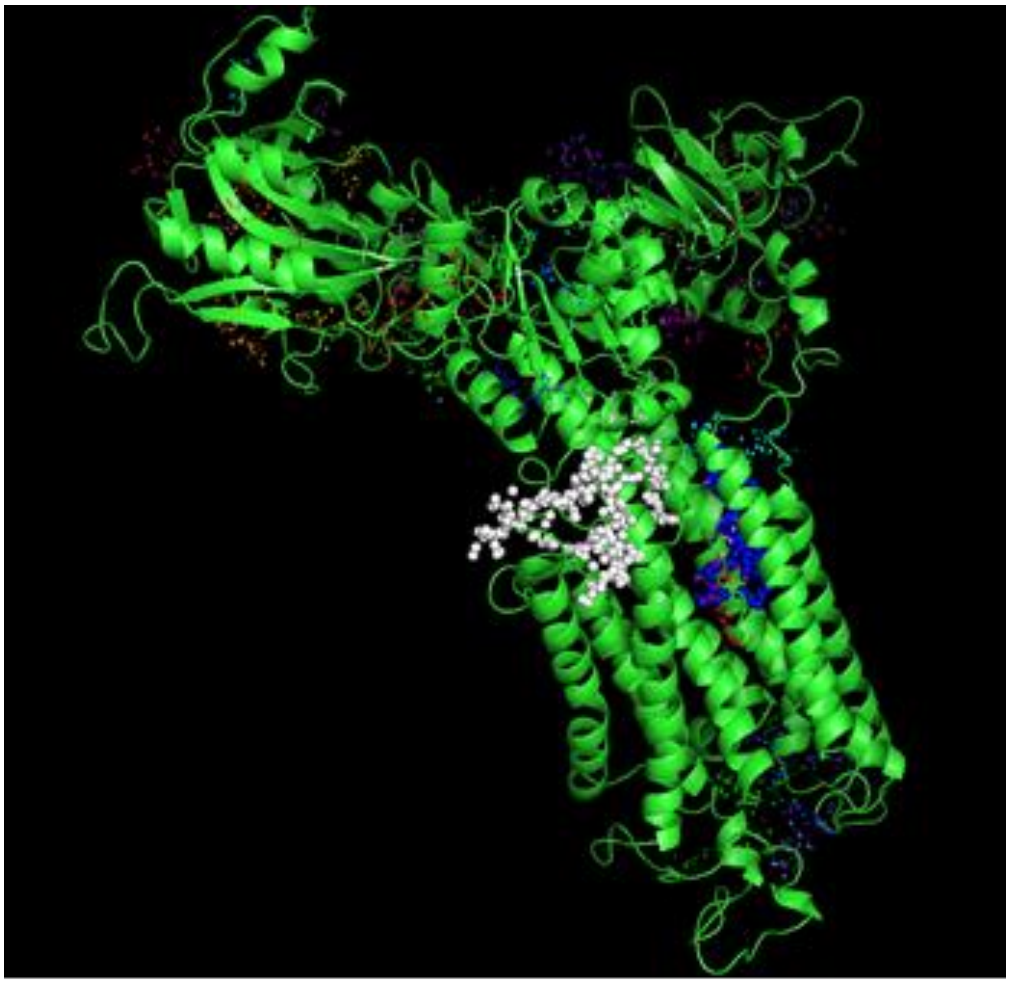

Figure 3.18: Model of PfATP6 showing the 51 pockets (in various colors and different sized spheres) found by fpocket.

3.4 BLIND DOCKING

Blind docking is used when only the structure of the macromolecule or protein and the structure of the ligand are known. There is no prior knowledge of the binding site. This application is named blind docking because the docking algorithm is not able to "see" the binding site but can still find it.[64]

The most important requirement of a blind docking calculation is its ability to distinguish between the actual binding site and nonspecific and/or energetically unfavorable sites. AutoDock packages have been proven to be efficient and robust at finding binding pockets and binding orientations of ligands. This makes this program particularly attractive because one method can be used to search for the binding site and to accurately dock the ligands.[64]

Since the AutoDock packages have been recognized for their ability not only to identify the binding site of ligands but also to dock the ligands well, we decided to use AutoDock Vina to identify all of the artemisinin binding sites in PfATP6. The structure of artemisinin was drawn and minimized in the Maestro workspace and then saved as a pdb file. The pdb file of the PfATP6 homology model was uploaded into AutoDock Vina. Hydrogens were added, and the protein was saved as a pdbqt file. A grid box of the protein was created to tell the program where to dock the ligand. Since this is blind docking, the entire protein structure was included in the grid box. The minimized structure of artemisinin was then uploaded to AutoDock Vina and saved as a pdbqt file. Torsions were not required as there are no rotatable bonds in artemisinin. A text file was used to identify the protein, ligand, grid box, grid spacing, and the exhaustiveness of the program. The command prompt was used to run the docking algorithm using a specified input text file. Nine results were obtained, but only 4 artemisinin binding sites were found.

Interestingly, these four sites were the sites ranked the most druggable by the fpocket pocket searching software. These sites were then extensively analyzed.

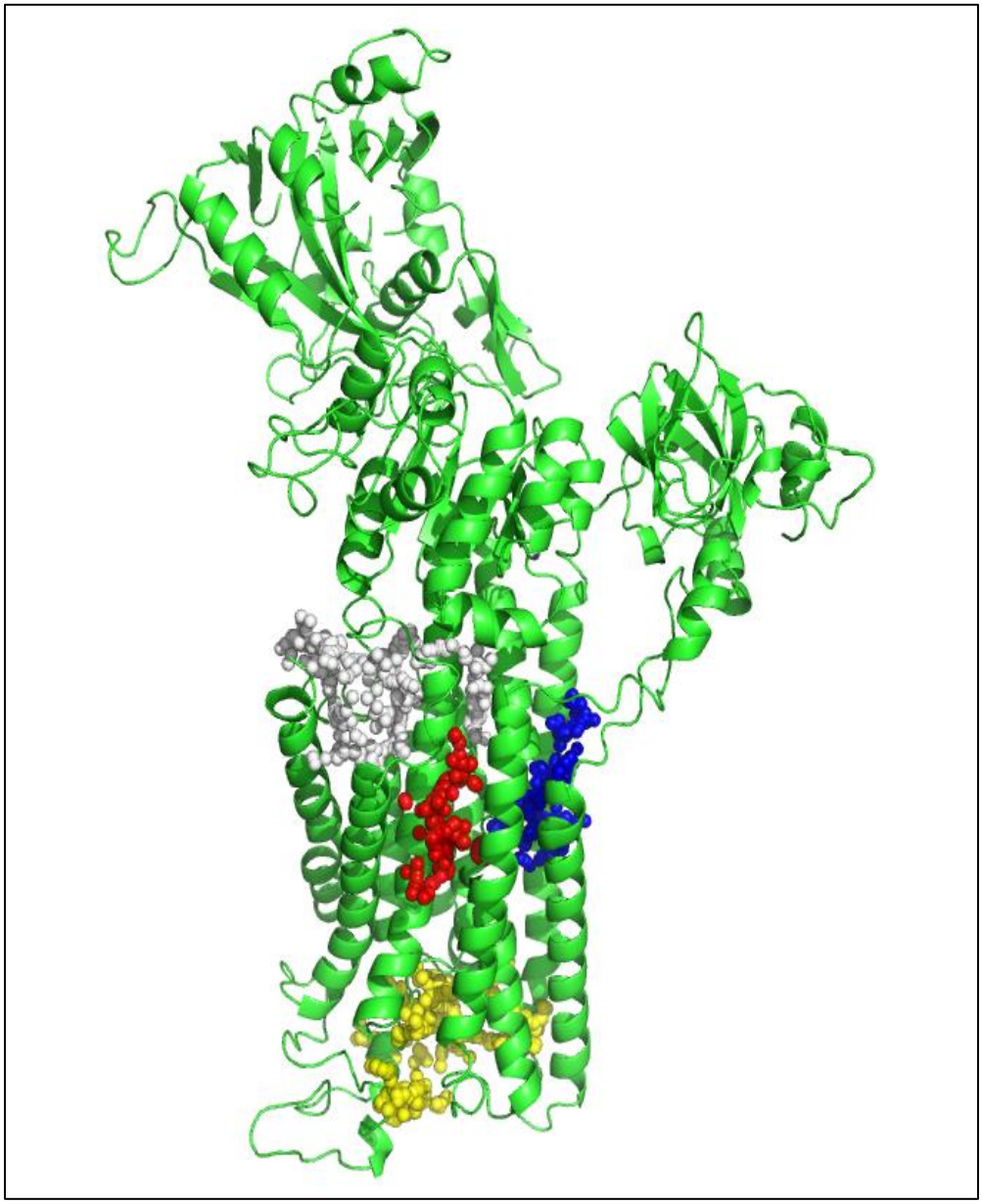

Figure 3.19: These are the four pockets that AutoDock Vina found that are able to be artemisinin binding sites, shown as white, red, blue, and yellow spheres.

Two of the pockets have been explored previously, as the pocket indicated by the red spheres is the thapsigargin binding pocket, and the pocket indicated by the blue spheres is the cyclopiazonic acid (CPA), another mammalian SERCA inhibitor, binding pocket. However, two of the pockets, indicated by the white and yellow spheres, have not been examined before, so these were the pockets that we decided to explore further. Upon examination, it was discovered that both of these new sites have an accessible cysteine residue present, and we found that to be quite promising.

3.5 ION PREDICTION AND MODELING

Approximately one-third of all proteins bind at least one metal ion, and many different metal ion binding proteins are found in humans. The structure of a protein determines its function and interactions with other biomolecules. Metal ions function in stabilizing the protein, inducing conformational changes upon binding, and may even participate in catalysis. Hence, identifying metal ion binding sites is the key to understanding the functional mechanisms of metal ion binding proteins.[65]

Metal ion binding proteins are identified and characterized experimentally by numerous processes such as nuclear magnetic resonance spectroscopy, gel electrophoresis, metal affinity column chromatography, electrophoretic mobility shift assay, absorbance spectroscopy, and mass spectroscopy. These techniques require complex steps, special equipment, and are unsuitable for unknown targets. Therefore, other means of detecting metal ion binding sites are in high demand, and computational methods can offer some assistance to meet this demand.[65]

Generally, the part of the protein that interacts with substrates, ligands, or other proteins are well conserved and are in close spatial proximity to each other although they may be far apart

in the sequence. These residues usually make up approximately 10 to 30% of a protein sequence. Cysteine, histidine, glutamate, and aspartate are the residues that most commonly bind metal ions because the atoms in their polar or charged side chains are able to coordinate the ion.[65]

The fragment transformation method combines sequence and structural information contained within spatially local fragments. Since the three-dimensional structure and residue type are often conserved, similar binding regions can be found by comparing the types of residues and their relative locations with those of computationally constructed metal ion binding residue templates. First, structures of known metal ion binding proteins were obtained from the Protein Data Bank. To be considered a metal ion binding protein, the protein must contain a polypeptide chain. If more than one polypeptide chain is present, then only chains that contain residues involved in metal ion binding were included. Also the length of the chain must be more than 50 residues. Next, these proteins were used to generate a template database. The residues that were considered to be template residues must be at least partially within 3 Å of the metal ion center. Also, a site needed to contain more than two metal ion binding residues in order to be considered as a template.[65]

Once the template has been completely constructed, the fragment transformation method aligns similar fragments that contain residues that are discontinuous in sequence but still spatially close. Each residue is treated as an individual unit, and the unit used to align the query protein and the templates is a triplet formed by the backbone N-Ca-C atoms of a given residue.[65]

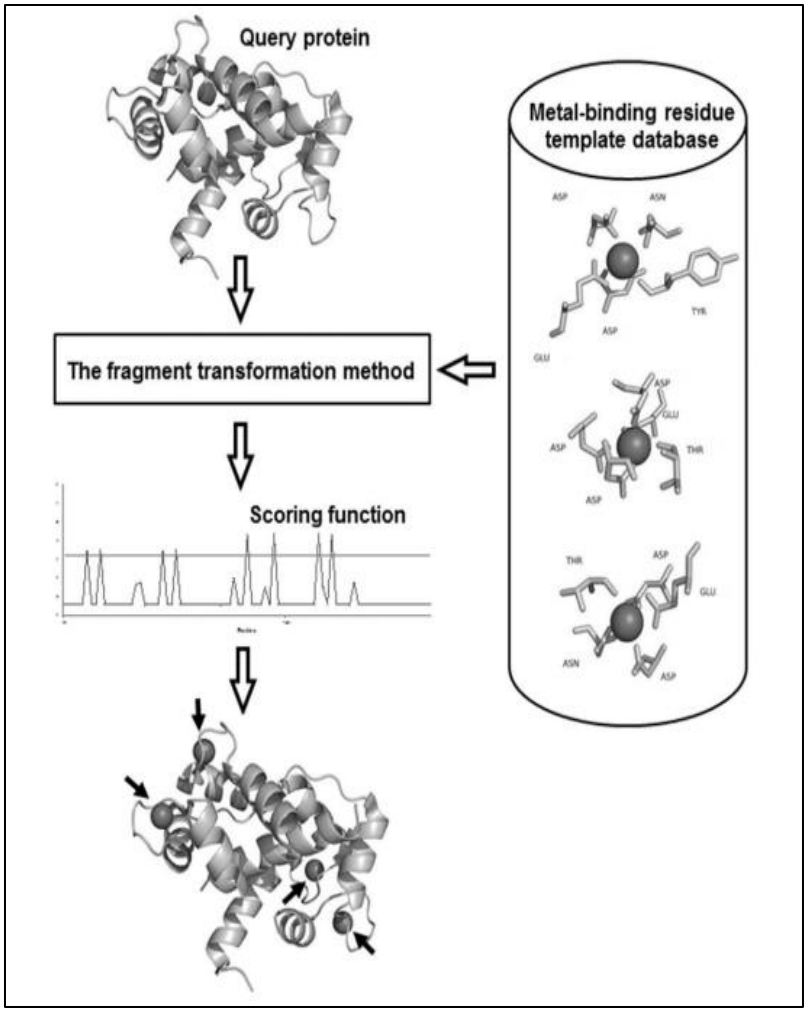

Figure 3.20: Schematic of the fragment transformation method for the prediction of metal ion binding sites in proteins. (Figure duplicated with permission from Dr. Chih-Hao Lu at China Medical University.)[65]

This method was able to outperform other methods and discovered that Ca^{2+} preferentially binds backbone oxygens of aspartate, glutamate, asparagine, and glycine; Cu^{2+} preferentially binds side chain oxygens and nitrogens of histidine; Mg^{2+} preferentially binds the side chain oxygens of aspartate and glutamate; Fe^{3+} preferentially binds the side chain oxygens, nitrogens, and sulfurs of histidine, glutamate, aspartate, cysteine, and tyrosine; Mn^{2+} preferentially binds side chain oxygens of aspartate, histidine, and glutamate; and Zn^{2+} preferentially binds side chain oxygens and nitrogens of cysteine and histidine. The method was

also able to predict Ca^{2+} binding sites with 94.1% accuracy, Cu^{2+} binding sites with 94.9% accuracy, Fe^{3+} binding sites with 94.9% accuracy, Mg^{2+} binding sites with 94.6% accuracy, Mn^{2+} binding sites with 95% accuracy, and Zn^{2+} binding sites with 94.8% accuracy. This averages to 94.6% accuracy overall.[65]

These are the results after our homology model of PfATP6 was submitted for metal ion binding prediction via the fragment transformation method:

Table 3.1: Residues in PfATP6 that are able to bind Fe^{2+}. The residues and their Fe^{2+} binding scores are listed in the table. A residue with a score greater than 1.9 is predicted as being an Fe^{2+} binding residue.

Residue Number	Residue Type	Fe Predicted Score	Fe^{2+} Positive
9	HIS	3.12862	3.12862
31	GLU	4.19643	4.19643
34	ASP	4.19643	4.19643
44	GLU	2.1846	2.1846
55	GLU	3.79203	3.79203
85	LYS	2.38	2.38
86	HIS	5.57443	5.57443
90	GLU	5.57443	5.57443
93	ASP	2.80675	2.80675
96	GLU	2.80675	2.80675
115	GLU	3.79203	3.79203
129	GLN	2.1846	2.1846
199	GLU	3.12862	3.12862
200	ASP	3.12862	3.12862
204	ASN	2.26405	2.26405
237	GLU	4.80251	4.80251
240	HIS	4.80251	4.80251
252	ASP	2.26257	2.26257
254	GLN	2.26257	2.26257
289	ASP	1.99473	1.99473
348	THR	2.00946	2.00946
351	CYS	2.00946	2.00946
358	ASP	2.29645	2.29645

380	ASP	3.00557	3.00557
383	THR	2.61077	2.61077
386	GLN	1.97509	1.97509
388	CYS	2.61077	2.61077
389	GLN	3.00557	3.00557
392	ASP	4.989	4.989
395	TYR	4.989	4.989
429	ASP	5.18091	5.18091
479	GLU	5.18091	5.18091
514	CYS	3.46772	3.46772
518	CYS	3.83556	3.83556
520	GLU	3.14781	3.14781
687	GLN	3.14781	3.14781
696	GLU	3.01132	3.01132
697	ARG	3.01132	3.01132
702	VAL	3.46772	3.46772
714	TYR	3.12309	3.12309
715	CYS	3.83556	3.83556
729	TYR	4.989	4.989
734	ASP	2.14142	2.14142
739	ASN	4.989	4.989
747	HIS	3.49934	3.49934
751	GLN	3.49934	3.49934
769	SER	3.12309	3.12309
781	TYR	3.01132	3.01132
782	TYR	3.12309	3.12309
846	ASP	3.69845	3.69845
847	GLU	3.69845	3.69845
849	ASP	3.69845	3.69845
852	THR	2.2741	2.2741
873	GLU	5.30663	5.30663
877	HIS	5.30663	5.30663
881	ASN	2.2741	2.2741
891	GLU	2.29645	2.29645
997	ASP	1.99473	1.99473
1003	GLN	3.82936	3.82936
1025	GLU	2.59582	2.59582
1026	HIS	3.15869	3.15869
1034	ARG	2.23251	2.23251
1035	HIS	4.04348	4.04348
1038	ASP	4.04348	4.04348

1082	PHE	3.89074	3.89074
1083	TYR	3.89074	3.89074
1087	HIS	3.65093	3.65093
1090	GLN	3.65093	3.65093
1103	TYR	3.65093	3.65093
1108	ASP	1.95727	1.95727
1109	HIS	1.95727	1.95727
1144	ASN	2.59582	2.59582
1148	GLU	3.15869	3.15869
1168	HIS	3.82936	3.82936
1210	PHE	5.42567	5.42567
1211	TYR	5.42567	5.42567

We were not interested in every iron binding site in the protein, however. We were only interested in the residues that are in the two unexplored pockets that AutoDock Vina found to be artemisinin binding pockets and that were in close vicinity to the pocket's cysteine residue. Those residues are Lys85, His86, Glu1025, His1026, His1035, and Asn1144.

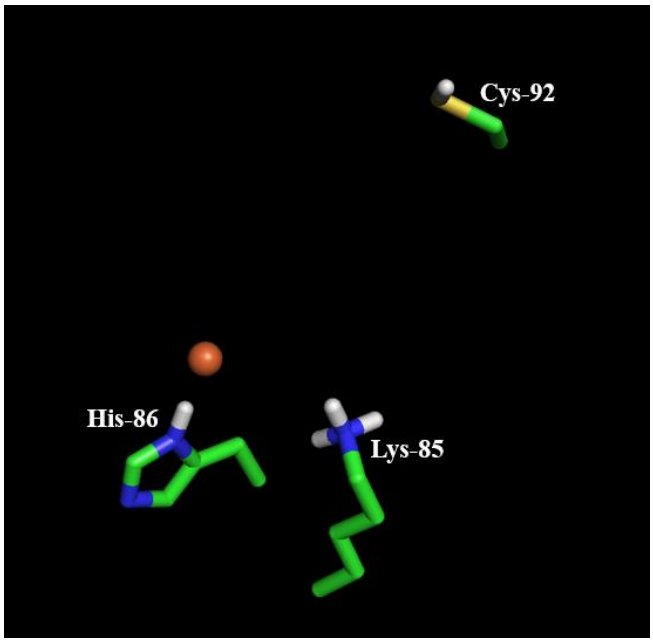

Figure 3.21: Fe^{2+} modeled into PfATP6 in the Cys-92 site using the fragment transformation method. Fe^{2+} is shown as an orange sphere, Cys-92 and the Fe^{2+}-binding residues, Lys-85 and His-86, are also shown.

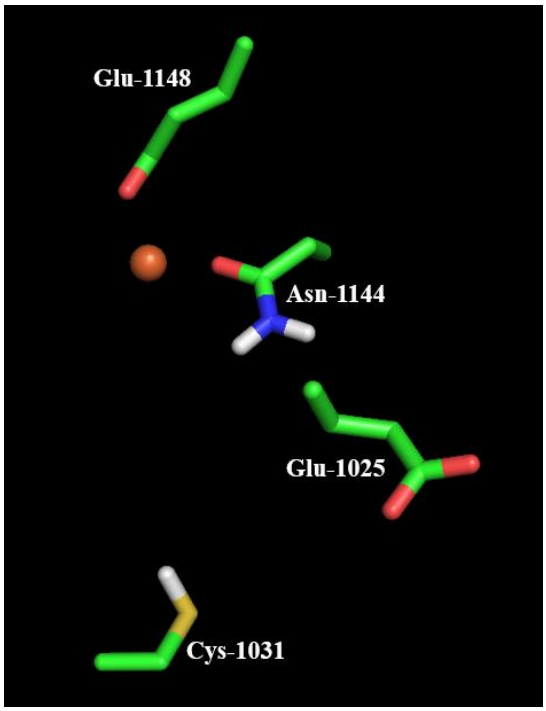

Figure 3.22: Fe^{2+} modeled into PfATP6 in the Cys-1031 site using the fragment transformation method. Fe^{2+} is shown as an orange sphere, Cys-1031 and the Fe^{2+}-binding residues, Glu-1025, Asn-1144 and Glu-1148, are also shown.

It can be clearly observed from **Figures 3.21** and **3.22** that the modeled iron atom is very far away (>10 Å) from the all-important cysteine residue in the pocket in both cases. In these regions of the protein, the residues are located on loops which are highly flexible, so to get the cysteine residues closer to the iron atom, we performed a loop refinement. We used the Prime module of Schrödinger and selected the protein refinement option. We then chose the refine loops option. The loop containing residues 83-95 for the Cys92 site and the loops containing residues 1018-1042 and 1139-1154 were selected for the Cys1031 site. Ultra-extended serial loop sampling was selected and constraints were chosen. For the Cys92 site: the sulfur atom of Cys92 was constrained to 3 Å away from the iron atom with a force constant of 350 [all force constants are given in units of kcal / (mol $Å^2$)]; the delta nitrogen of His86 was constrained to 3

Å away from the iron atom with a force constant of 350; and the zeta nitrogen of Lys85 was constrained to 3 Å away from the iron atom with a force constant of 200. Default options were chosen for the rest. For the Cys1031 site: the sulfur atom of Cys1031 was constrained to 3 Å from the iron atom with a force constant of 100; the epsilon oxygen of Glu1025 was constrained to be 3 Å from the iron atom with a force constant of 100; the epsilon oxygen of Asn1144 was constrained to be 3 Å from the iron atom with a force constant of 250; and the delta oxygen of Glu1148 was constrained to be 3 Å from the iron atom with a force constant of 350. Default options were chosen for the rest. This procedure resulted in a better position of the cysteine residues.

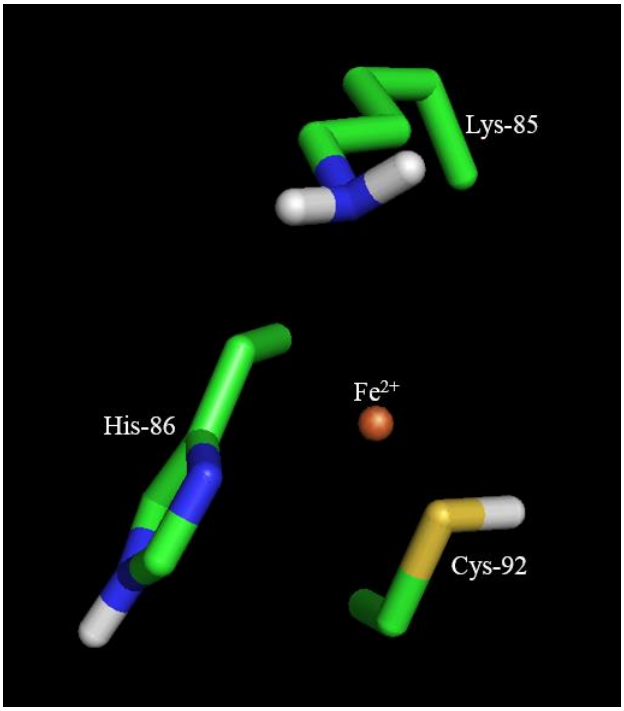

Figure 3.23: Cys-92 site results after loop refinement.

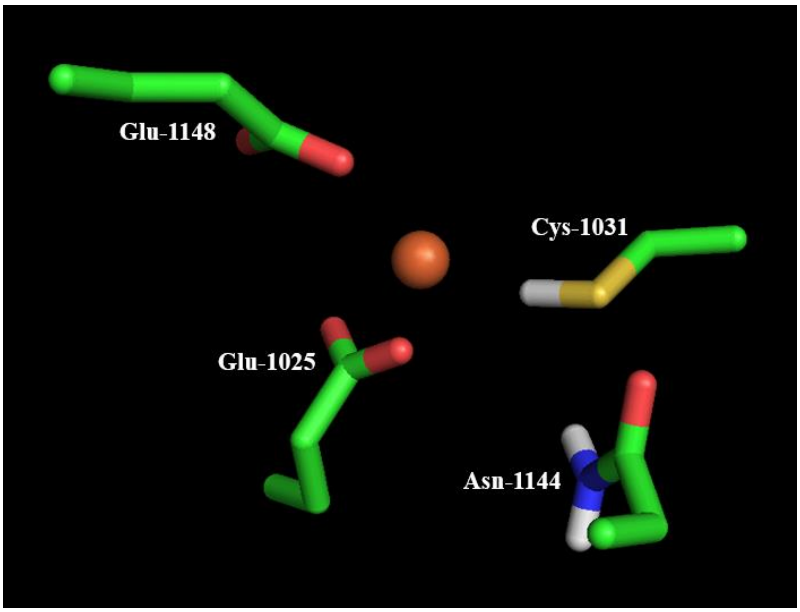

Figure 3.24: Cys-1031 site results after loop refinement.

3.6 PRE-TRANSITION STATE CALCULATION

Yikang Wu *et. al.* found that artemisinin is fully degraded by cysteine very rapidly *in vivo*. However, artemisinin is fully consumed instantly in the presence of one equivalent each of cysteine and $FeSO_4$. This demonstrated the importance of the iron activation of cysteine.[58] It was important to find the optimum geometry, or pre-transition state, that should occur between the Fe^{2+}, artemisinin, and the cysteine residue in order for our proposed reaction to occur. *Ab initio* quantum mechanics calculations were then utilized to determine the pre-transition state of our complex for our reaction.

Ab initio is a Latin term that means "from the beginning". In science, a calculation is *ab initio*, or from first principles, if it is based on established and basic laws of nature without making any assumptions.[66] To find our pre-transition state, the Jaguar[62] 8.4 *ab initio* and simulations module of the Schrödinger suite was utilized. The density functional theory hybrid

functional B3LYP and the 6-31G basis set with polarized and diffuse functions that are parameterized for transition metals (6-31G™*+) was used. Before the quantum mechanics calculations could be commenced, however, we first needed a model system. To generate a model, artemisinin was docked into the two sites using the Glide module of the Schrödinger suite and a ferrous ion was placed nearby. During the docking procedure, artemisinin was allowed to vary its conformation, but the protein was kept rigid. Since the protein naturally undergoes certain conformational changes to accommodate the docked ligand, we altered the cysteine residues in the sites so that the sulfurs would be closer to the O1 oxygen of artemisinin's peroxide bridge. Having the artemisinin accommodated in the geometry that we believe could be the starting point of our reaction but having produced some extra steric clashes from rotamer modifications, we performed side chain refinement of the rotamers using the default settings of the Prime module of the Schrödinger suite. Subsequently, we performed a constrained minimization of the whole complex while setting three constraints: the distance between the oxygen of the water molecule and iron, the distance between O1 of artemisinin and the iron atom, and the distance between the cysteine sulfurs and the iron atom were all set to 3±1 Å. Having all the parameters for our model systems, we removed the protein and continued the calculations on just the model system. Instead of using the entire cysteine residue, a methyl group replaced the beta carbon on the cysteines and hydrogen atoms were added to have methylthiol instead, and instead of simply a ferrous ion, we used ferrous chloride. The structure was then minimized using the quantum mechanical method DFT B3LYP with the 6-31G™*+ basis set in vacuo. The geometry of the pre-transition state can be seen in **Figure 3.25**. The end product of the proposed complex reaction was built by the modification of artemisinin and can be viewed in **Figure 3.26**.

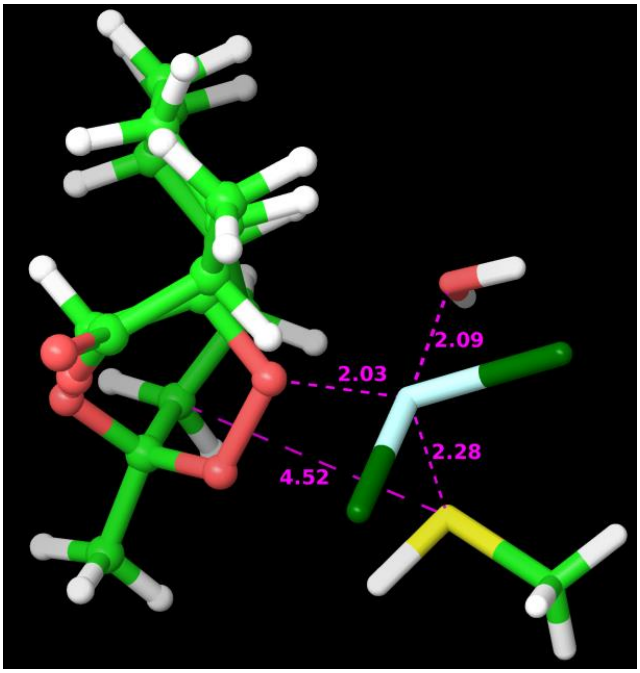

Figure 3.25: Geometry of the pre-transition state calculated by Prime. Carbons are shown in green, oxygens in red, hydrogens in white, sulfur in yellow, iron in light blue, and chlorines in dark green. The distances between the atoms (in Å) are shown in magenta.

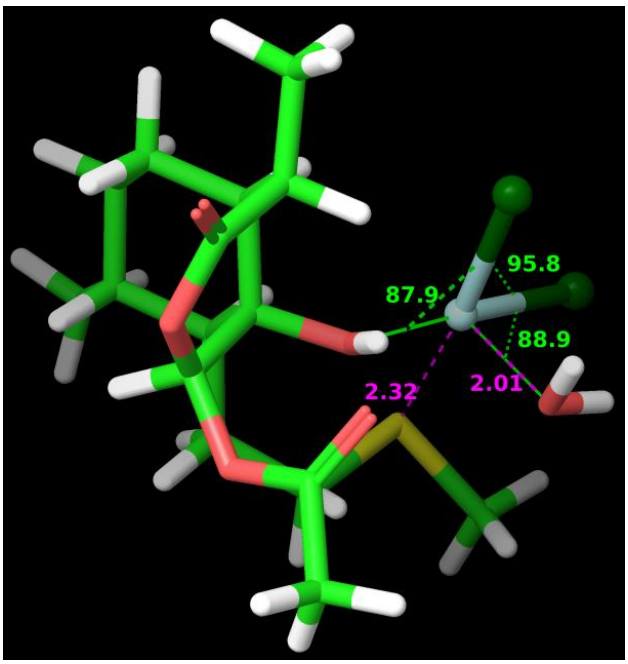

Figure 3.26: End product of the proposed complex reaction. Carbons are shown in green, oxygens in red, hydrogens in white, sulfur in yellow, iron in light blue, and chlorines in dark green. The distances between the atoms (in Å) can be seen in magenta, and the angles (in °) are shown in green.

3.7 GLIDE DOCKING AND INDUCED FIT DOCKING

Molecular docking is a method that is used to predict the preferred orientation of one molecule relative to another when bound to each other in a stable complex. It is frequently used to predict the binding orientation of small molecule drug candidates to their protein targets in order to predict their binding affinity and activity.[67]

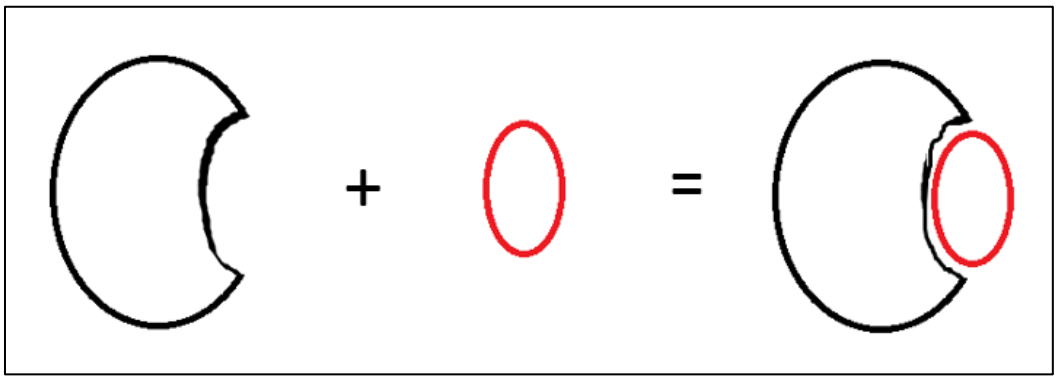

Figure 3.27: Schematic diagram illustrating the docking of a small molecule ligand (red) to a protein receptor (black) to produce a complex.

We used both Glide standard precision docking, which assumes a rigid protein, and Induced Fit Docking, which takes into account that many receptors alter their binding site to conform to the shape and binding mode of the ligand. Both were used to determine which program would produce the pre-transition state that was calculated previously. For the site containing Cys-92, Induced Fit Docking was able to produce the desired pre-transition state geometry better than Glide docking. The pre-transition state for the residues in the site containing Cys-1031 was somewhat more difficult to retrieve. Glide docking and Induced Fit Docking failed to give us an appropriate pose. We therefore used the best output that was retrieved from Induced Fit Docking and used an appropriate, low energy rotamer of Cys-1031. The requirements for our proposed active site were thus fulfilled. We then chose to perform a

protein-ligand complex refinement using Prime. The Refine Protein-Ligand Complex option was selected, and we chose to refine the atoms within 10 Å of the ligand using Monte Carlo minimization. Then we constrained the distances between iron and O1 of artemisinin and between C4 of artemisinin and the sulfur of Cys-1031 to be 2.5 Å, both with a force constant of 350. This procedure resulted in the retrieval of the pre-transition state that we sought.

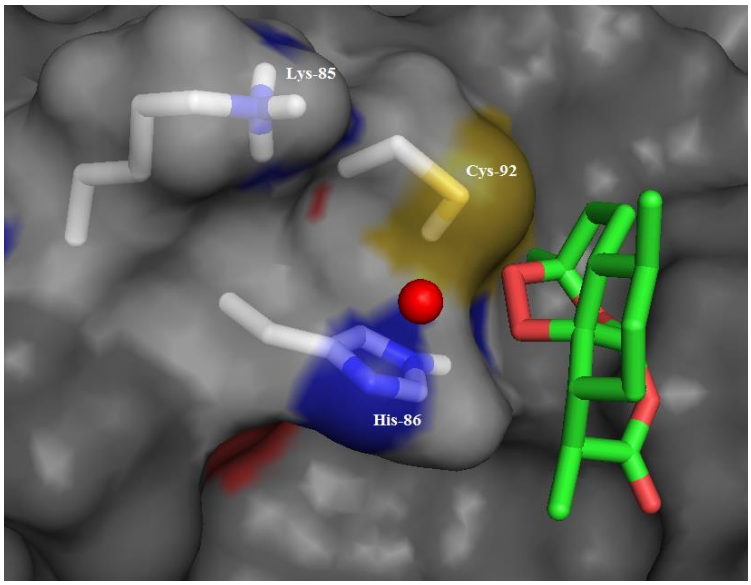

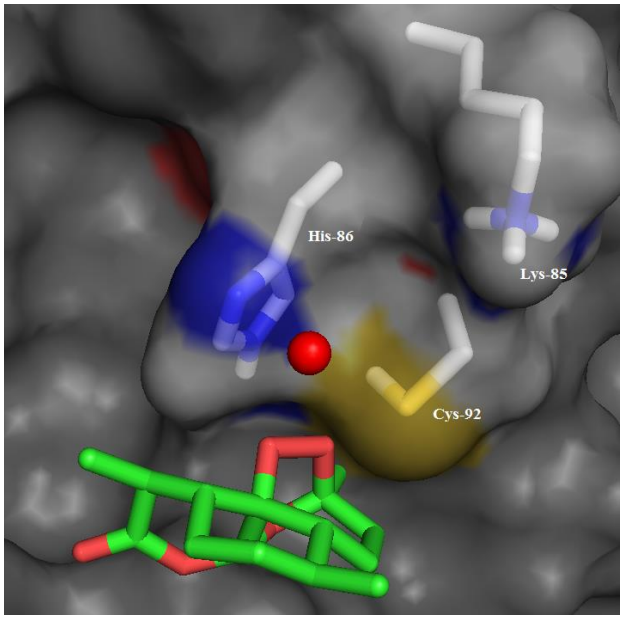

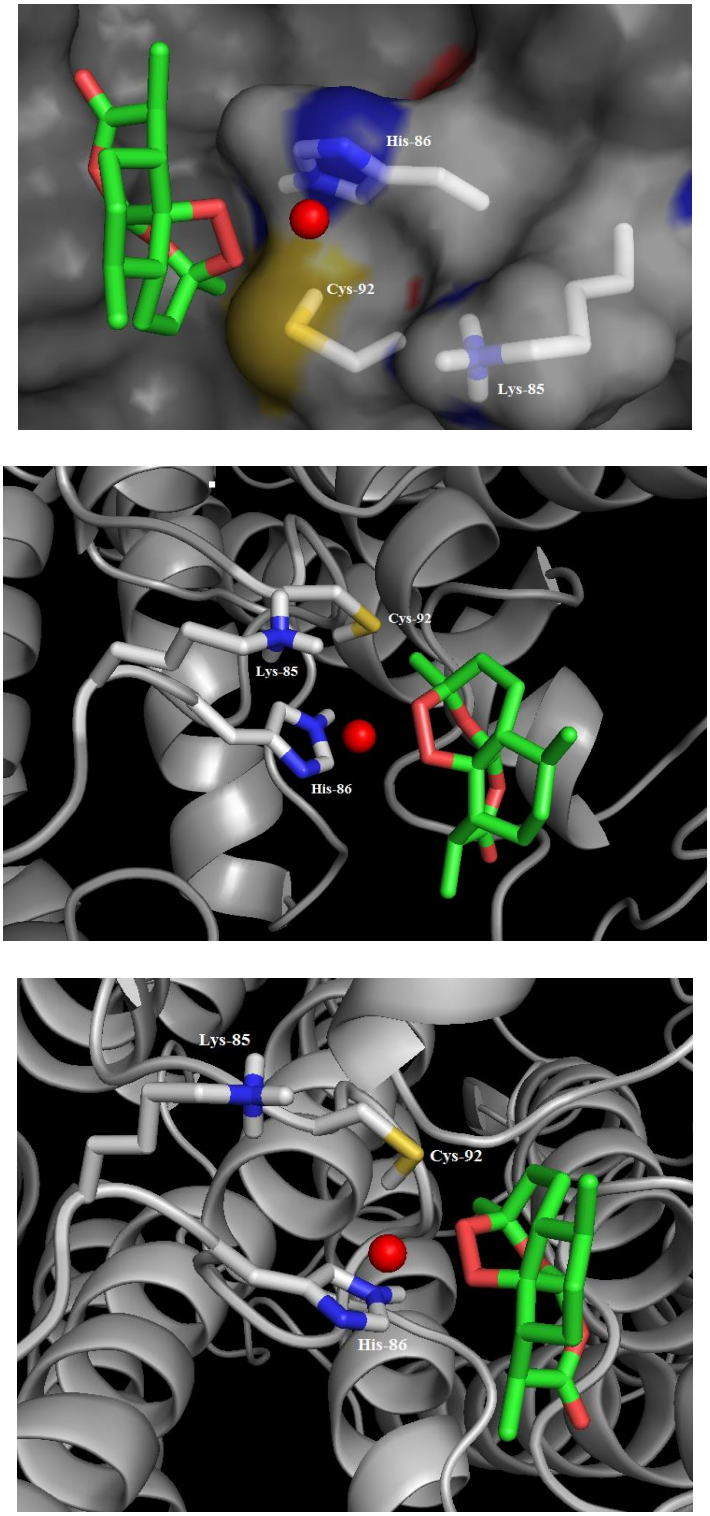

Figure 3.28: Different views of the docked pose of artemisinin in Cys-92 site. The coordinating residues, Lys-85 and His-86, are shown a close distance from the iron atom which, in turn, is in close proximity to the peroxide bridge of artemisinin. Cys-92 is also seen to be only a few Å away from C4 of artemisinin, which is the optimal location to intercept the carbon radical.

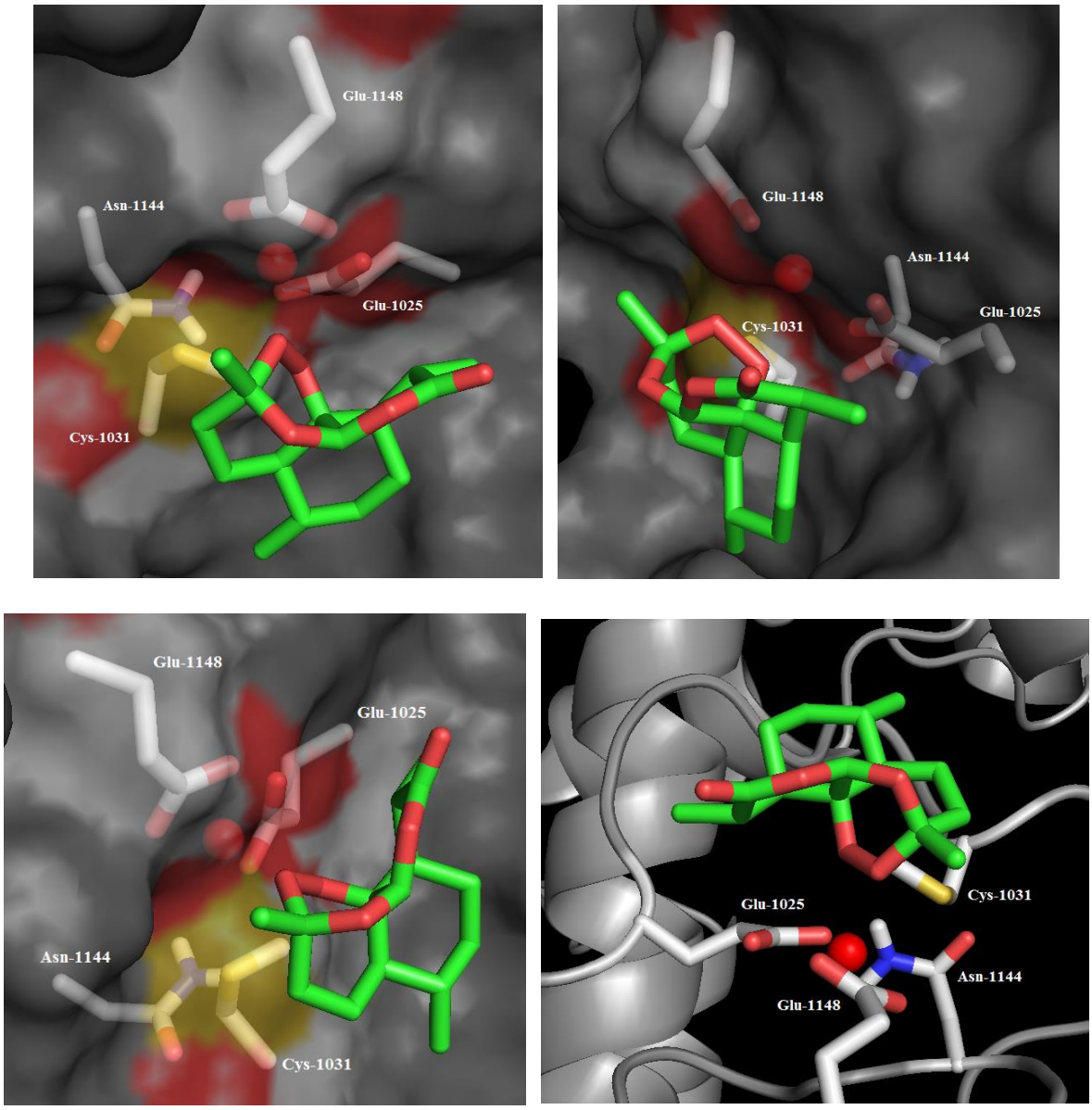
Glu-1148
Asn-1144
Glu-1025
Cys-1031
Glu-1148
Asn-1144
Glu-1025
Cys-1031
Glu-1148
Glu-1025
Asn-1144
Cys-1031
Cys-1031
Glu-1025
Asn-1144
Glu-1148

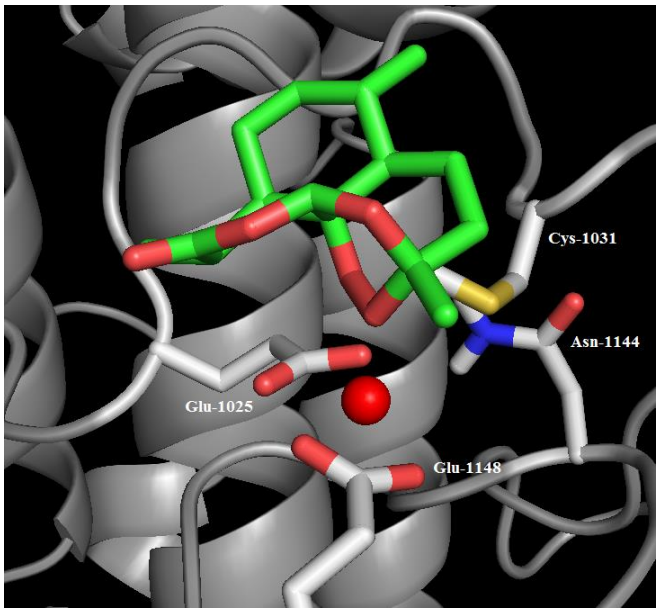

Figure 3.29: Different views of the docked pose of artemisinin in Cys-1031 site. The coordinating residues, Glu-1025, Asn-1144, and Glu-1148, are shown a close distance from the iron atom which, in turn, is in close proximity to the peroxide bridge of artemisinin. Cys-92 is also seen to be only a few Å away from C4 of artemisinin, which is the optimal location to intercept the carbon radical.

After receiving favorable results thus far, we enlisted the assistance of Dr. Sanjeev Krishna to perform PfATP6 enzyme-specific assays. Our results were shared with him, and he agreed to perform an experimental mutagenesis of residues in our two sites, and then assay artemisinin against the mutants to determine if variations at these sites will alter the inhibitory activity of artemisinin.

3.8 "MALARIA BOX"

In 2011, the Medicines for Malaria Venture (MMV) formed the Malaria Box project. Extensive high-throughput screenings of millions of proprietary and publicly-available compounds have led to the discovery of thousands of compounds with confirmed antimalarial activity. Structures and descriptions of these compounds are publicly available. Researchers who are part of the MMV analyzed over four million compounds that they acquired from companies

such as GlaxoSmithKline and Novartis, and St. Jude Children's Hospital. The program works by mailing interested researchers a complete box-set of malaria tools, free of charge. The kit contains over 400 antimalarial compounds in quantities large enough to run approximately 10 assays. The only stipulation to receiving the box is that receivers must promise to release any and all research findings within two years.[68, 69]

Dr. Sanjeev Krishna, a collaborator at St. George's University of London, has received the malaria box compounds and assayed the compounds against PfATP6. Of the 400 compounds, 4 were found to be PfATP6 inhibitors. However, the binding site and mechanism of action for these compounds are unknown. As a starting point, we decided to first find out where in PfATP6 the compounds bind. Using the same procedure that we used to find alternative artemisinin binding sites, we proceeded to do blind docking studies for each of the compounds.

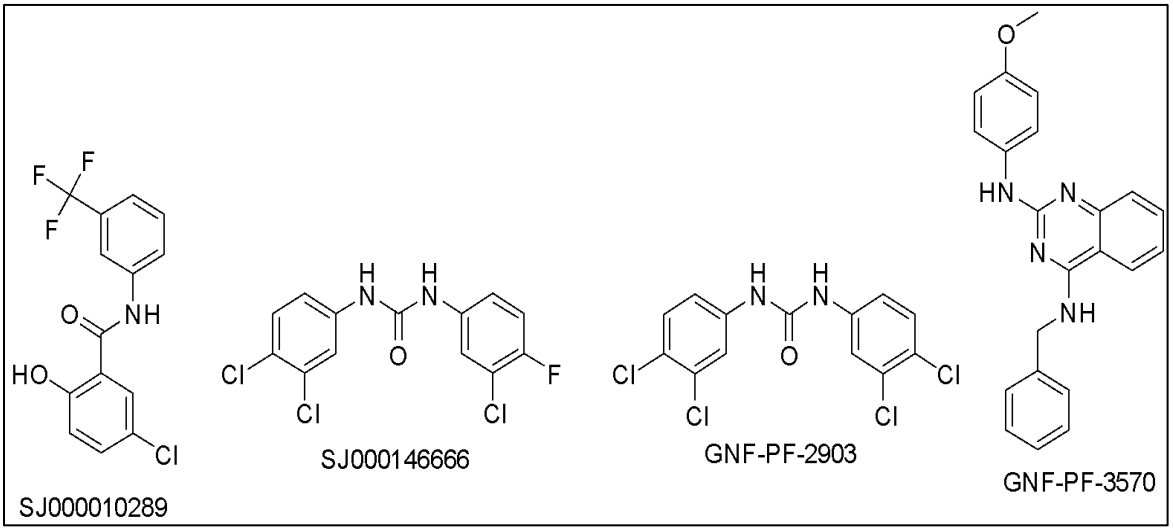

Figure 3.30: The structures and codes for the four malaria box compounds.

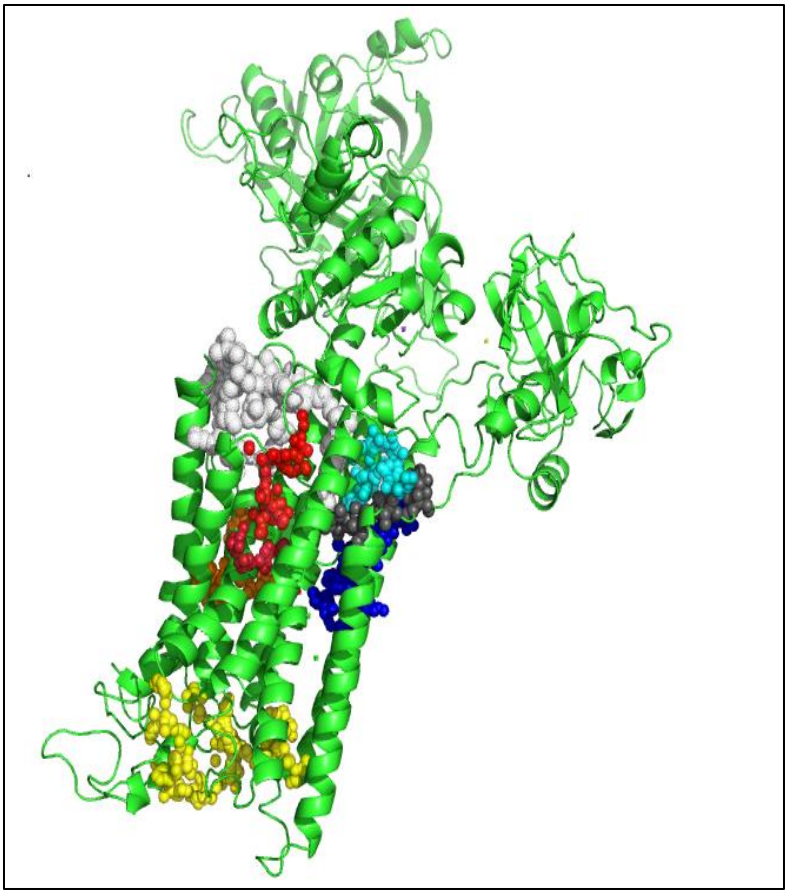

Figure 3.31: AutoDock Vina results showing the pockets able to bind the four malaria box compounds.

Using AutoDock Vina, we found approximately six pockets that are capable of binding the malaria box compounds. Opportunely, two of the malaria box binding pockets are our two unexplored artemisinin binding sites. The residues in these pockets were listed and sent to Dr. Krishna. Mutagenesis studies will commence on these residues and the compounds will be assayed again to find out if any of the mutations caused a decrease in the antimalarial activity of any of the compounds.

3.9 IN SILICO MUTAGENESIS

Mutagenesis is the term given to the procedure used to change the genetic information of an organism. This can happen spontaneously in nature, from exposure to mutagens, or experimentally.[70] Site-directed mutagenesis is a technique that is used to make specific and intentional changes to genes and it can be used to explore the biological activity of proteins.[71] It is a potent research tool used to study protein function, identify enzyme active sites, and design novel proteins in drug discovery.[72]

There are numerous approaches to perform site-directed mutagenesis. While these experimental methods are more reliable, they are more difficult than computational studies. Computational studies can add efficiency and speed to experimental methods by pre-filtering with *in silico* predictions of non-synonymous single nucleotide polymorphisms (nsSNP). Although it may never be accurate enough to completely replace wet-lab experiments, computational methods may help in selecting and prioritizing a small number of likely candidates from available data. Studies have shown a range of computational approaches that are capable of producing estimates of the functional effects of polymorphisms.[73]

In order to truly know if our two new sites are actual artemisinin binding sites, certain residues in the pockets will need to be mutated. The mutant protein will then be treated with artemisinin to determine if the mutations had any effect on the activity of artemisinin. To aid in our experimental mutagenesis, a program named SNAP (screening for non-acceptable polymorphisms) was utilized to find if the mutation of certain residues in our protein would affect its function. SNAP is a neural network-based method for the prediction of the functional effects of nsSNPs. Sequence information is the only needed input. In a cross-validation test on

over 80,000 mutants, SNAP was able to identify 80% of the non-neutral (functionally-distinct) substitutions with 77% accuracy and 76% of the neutral substitutions with 80% accuracy. This was a marked improvement over existing methods. More importantly, SNAP introduced a well-calibrated measure for the reliability of each prediction.[73]

Experimental mutagenesis studies have previously been performed on PfATP6. This study demonstrated that if Leu263 is mutated to E263, the protein's function changes and artemisinin's activity on the protein decreases.[44] We wanted to find out if SNAP would classify this mutation as non-neutral. The sequence for PfATP6 was uploaded into the SNAP software and the L263E mutation was selected. The software was able to accurately classify this mutation as non-neutral with 58% predicted accuracy as shown in **Figure 3.32.** Another documented mutation, S769N, was reported as having no effect on PfATP6[74], so this mutation was selected in the SNAP software. SNAP found this mutation to be neutral with 92% predicted accuracy as seen in **Figure 3.33**. Based on these results, SNAP software may be a reliable source for predicting the effect of mutations in our protein.

#Query sequence: snapfasta
Including only predictions with:
RI >= 0
Expected Accuracy >= 50%

nsSNP	Prediction	Reliability Index	Expected Accuracy
L263E	Non-neutral	0	58%

Figure 3.32. SNAP prediction for the L263E mutation.

#Query sequence: snapfasta
Including only predictions with:
RI >= 0
Expected Accuracy >= 50%

nsSNP	Prediction	Reliability Index	Expected Accuracy
S769N	Neutral	6	92%

Figure 3.33: SNAP prediction for the S769N mutation.

As a starting point, we decided to use the cysteine residues in the pockets. We chose to mutate them to similar residues and see if the SNAP program would classify the mutation as being neutral or non-neutral. The mutations we chose were Cys-Asp, Cys-Asn, Cys-Ala, Cys-Val, and Cys-Ser.

Table 3.2: SNAP predictions for numerous mutations in PfATP6.

Original Residue	Mutated Residue	Result
Cys92	Asp92	Non-neutral
Cys92	Asn92	Non-neutral
Cys92	Ala92	Non-neutral
Cys92	Val92	Non-neutral
Cys92	Ser92	Non-neutral
Cys1031	Asp1031	Neutral
Cys1031	Asn1031	Neutral
Cys1031	Ala1031	Neutral
Cys1031	Val1031	Neutral
Cys1031	Ser1031	Neutral

From **Table 3.2**, it is predicted that any of these mutations occurring at Cys92 will cause a non-neutral change. This means that mutating Cys92 will change either the shape or the function of PfATP6. It is also worth noting that any of these mutations occurring at the Cys1031 position was predicted to be a neutral mutation meaning it will not cause a change in the shape or function of the protein. These results were given to our collaborator who will perform the experimental mutagenesis. The results of the experimental mutagenesis will not only prove or disprove our hypothesis, but it will either offer more evidence for the accuracy of SNAP or condemn its practicality.

To determine if our docking algorithm could also detect how the mutation of certain residues could alter the docking poses and scores and to test for any correlation between them, we mutated Cys92 and Cys1031 to the residues that we submitted to the SNAP program. The mutant proteins were then prepared and minimized, and receptor grids were generated for each. Artemisinin was then docked into each receptor to retrieve the best docking score for each mutant-artemisinin complex. **Table 3.3** shows the differences in the docking scores of artemisinin against the mutant proteins in comparison to the native protein.

Table 3.3: Docking scores of artemisinin against mutant PfATP6 proteins.

Residue	**Docking score**
Cys92	-4.045
Asp92	-4.016
Asn92	-3.215
Ala92	-3.811
Val92	-3.580
Ser92	-3.670
Cys1031	-4.380
Asp1031	-4.780
Asn1031	-4.740
Ala1031	-4.802
Val1031	-4.575
Ser1031	-4.786

According to the docking scores, all of the mutations at the Cys92 residue resulted in artemisinin binding poses with worse docking scores (more positive) as compared to the native

protein, and all of the mutations at the Cys1031 residue resulted in artemisinin binding poses with better docking scores (more negative) as compared to the native protein. So the SNAP program and the manual in silico mutagenesis/docking of artemisinin show an opposite trend in the two sites. Only the experimental mutagenesis will show which one was more accurate.

CHAPTER 4. STRUCTURE-BASED VIRTUAL SCREENING

***Shuneize E. Slater, Khaled M. Elokely, Kuldeep K. Roy, Manal A. Nael, Robert J. Doerksen, Mitchell A. Avery, Unpublished.**

4.1 INTRODUCTION

High throughput screening (HTS) involves the biological testing of large numbers of small molecules for a specific pharmaceutical effect. It is a major route toward discovering novel compounds. Advances in computational methods have allowed virtual screening to speed up modern drug discovery programs. Virtual screening, or *in silico* screening, is the selection of compounds by evaluating their desirability in a computational model. Since its debut over a decade ago, there has been a clear upward trend in publications on this particular subject area. The progress that has been made in this field has fostered its high acceptance in use, and it can be easily integrated in the drug discovery and development process. Virtual screening can be divided into two main categories: similarity- or ligand-based virtual screening (LBVS) and target- or structure-based virtual screening (SBVS).[75]

Ligand-based virtual screening relies on the assumption that structurally similar molecules will exhibit similar binding properties towards a target protein. It generally provides significant enrichment over the random selection of compounds and has been successfully applied for the identification of bioactive lead compounds for a wide range of drug targets. There is a diverse set of LBVS techniques such as small molecule alignment, 1D, 2D, and 3D descriptor-based screening, shape-based searching, pharmacophore-based searching, recursive partitioning, and graph-based similarity assessment.[76]

Structure-based virtual screening is used if structural information is available for a target. Quick SBVS algorithms are used to place the molecules inside the active site or a specified pocket of the biological target (docking), after which they are then ranked according to their calculated binding affinity estimations (scoring). There are currently a vast number of different

docking and scoring methodologies employed in the pharmaceutical industry. Most docking algorithms can be classified into four methods: force field-based, evolutionary, fragment-based incremental, and shape complementary-based methods. These provide approximations of the expected conformation and orientation of the ligands in the binding site. Protein flexibility and the importance of water molecules have also been incorporated into most docking schemes. Although a large amount of research has been undertaken in the generation of better docking algorithms and scoring functions, the discrimination of true binders from the decoys remains a challenge.[77]

4.2 PROCEDURE

To determine whether targeting our two new pockets will result in the discovery of novel PfATP6 inhibitors, we performed virtual screening into the pockets. All purchasable compounds were downloaded from the ZINC database. This was approximately 20 million compounds. Filter 2.1.1, a drug filter, was used to eliminate the compounds that do not follow Lipinski's rule of five and structures with metabolically vulnerable groups. This resulted in approximately 11 million compounds remaining. We then used OMEGA 2.4, a program from OpenEye Scientific that is able rapidly and effectively to generate conformers of large databases, to generate a maximum of 300 conformers per ligand within an energy window of 10 kcal/mol. These conformers were docked into the two sites using OpenEye Scientific software. The one thousand best scoring compounds were selected. Canvas from Schrödinger, which uses fingerprinting and substructure matching to screen millions of compounds in seconds, was used to select approximately fifty of the most diverse compounds from the set.

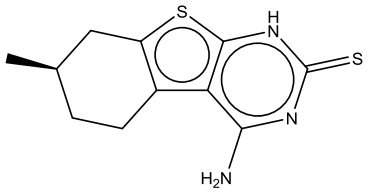

ZINC00506860

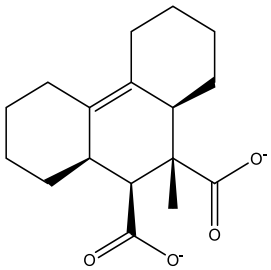

ZINC00192016

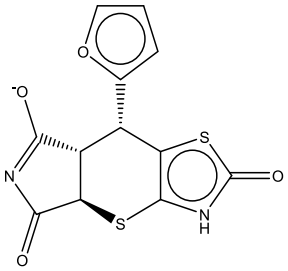

ZINC04337585

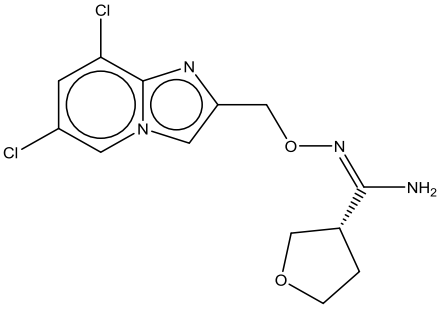

ZINC80290460

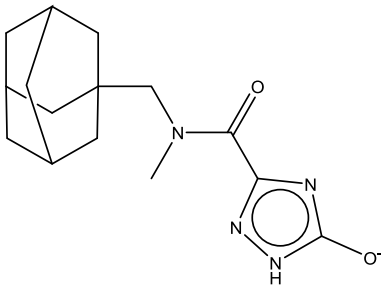

ZINC80212637

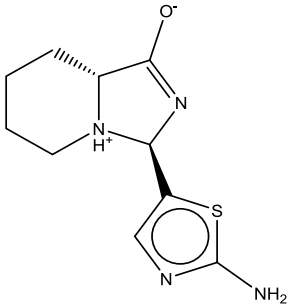

ZINC77506749

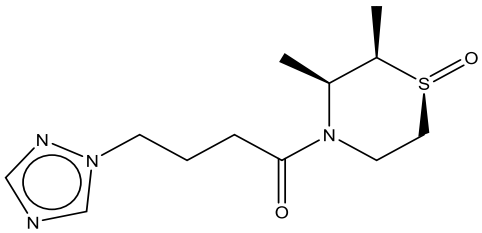

ZINC76658501

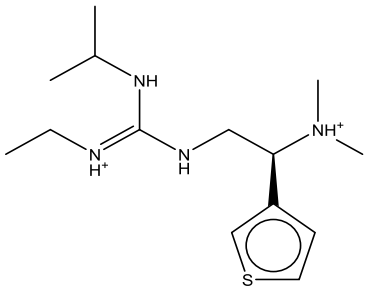

ZINC72623135

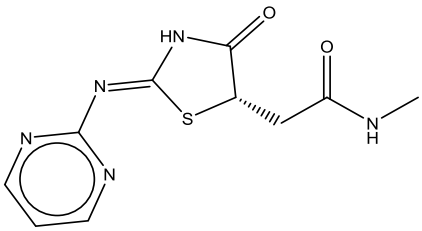

ZINC72435140

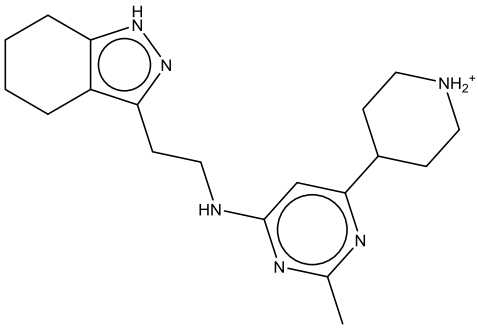

ZINC67867915

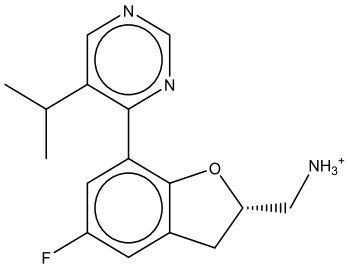

ZINC67786201

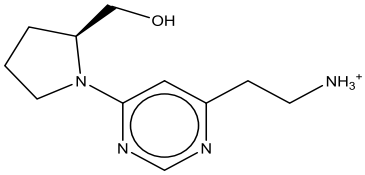

ZINC67688838

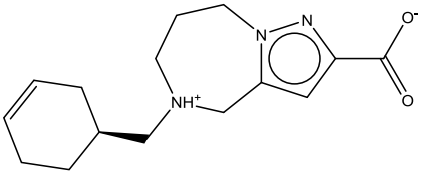

ZINC65375585

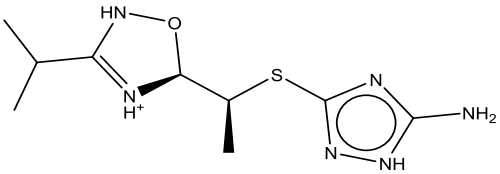

ZINC64025512

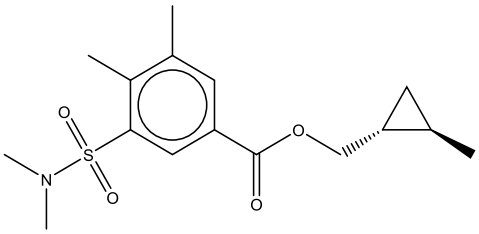

ZINC63846532

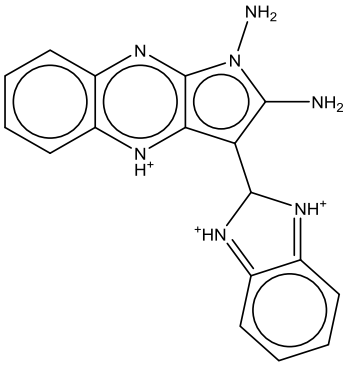

ZINC63388047

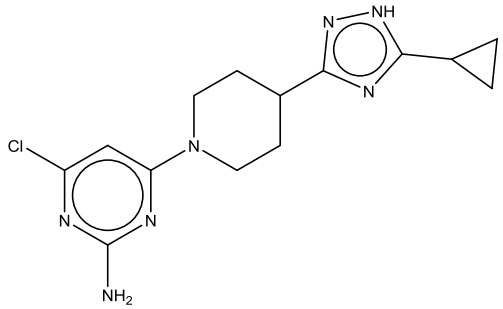

ZINC58218624

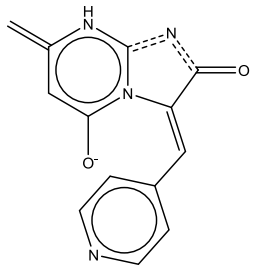

ZINC51331099

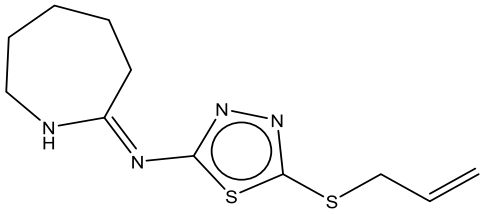

ZINC02659645

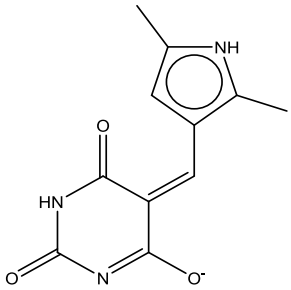

ZINC03002706

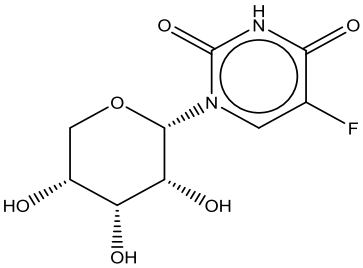

ZINC04127198

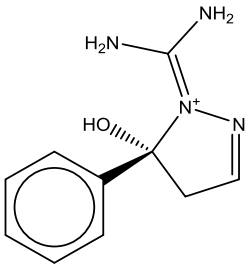

ZINC05604299

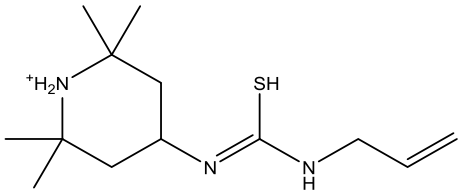

ZINC08683581

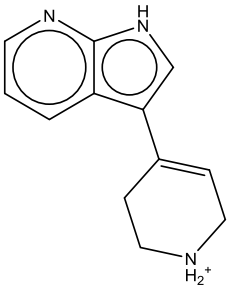

ZINC08780032

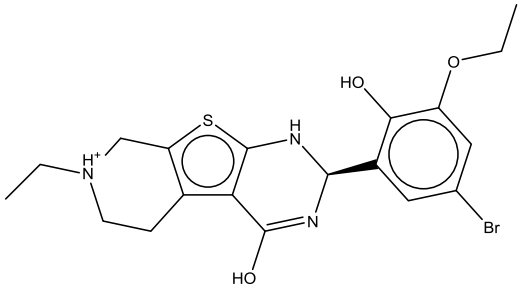

ZINC08928022

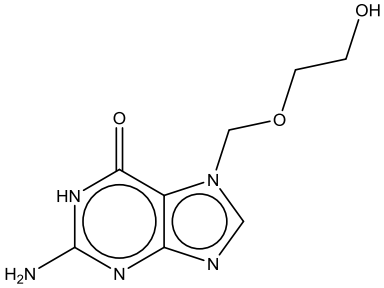

ZINC13831596

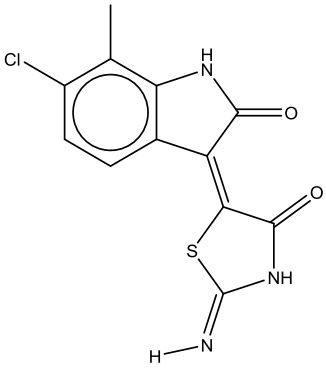

ZINC15018344

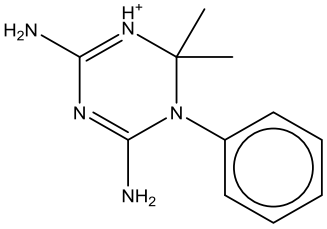

ZINC16981849

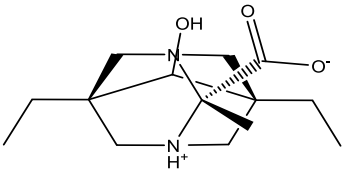

ZINC19331111

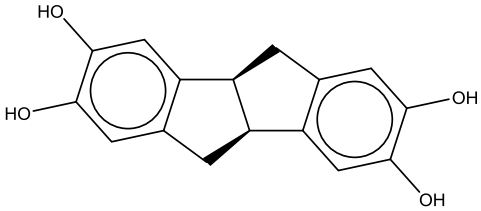

ZINC25500407

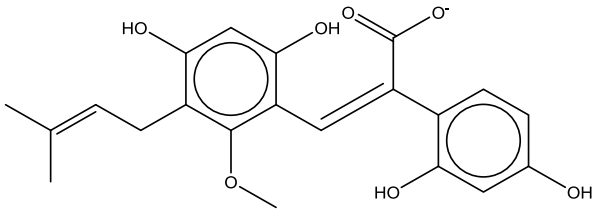

ZINC31169813

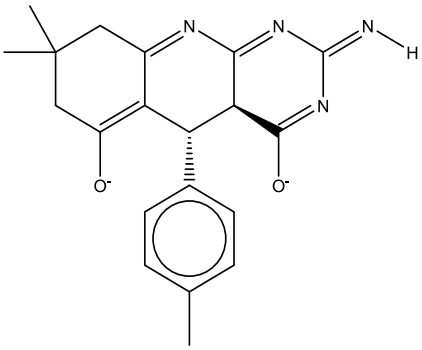

ZINC39001420

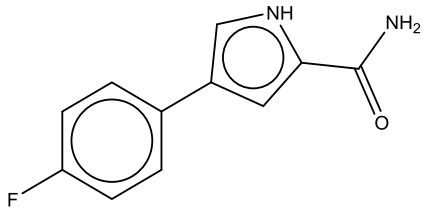

ZINC42384326

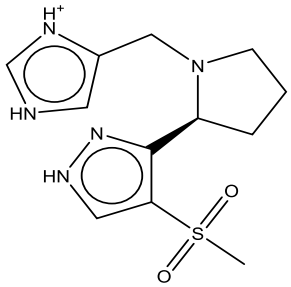

ZINC72388585

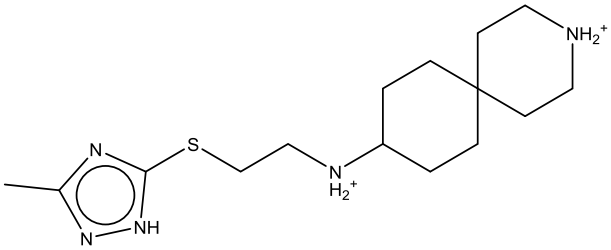

ZINC67757786

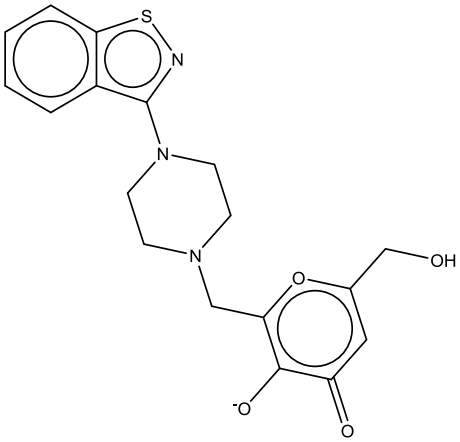

ZINC57160091

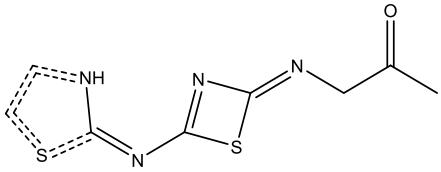

ZINC59349840

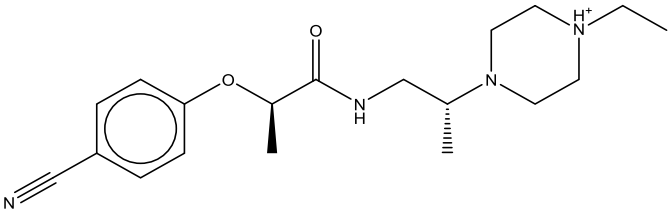

ZINC46947075

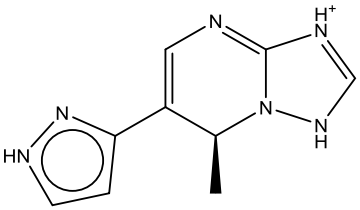

ZINC39605861

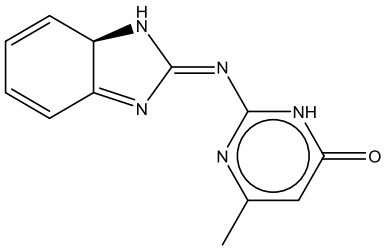

ZINC39446033

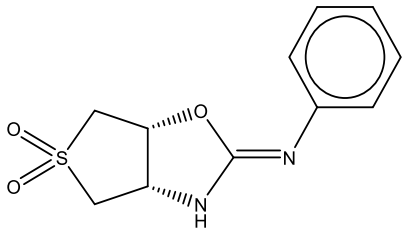

ZINC04742288

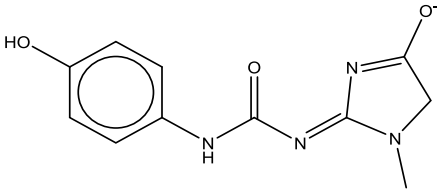

ZINC08133013

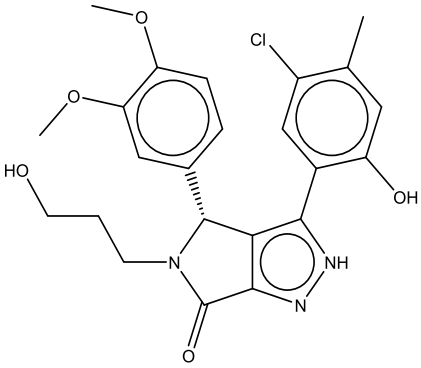

ZINC09124247

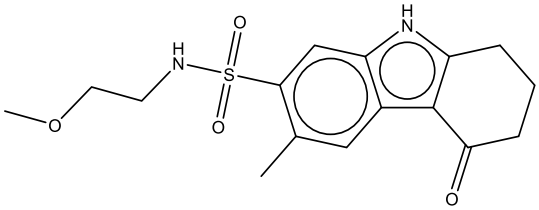

ZINC15733800

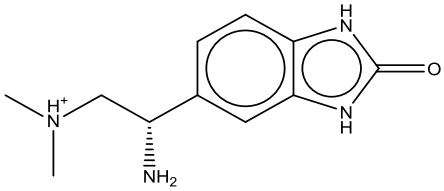

ZINC19821533

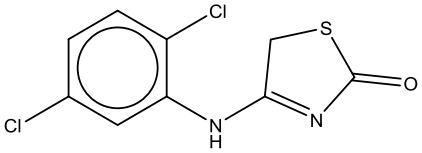

ZINC20391478

Figure 4.1: The 46 most diverse compounds from the virtual screening. The 18 remaining after visual inspection and determination of commercial availability are shown in red.

The 46 diverse compounds were then visually inspected for ionization issues and problematic functional groups. Other than the docking scores and poses, selection was also based

on a combination of the number of good interactions, the general match of hydrophobic or hydrophilic space, logP, and the potential for metabolism. This resulted in twenty-five compounds remaining. Of these 25, seven were not commercially available at the time. A quote was requested and a price list was obtained from Ambinter. These eighteen compounds, or a subset thereof, will be purchased and tested for both their antimalarial activity and their PfATP6 inhibitory activity.

Table 4.1: The clogP values and docking scores for the eighteen compounds chosen for antimalarial assay and PfATP6 inhibition.

COMPOUND	clogP	DOCKING SCORE
ZINC00506860	0.935	-11.922
ZINC00192016	-2.1446	-11.462
ZINC67867915	2.7312	-11.547
ZINC67786201	2.4537	-11.971
ZINC58218624	1.4802	-12.099
ZINC02659645	2.482	-11.408
ZINC03002706	-0.297	-11.534
ZINC04127198	-1.8566	-12.008
ZINC08780032	1.726	-11.495
ZINC13831596	-2.4224	-11.563
ZINC15018344	1.3826	-11.582
ZINC16981849	1.247	-11.401
ZINC19331111	1.4276	-11.405
ZINC31169813	-0.8467	-11.500
ZINC67757786	3.0399	-12.789
ZINC57160091	-2.670	-13.757
ZINC09124247	3.1904	-11.71
ZINC15733800	2.2095	-11.404

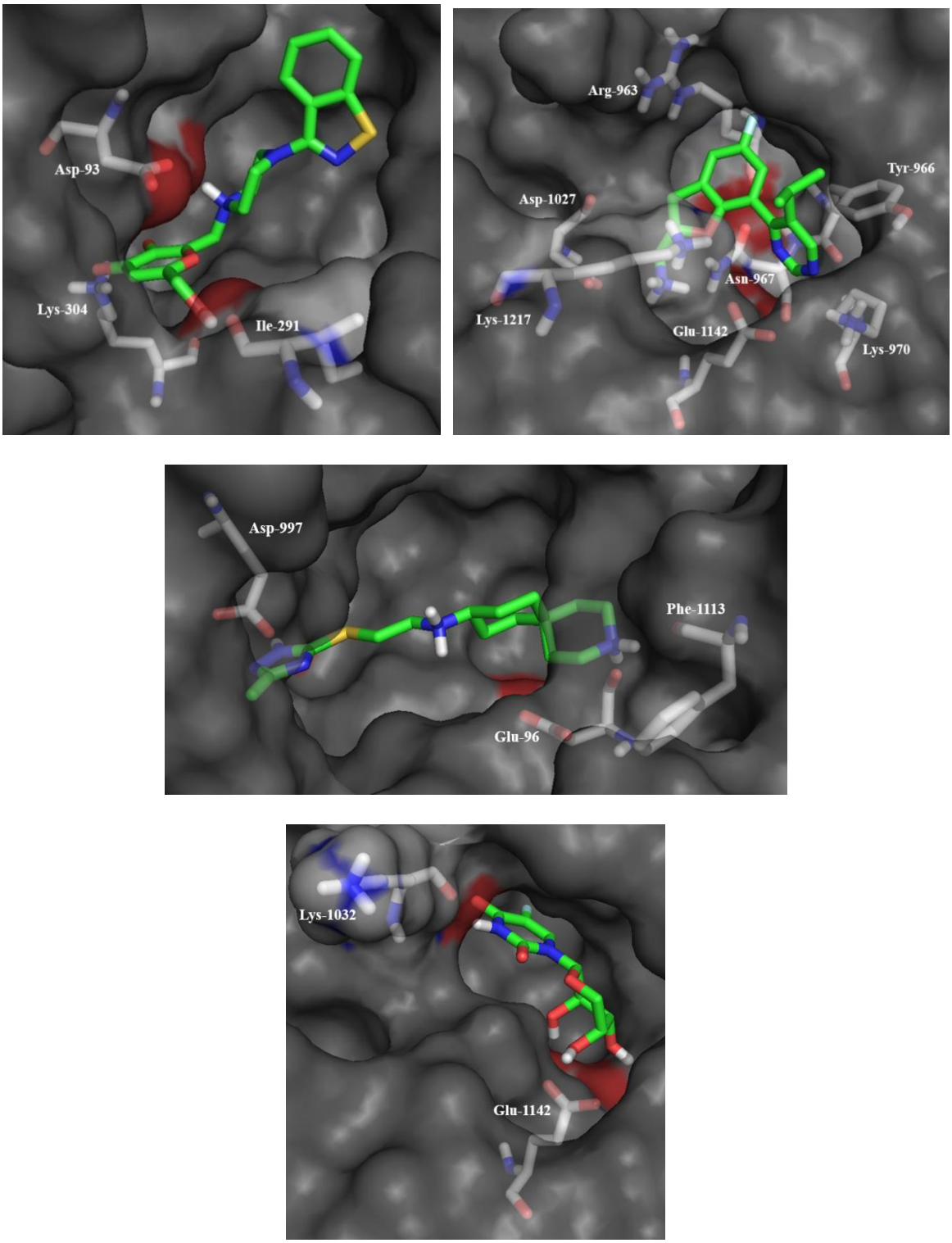

Figure 4.2: Docking poses of the 2 best-scoring virtual screening hits in each site, shown with green carbons, and the residues that interact with them, shown with gray carbons. Top left, **ZINC57160091**; top right, **ZINC67786201**; middle, **ZINC67757786**; bottom, **ZINC04127198**.

CHAPTER 5. DEVELOPING A STRUCTURE-ACTIVITY RELATIONSHIP FOR THE TWO NEW ARTEMISININ BINDING SITES

***Shuneize E. Slater, Mohamed Jihan, Robert J. Doerksen, Mitchell A. Avery, Unpublished.**

5.1 INTRODUCTION

Structure-activity relationship, or SAR, is the study of the correlation between the structure of a drug and its biological activity. SARs are essential for the design of therapeutics with the highest potency but the least adverse effects.[78] Developing a SAR helps in determining the chemical groups at a specified position in the drug structure that are responsible for producing a biological effect in the target organism. Medicinal chemists use SARs to modify drug structures and test the modifications for their biological activities.[79]

5.2 PROCEDURE

Currently in our research group, sixteen derivatives of artemisinin were designed. These were used to develop a SAR against the two new sites that we discovered in PfATP6. To begin, the sixteen compounds were drawn in ChemDraw and saved as individual .sdf files. The files were then uploaded to the Maestro interface of the Schrödinger suite and minimized to obtain their 3-D conformations. The 3-D structures were then prepared using the LigPrep module of Schrödinger which prepares the ligands by converting them based on their tautomeric and protonation states at certain pH ranges. Next the compounds were docked into both sites using both Glide docking and Induced Fit Docking to retrieve their docking scores and poses.

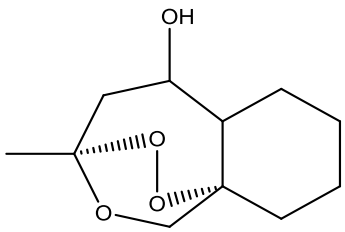

1

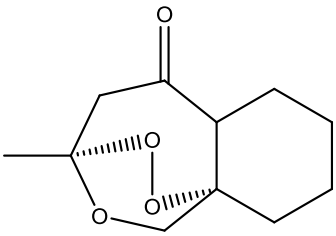

2

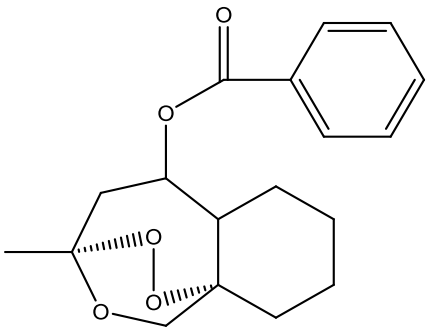

3

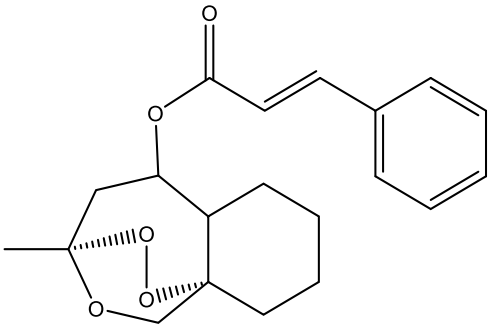

4

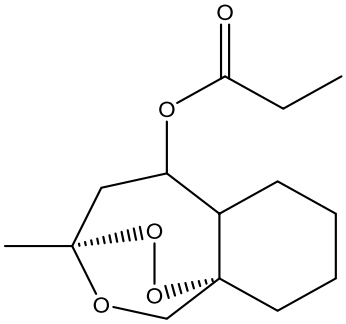

5

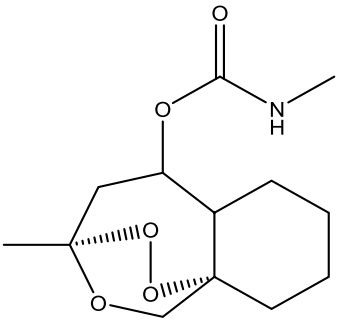

6

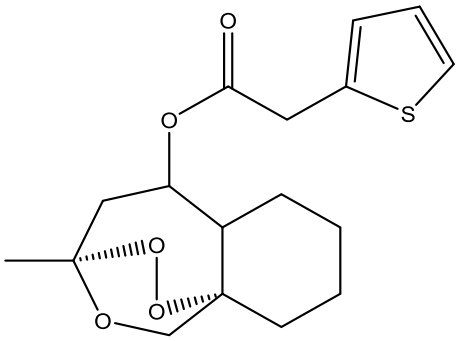

7

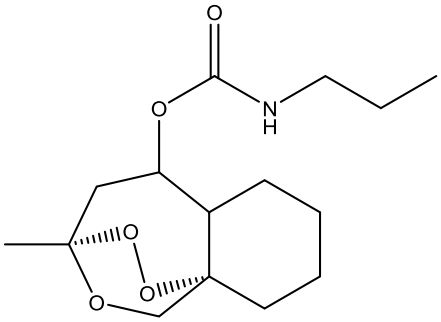

8

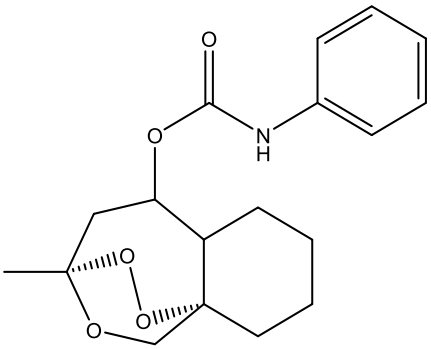

9

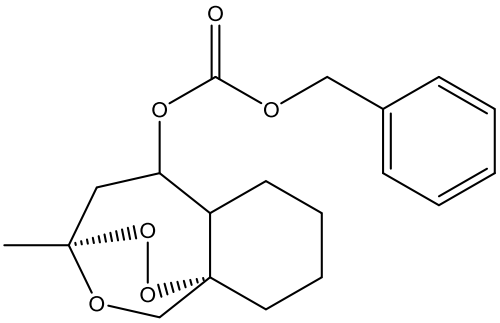

10

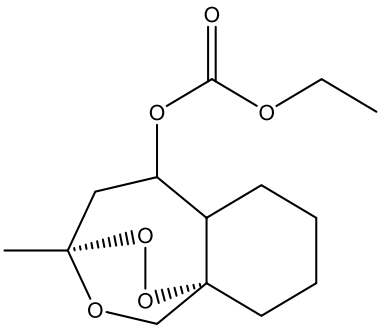

11

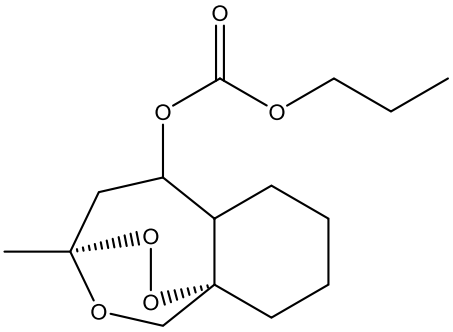

12

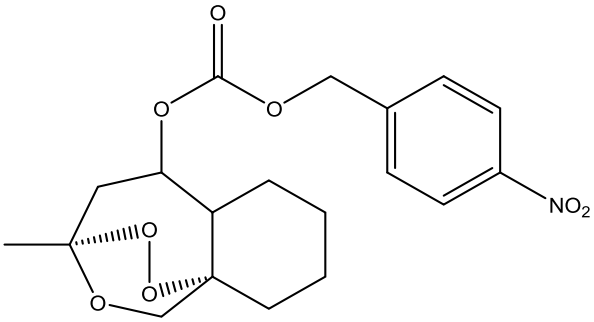

13

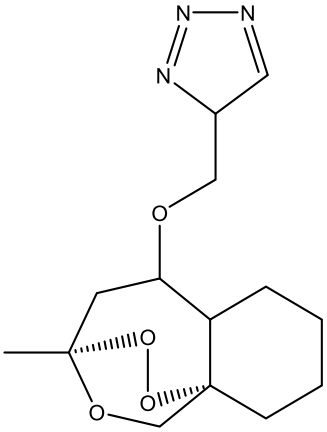

14

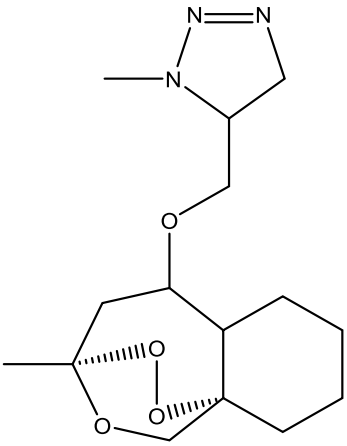

15

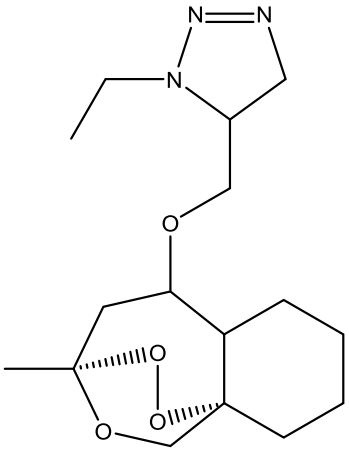

16

Figure 5.1: Structures of the 16 artemisinin derivatives used in this study.

Table 5.1: Docking scores of artemisinin derivatives in Cys92 site.

Compound	Docking Score
1	-4.567
2	-3.837
3	-4.593
4	-4.370
5	-3.088
6	-3.626
7	-4.379
8	-3.534
9	-4.130
10	-4.273
11	-4.050
12	-3.466
13	-3.381
14	-3.568
15	-3.633
16	-3.753
artemisinin	-4.045

Table 5.1 shows the docking scores of artemisinin and the sixteen artemisinin derivatives used in this study against the site containing Cys92. Seven of these derivatives, **1, 3, 4, 7, 9, 10,** and **11** are predicted to be better binders to PfATP6 at this site than artemisinin itself.

Table 5.2: Docking scores of artemisinin derivatives in Cys1031 site.

Compound	Docking Score
1	-6.456
2	-6.197
3	-5.140
4	-4.666
5	-4.805
6	-5.237
7	-4.541
8	-4.689
9	-4.393
10	-5.331
11	-5.211
12	-4.801
13	-4.743
14	-3.061
15	-4.543
16	-4.298
artemisinin	-4.380

Table 5.2 shows the docking scores of artemisinin and the sixteen artemisinin derivatives used in this study against the site containing Cys1031. Amazingly, all of the derivatives scored better than artemisinin in this site except for compounds **14** and **16**. All sixteen of these compounds are currently being synthesized and will be assayed for their antimalarial activities and PfATP6 inhibitory activities. Once the assays are completed, we will be able to determine if there is indeed a correlation between the structures and their biological activities.

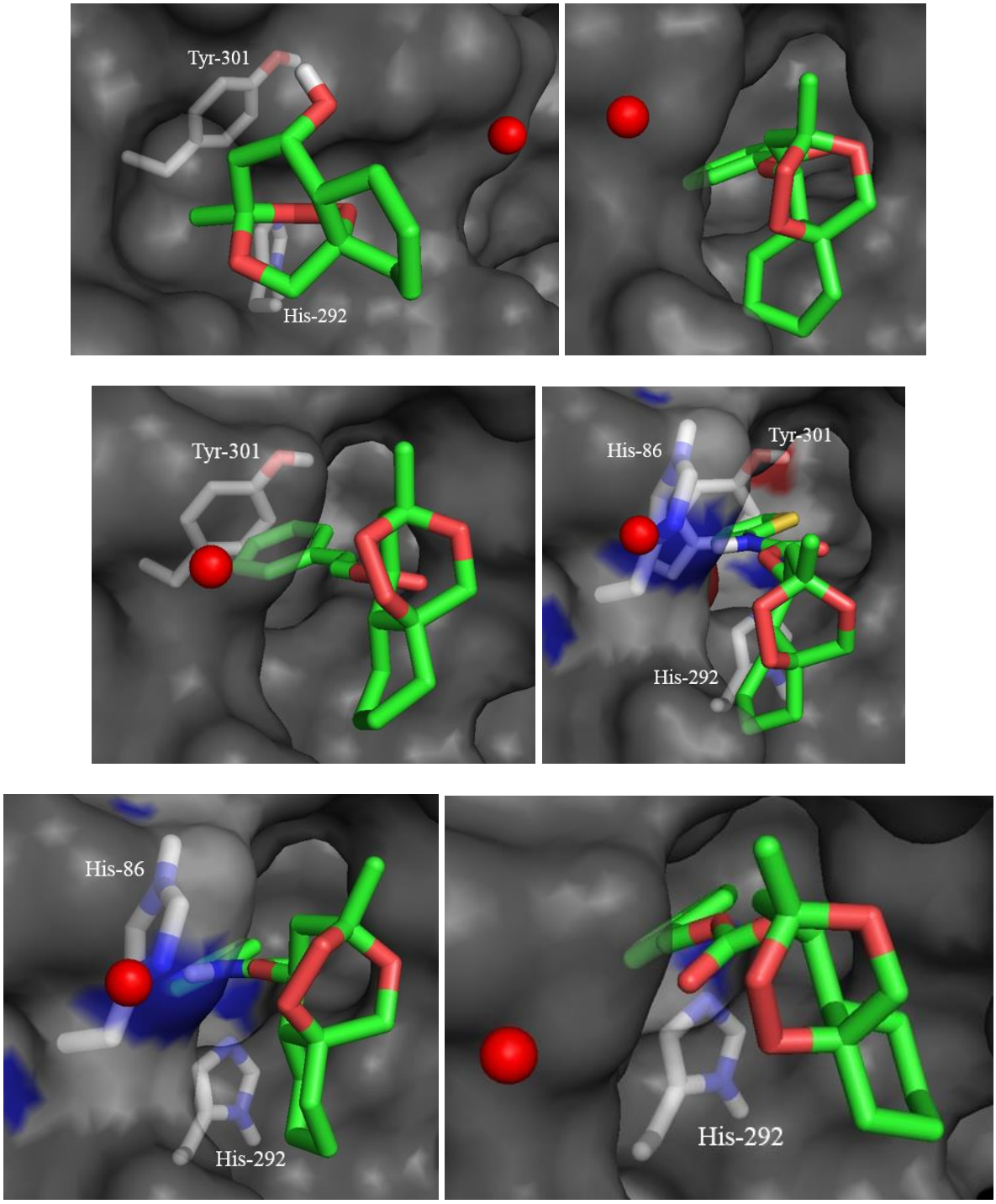

Figure 5.2: The top ranked compounds in the site containing Cys92. Top left, **1**; top right, **3**; middle left, **4**; middle right, **7**; bottom left, **9**; bottom right, **10**.

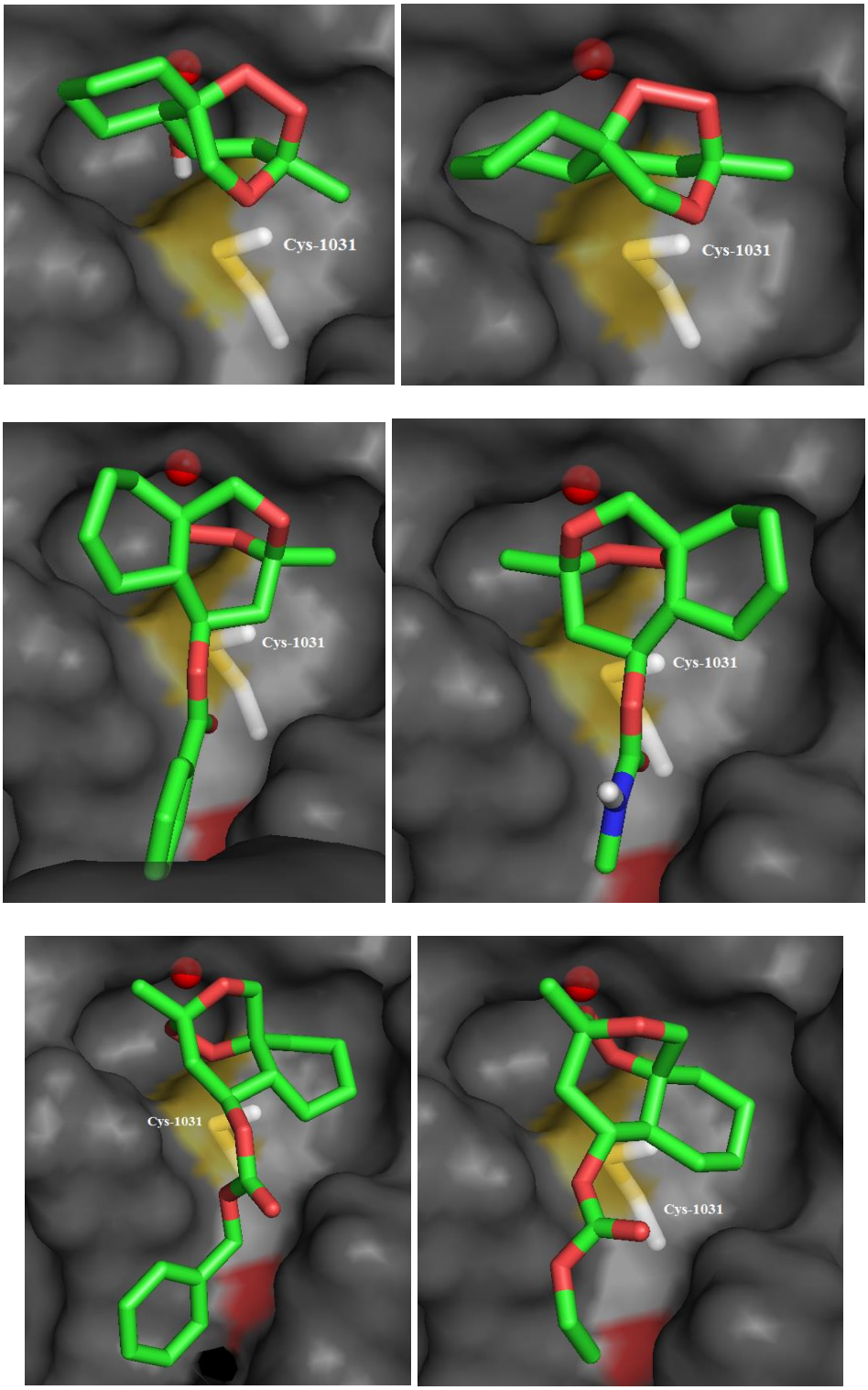

Figure 5.2: The top ranked compounds in the site containing Cys92. Top left, **1**; top right, **2**; middle left, **3**; middle right, **6**; bottom left, **10**; bottom right, **11**.

CHAPTER 6. PfATP6 AND PfTCTP

***Shuneize E. Slater, Chinni Yalamanchili, Amar Chittiboyina, Mitchell A. Avery,**

Unpublished.

6.1 INTRODUCTION

It is well known that artemisinin derivatives are very potent antimalarials. Specific malaria proteins become labeled when intact *Plasmodium falciparum*-infected blood cells are exposed to radiolabeled artemisinin. One of the proteins, a translationally controlled tumor protein (TCTP), was eluted from 2-dimensional gels, partially sequenced, then cloned and expressed in *E. coli*.[80] TCTP was first described in the 1980s and was preciously named fortilin, Q23, p23, and p21.[81]

PfATP6 is found in the membrane of the parasite's food vacuole. Here, there is an abundance of heme and iron from digested hemoglobin. To determine if PfTCTP is located in the food vacuoles as well, isolated food vacuoles and hemozoin were examined by immunofluorescence. The results suggest that PfTCTP is either located in the food vacuole stroma or the membrane. To find its exact location, immunoelectron microscopy with immunogold labeling was used. Gold particles were found in the cytoplasm, the food vacuolar membrane and in other parasite-derived membranes. It is also known that PfATP6 is able to bind calcium ions. To discover if PfTCTP is also able to bind calcium ions, a ^{45}Ca overlay assay was used. Calcium binding proteins tend to migrate more rapidly in SDS gels in the presence of calcium. The results of the assay indicated that PfTCTP does in fact bind calcium ions.[81]

All of the previous information suggested that PfTCTP is a target molecule for artemisinin; however, the site of interaction had not been elucidated. It was believed that the single cysteine residue of the protein was responsible for drug binding. However, once the crystal structure of PfTCTP was determined, the structure revealed that the cysteine residue is buried deep inside the protein and is inaccessible. So, *in silico* blind docking was performed to

find potential binding sites in the protein. Out of thirteen sites found, two were selected for further analysis based on their correlation with experimental evidence.[81]

6.2 PROCEDURE

After finding this information, we decided to compare the two potential artemisinin binding sites in PfTCTP to our two potential artemisinin binding sites in PfATP6. The idea is that if artemisinin is able to bind to both proteins, then there should be some similarities between the binding sites. Since crystals of the artemisinin-PfTCTP complex could not be obtained, we downloaded the crystal structure of PfTCTP (PDB ID: 3P3K) from the Protein DataBank and prepared and minimized it using the Protein Preparation Wizard of the Schrödinger suite. Glide was then used to generate receptor grids for the two sites by specifying the binding site residues. For position 1, the binding site residues were Ile95, Met99, Glu100, Ala103, Phe117, Lys118, Ala121, Gln122, and Ile125. For position 2, the specified residues were Phe28, Glu29, His127, Asn131, Asp134, Phe135, Ser152, Tyr153, Tyr154, and Gly156. After the receptor grids were generated, we docked artemisinin into the two sites in order to attempt to reproduce the exact binding poses that were reported. Once the best matching poses were retrieved, we superimposed the two complexes of PfTCTP with our two complexes of PfATP6 by aligning the artemisinin structures in the sites. By doing so, this allowed us to compare the residues in both proteins that are interacting with certain features in artemisinin and to study whether these residues share any similarities.

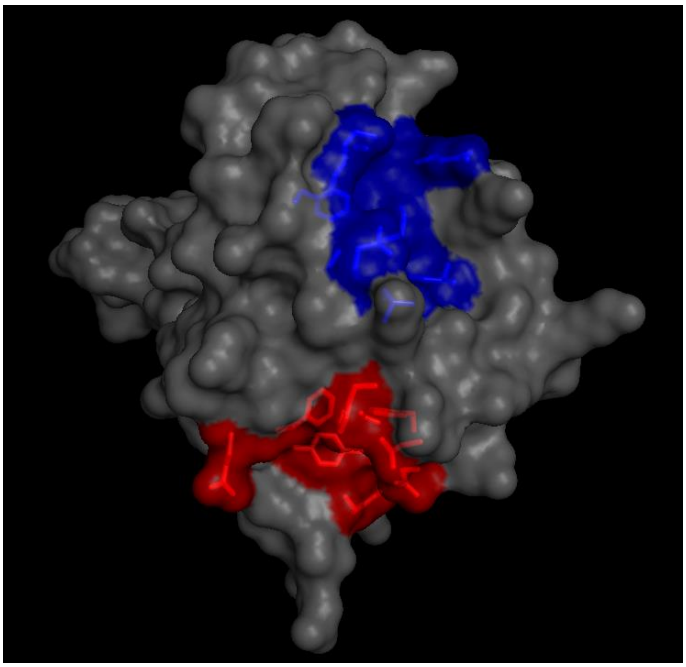

Figure 6.1: Structure of PfTCTP. The location of artemisinin binding position 1 is shown in blue and of artemisinin binding position 2 is shown in red.

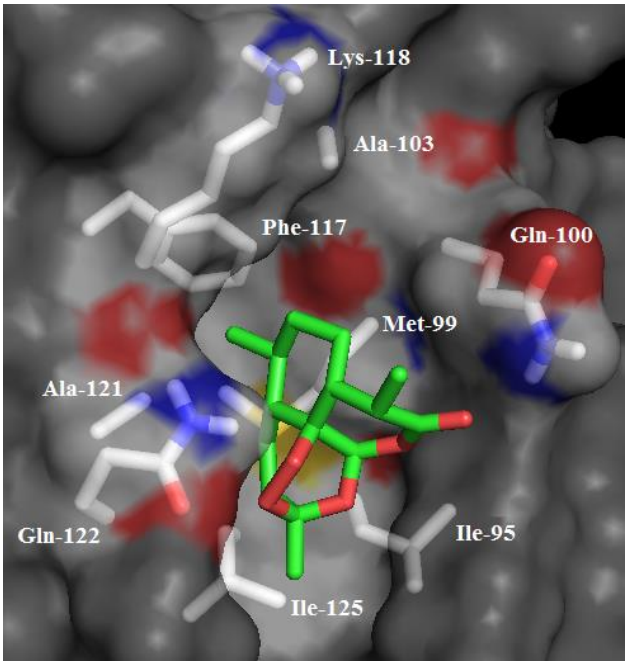

Figure 6.2: Artemisinin docked into position 1 of PfTCTP.

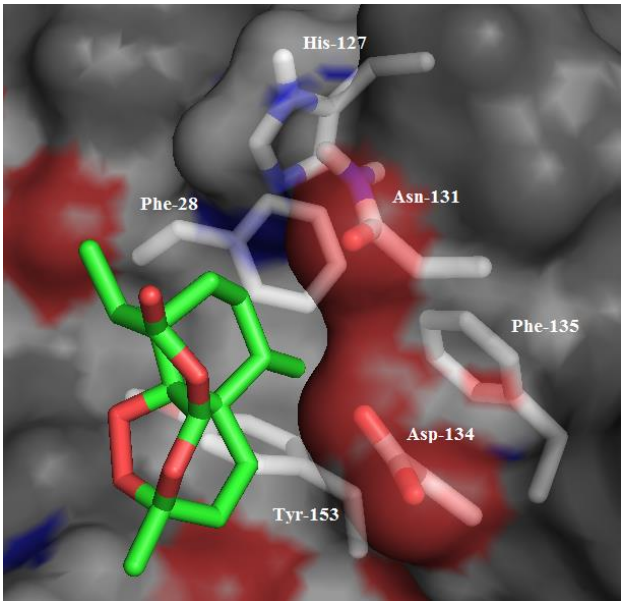

Figure 6.3: Artemisinin docked into position 2 of PfTCTP.

Once the superimposition of the sites is complete and the similarities between the sites have been documented, we will take approximately 50 compounds that were synthesized and assayed *in house* and dock them into both sites of the proteins to determine whether *in silico* studies can aid in explaining the activity trend of the compounds.

CHAPTER 7. CONCLUSIONS AND FUTURE PLANS

In conclusion, malaria has been a major problem in our world for centuries. It is an extremely fatal, yet preventable and treatable disease. Over the years, numerous efforts have been made in the discovery of both natural and synthetic therapeutics to treat malaria. Quinoline derivatives such as quinine and chloroquine have offered relief for years, but resistance towards these drugs has emerged. To thwart malaria, many ventures went underway to find novel therapeutics. One such venture isolated the compound artemisinin from *Artemisia annua*. This compound was found to be a very potent antimalarial. Although artemisinin has been used for decades to treat malaria, exactly how is exerts its antimalarial effects is still a mystery. Many research groups have offered hypotheses as to its exact mechanism of action, but no consensus has been reached. One group offered the protein *Plasmodium falciparum* ATPase 6 as the possible target for artemisinin. They predicted that artemisinin acts in the same manner as the compound thapsigargin towards the mammalian ATPase. However, we found a few concerns with that mechanism of action and ventured out to find a more plausible mechanism of action for artemisinin against PfATP6. Many computational methods, such as pocket searching, blind docking, ion prediction and modeling, and in silico mutagenesis, have been exhausted in the search to verify our hypothesis. Our results are proving to be quite favorable. We also searched for PfATP6 binding sites for four “malaria box” compounds that were first found to possess antimalarial activity and then PfATP6 inhibitory activity. To verify both our hypothesis of the two new PfATP6 binding sites for artemisinin and the four “malaria box” compounds, an experimental mutagenesis study will be performed by collaboration with Krishna and colleagues at St. George’s University of London. This will determine whether our two sites truly are artemisinin binding sites and will verify the “malaria box” binding sites as well.

To further determine if targeting our new sites could result in the discovery of novel antimalarials, virtual screening was executed utilizing docking into the pockets. A library of approximately 20 million compounds was downloaded and after a few steps, nineteen remained. These compounds will be purchased, and both an antimalarial assay and a PfATP6 enzyme-based assay will be performed on these compounds to determine their activities.

In the very near future, the synthesis of the artemisinin derivatives will be completed and they will be tested for both their antimalarial activity and their PfATP6 inhibitory activity. This will aid in the development of a structure-activity relationship for PfATP6 inhibitors. The work on PfTCTP will also be completed.

Finally, with the occurrence of so many reasonable mechanisms of action, many of them being difficult to refute, we think it is likely that artemisinin and its derivative peroxides act by a combination of various mechanisms. If true, it will be extremely difficult to construct a predictive single pharmacophore model for this class of drugs. Future researchers will face these difficulties. As a final note, how do we explain the activities of so many diverse peroxides against *P. falciparum*? How do we reconcile bioactive 13-Carbaartemisinin with these mechanisms, and finally, how do we explain the potent antimalarial activity of 4,5-secoartemisinin **1** (**Scheme 7.1**)[82], prepared by total synthesis by the Avery research group many years ago? For example, as shown in **Scheme 7.1**, formation of a C-4 radical seems impossible upon exposure to Fe(II). Instead, we see the loss of acetone from **2** to give **3**, a carboxyl radical, which is known to lose CO_2 to form a carbon radical such as **4**. One can conceive of **4** undergoing ring opening to form an enolate radical **5**, which is more stable than the carbon radical **4**. Which, if any, of these intermediates can be reconciled with the MOA forwarded in

this proposal for PfATP6? Is the Haynes MOA more compatible with this ring-scissioned version of artemisinin? Also, can **4** or **5** achieve an orientation within the proposed sites containing C1031 or C92 to bind with their cysteine thiols? These are the sorts of questions that are to be struggled with in the future and support a multi-mechanistic view of the MOA for artemisinin.

Scheme 7.1: Fe(II)-mediated ring opening.

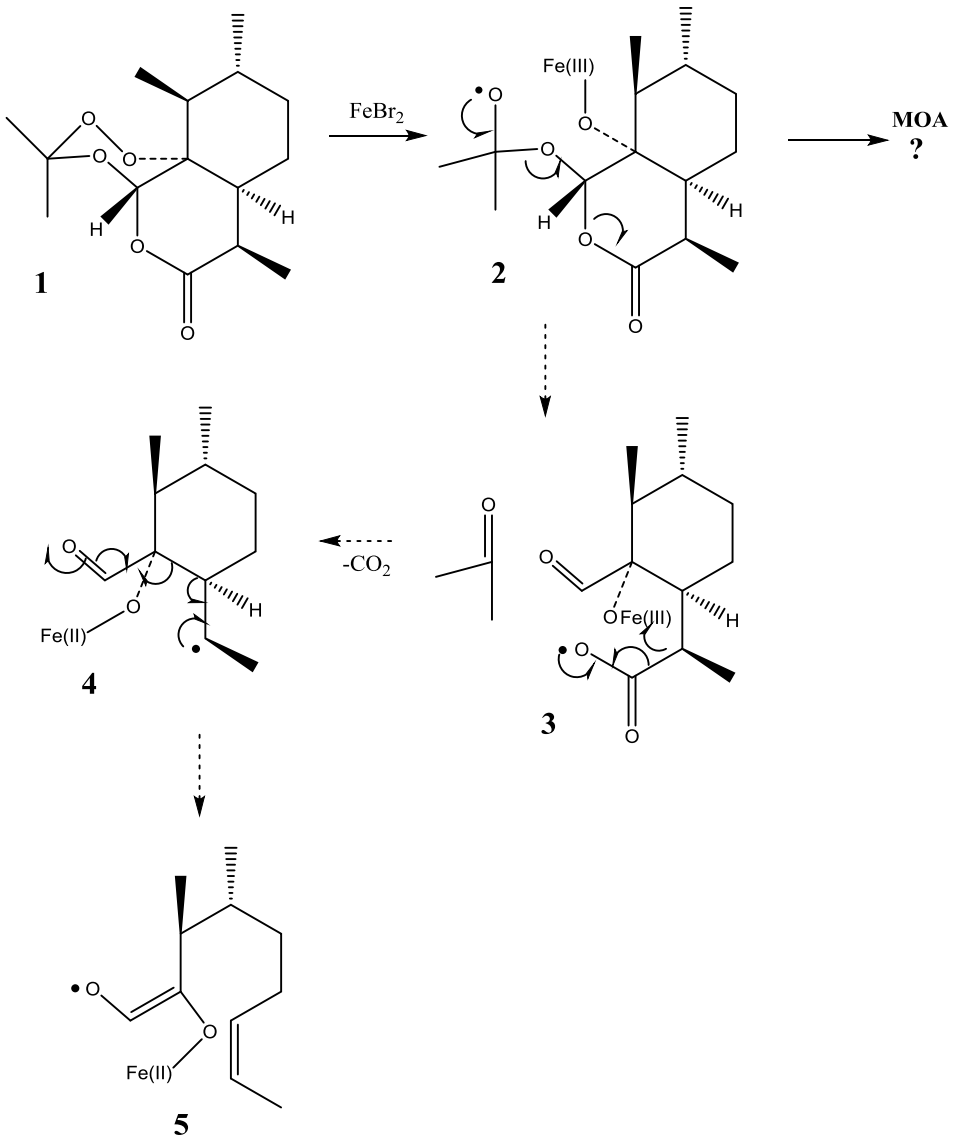

LIST OF REFERENCES

1. Kokwaro, G. *Malaria Journal* (2009) **8** (Suppl 1), S2.

2. Nayyar, G.M.; Breman, J.G.; Newton, P.N.; Herrington, J. (2012) Poor-quality antimalarials drugs in southeast Asia and sub-Saharan Africa. *Lancet Infect Dis*. **12**(6): 488-96.

3. World Malaria Report 2013, W.H. Organization, Editor. 2013.

4. Success. http://successimg.com/malaria-world-map/

5. Sarkar, P.K.; Ahluralia, G; Vijayan, V.K.; Talwar, A. (1999) Critical care aspects of malaria. *Journal of Intensive Care Medicine*. **25**(2): 93-103.

6. Cowman, A.F.; Berry, D.; Baum, J. (2012) The cellular and molecular basis for malaria parasite invasion of the human red blood cell. *J. Cell Biol*. **198**(6): 961-971.

7. Nantong Egens Bio Technology Company Blog. http://www.egensdiagnostics.com/blog/worldwide-usage-of-malaria-diagnostics-kits/

8. Nadjm, B. and Behrens, R.H. (2012) Malaria: an update for physicians. *Infect Dis Clin North Am.* **26**(2): 243-59.

9. Rich, S.M.; .Leendertz, F.H.; Xu, G.; Le Breton, M.; Djoko, C.F.; Aminake, M.N.; Takang, E.E.; Diffo, J.L.D., Pike, B.L.; Rosenthal, B.M.; Formenty, P.; Boesch, C.; Ayala, F.J.; Wolfe, N.D. (2009) The origin of malignant malaria. *Proc. Natl. Acad. Sci*. **106**(35): 14902-14907.

10. World Health Organization (2006). Guidelines for the treatment of malaria: (http://apps.who.int/malaria/docs/TreatmentGuidelines2006.pdf) (PDF). World Health Organization. Retrieved 10 February 2015.

11. Dorndorp, A.; Nosten, F.; Stepniewska, K.; Day, N.; White, N. (2005) Artesunate versus quinine for treatment of severe *falciparum* malaria: a randomized trial. *Lancet* **366**(9487): 717-725.

12. Reyburn, H.; Mtove, G.; Hendriksen, I.; Seidlien, L. (2009) Oral quinine for the treatment of uncomplicated malaria. *Brit. J. Med*. **339**: b2066.

13. Achan, J.; Tibenderana, J.K.; Kyabayinze, D.; Mangen, F.W.; Kamya, M.R.; Dorsey, G.; D'Alessandro, U.; Rosenthal, P.J.; Talisuna, A.O. (2009) Effectiveness of quinine versus artemether-lumefantrine for treating uncomplicated *falciparum* malaria in Ugandan children: randomized trial. *Brit. J. Med*. **338**: b2763.

14. Paintaud, G.; Alvan, G.; Berninger, E.; Gustafsson, L.L.; Idrizbegovic, E.; Karlsson, K.K.; Wakelkamp, M. (1994) The concentration-effect relationship of quinine-induced hearing impairment. *Clin. Pharmacol. Ther*. **55**(3): 317-323.

15. Malaria: Past and Present: History of Treatment and Prophylaxis. NobelPrize.com. http://www.nobelprize.org/educational/medicine/malaria/readmore/treatment.html

16. Uhlemann, A.-C.; Krishna, S. (2005) Antimalarial multi-drug resistance in Asia: Mechanisms and assessment. *Curr. Top. Microbiol. Immunol*. **295**: 39-53.

17. Hempelmann, E. (2007) Hemozoin biocrystallization in *Plasmodium falciparum* and the antimalarial activity of crystallization inhibitors. *Parasitol. Research*. **100**(4): 671-676.

18. Savarino, A.; Boelaert, J.R.; Cassone, A.; Majori, G.; Cauda, R. (2003) Effects of chloroquine on viral infections: an old drug against today's diseases? *Lancet Infect Dis*. **3**(11): 722-727.

19. Wall, J.E.; Buijs-Wilts, M.; Arnold, J.T.; Wang, W.; White, M.M.; Jennings, L.K.; Jackson, C.W. (1995) A flow cytometric assay using mepacrine for study of uptake and release of platelet dense granule contents. *Br. J. Haematol*. **89**(2): 380–385.

20. Drugs.com: Quinacrine. Retrieved on 24 April 2015

21. Zipper, J.; Cole, L.P.; Goldsmith, A.; Wheeler, R.; Rivera, M. (1910) Quinacrine hydrochloride pellets: preliminary data on a nonsurgical method of female sterilization. *International Journal of Gynaecology and Obstetrics: the official organ of the International Federation of Gynaecology and Obstetrics*. **18**(4): 275–90.

22. "Lariam". The American Society of Health-System Pharmacists. Retrieved 3 April 2015.

23. "Lariam medication guide" (PDF). Hoffman La Roche. Retrieved 3 April 2015.

24. Alkadi, H.O. (2007) Antimalarial Drug Toxicity: A Review. *Chemotherapy* **53**(6): 385–391.

25. González, R.; Hellgren, U.; Greenwood, B.; Menéndez, C. (2014) Mefloquine safety and tolerability in pregnancy: a systematic literature review. *Malaria Journal*. **13**: 75.

26. de Villiers, K.A.; Marques, H.M.; Egan, T.J. (2007) Speciation and structure of ferriprotoporphyrin IX in aqueous solution: spectroscopic and diffusion measurements demonstrate dimerization, but not mu-oxo dimer formation. *Journal of Biological Inorganic Chemistry*. **12**(1): 101-117.

27. Wesche, D.L.; Schuster, B.G.; Wang, W.X.; Woosley, R.L. (2000) Mechanism of cardiotoxicity of halofantrine. *Clin. Pharmacol. Ther*. **67**(5): 521–9.

28. Etymologia: Artemisinin. Emerg Infect Dis [Internet]. 2014 July. http://dx.doi.org/10.3201/eid2007.ET2007

29. Burns, W. Qingaosu Project http://qinghaosu.blogspot.com/

30. Tu, Y. (2011) The discovery of artemisinin (qinghaosu) and gifts from Chinese medicine. *Nature Medicine.* **17**(10): 1217-1220.

31. Faurant, C. (2011) From bark to weed: the history of artemisinin. *Parasite*, **18**(3): 215-218.

32. Rehwagen, C. (2006) WHO ultimatum on artemisinin monotherapy is showing results. *BMJ* **332**(7551): 1176.

33. White, N.J. (2004) Antimalarial drug resistance. *J. Clin. Invest*. **113**(8): 1084–92.

34. Dondorp, A.M.; Fanello, C.I.; Hendriksen, I.C.; Gomes, E.; Seni, A.; Chhaganlal, K.D.; Bojang, K.; Olaosebikan, R.; Anunobi, N.; Maitland, K.; Kivaya, E.; Agbenyega, T.; Nguah, S.B.; Evans, J.; Gesase, S.; Kahabuka, C.; Mtove, G.; Nadjm, B.; Deen, J.; Mwanga-Amumpaire, J.; Nansumba, M.; Karema, C.; Umulisa, N.; Uwimana, A.; Mokuolu, O.A.; Adedoyin, O.T.; Johnson, W.B.; Tshefu, A.K.; Onyamboko, M.A.; Sakulthaew, T.; Ngum, W.P.; Silamut, K.; Stepniewska, K.; Woodrow, C.J.; Bethell, D.; Wills, B.; Oneko, M.; Peto, T.E.; von Seidlein, L.; Day, N.P.; White, N.J. (2010) Artesunate versus quinine in the treatment of severe *falciparum* malaria in African children (AQUAMAT): an open-label, randomised trial. *Lancet* **376**(9753): 1647–57.

35. Hou J, Wang, D., Zhang, R., Wang, H. (2008) Experimental Therapy of Hepatoma with Artemisinin and Its Derivatives: In vitro and In vivo Activity, Chemosensitization, and Mechanisms of Action. *Clin Cancer Res* **14**(17): 5519–5530.

36. Xiao, S.H. (2005) Development of antischistosomal drugs in China, with particular consideration to praziquantel and the artemisinins. *Acta Tropica*. **96**(2–3): 153–167.

37. Keiser, J., Utzinger, J. (2007) Artemisinins and synthetic trioxolanes in the treatment of helminth infections. *Current Opinion in Infectious Diseases* **20**(6): 605–612.

38. Douglas, N.M., Anstey, N.M., Angus, B.J., Nosten, F., Price, R.N. (2010) Artemisinin combination therapy for vivax malaria. *Lancet Infect Dis* **10**(6): 405–16.

39. Calcium Pumping: P-type ATPase. [cited; Available from: http://www.cs.stedwards.edu/chem/Chemistry/CHEM43/CHEM43/Projects04/ATPASES/PTYPE_CALCIUM.htm.

40. Stokes, D.L., Green, N.M. (2003) Structure and function of the calcium pump. *Annu. Rev. Biophys. Struct.* **32**: 445-468.

41. Stokes, D.L. (1997) Keeping calcium in its place: Ca(2+)-ATPase and phospholamban. *Curr. Opin. Struct. Biol*. **7**(4): 550-556.

42. Toyoshima, C. and Nomura, H. (2002) Structural changes in the calcium pump accompanying the dissociation of calcium. *Nature*. **418**(6898): 605- 611.

43. Shandilya, A.; Chacko, S.; Jayaram, B.; Ghosh, I. (2013) A plausible mechanism for the antimalarial activity of artemisinin: A computational approach. *Sci Rep*. **3**: 2513.

44. Eckstein-Ludwig, U.; Eckstein-Ludwig, U.; Webb, R.J.; van Goethem, I. D. A.; East, J. M.; Lee, A.G.; Kimura, M.; O'Neill, P.; Bray, P.; Ward, S.; Krishna, S. (2003) Artemisinins target the SERCA of *Plasmodium falciparum*. *Nature* (London, U. K.). **424**(6951): 957-961.

45. Thastrup, O., Cullen, P.J.; Drøbak, B.K.; Hanley, M.R.; Dawson, A.P. (1990) Thapsigargin, a tumor promoter, discharges intracellular calcium stores by specific inhibition of the endoplasmic reticulum calcium ATPase. *Proc. Natl. Acad. Sci.* **87**(7): 2466-2470.

46. Uhlemann, A.-C.; Cameron, A.; Eckstein-Ludwig, U.; Fischbarg, J.; Iserovich, P.; Zuniga, F.A.; East, M.; Lee, A.; Brady, L.; Haynes, R.K.; Krishna, S. (2005) A single

amino acid residue can determine the sensitivity of SERCAs to artemisinins. *Nat. Struct. Mol. Biol*. **12**(7): 628-629.

47. Batista, R.; García, P.A.; Castro, M.A.; Miguel Del Corral, J.M.; Speziali, N.L.; de P Varotti, F.; de Paula, R.C.; García-Fernández, L.F.; Francesch, A.; San Feliciano, A.; de Oliveira, A.B. (2013) Synthesis, cytotoxicity and antiplasmodial activity of novel ent-kaurane derivatives. *Eur. J. Med. Chem*. **62**:168-176.

48. Guimaraes, D.S.M.; de Fonseca, A.L.; Batista, R.; Junior, M.C.; de Oliveira, A.B.; Taranto, A.G.; de P. Varotti, F. (2015) Structure-based drug design studies of the interactions of ent-kaurane diterpenes derived from Wedelia paludosa with the *Plasmodium falciparum* sarco/endoplasmic reticulum Ca2+-ATPase PfATP6. *Mem Inst Oswaldo Cruz, Rio de Janeiro*. **110**(2): 255-258.

49. Shukla, A.; Singh, A.; Singh, A.; Pathak, L.P.; Shrivastave, N.; Tripatha, P.K.; Singh, K.; Singh, M.P. (2014) Inhibition of P. *falciparum* PFATP6 by curcumin and its derivatives: a bioinformatic study. *Cell. Mol. Biol*. **58**(1), 182-186.

50. Uhlemann, A.-C.; Wittlin S.; Matile, H.; Bustamante, L.Y.; Krishna, S. (2007) Mechanism of antimalarial action of the synthetic trioxolane RBX11160 (OZ277). *Antimicrob. Agents Chemother*. **51**(2): 667-672.

51. Bousejra-El Garah, F.; Stiglilani, J.-L.; cosledan, F.; Meunier, B. Robert, A. (2009) Docking Studies of Structurally Diverse Antimalarial Drugs Targeting PfATP6: No Correlation between in silico Binding Affinity and in vitro Antimalarial Activity. *ChemMedChem*. **4**(9): 1469-1479.

52. David-Bosne, S.; Florent, I.; Lund-Winther, A.-M.; Hansen, J.B.; Buch-Perdersen, M.; Machillot, P.; le Maire, M.; Jaxel, C. (2013) Antimalarial screening via large-scale

purification of *Plasmodium falciparum* Ca2+-ATPase 6 and in vitro studies. *FEBS Journal*. **280**(21): 5419-5429.

53. Sun, L. Shah, F. Helal, M. Wu, W.; Pedduri, Y.; Chittiboyina, A.G.; Gut, J.; Rosenthal, P.J.; Avery, M.A. (2010) Design, Synthesis, and Development of Novel Guaianolide-Endoperoxides as Potential Antimalarial Agents. *J. Med. Chem*. **53**(21): 7864-7868.

54. Valderramos, S. G.; Scanfeld, D.; Uhlemann, A.-C.; Fidock, D. A.; Krishna, S. (2004) Investigations into the role of the *Plasmodium falciparum* SERCA (PfATP6) L263E mutation in artemisinin action and resistance. *Antimicrob. Agents Chemother*. **54**(9): 3842-3852.

55. O'Neill, P.M. and Posner, G.H. (2004) A Medicinal Chemistry Perspective on Artemisinin and Related Endoperoxides. *J. Med. Chem*. 47(12):2945-2964.

56. Robert, A. and Meunier, B. (1997) Characterization of the First Covalent Adduct between Artemisinin and a Heme Model. *J. Am. Chem. Soc.* **119**(25): 5968-5969.

57. Avery, M.A.; Fan, P.; Karle, J.M.; Bonk, J.D.; Miller, R.; Goins, D.K. (1996) Structure-Activity Relationships of the Antimalarial Agent Artemisinin. 3. Total Synthesis of (+)-13-Carbaartemisinin and Related Tetra- and Tricyclic Structures. *J. Med. Chem*. **39**(9): 1885-97.

58. Wu, Y.; Yue, Z.-Y.; Wu, Y.-L. (1999) Interaction of qinghaosu (artemisinin) with cysteine sulfhydryl mediated by traces of non-heme iron. *Angew. Chem. Int. Ed*. **38**(17): 2580-2582.

59. Haynes, R.K.; Chan, W.-C.; Wong, H.-N.; Li, K.-Y.; Wu, W.-K.; Fan, K.-M.; Sung, H.Y.; Williams, I.D.; Prosperi, D.; Mealto, S.; Coghi, P.; Monti, D. (2010) Facile Oxidation of Leucomethylene Blue and Dihydroflavins by Artemisinins: Relationship

with Flavoenzyme Function and Antimalarial Mechanism of Action. *ChemMedChem*. **5**(8): 1282-1299.

60. Mount, D.M. Bioinformatics: Sequence and Genome Analysis 2. Cold Spring Harbor Laboratory Press. ISBN 0-87969-712-1.

61. Zhang, Y. (2008) Progress and challenges in protein structure prediction. *Curr Opin Struct Biol* **18**(3): 342–348.

62. Schrödinger Release 2014-4: Schrödinger, LLC, New York, NY, 2014.

63. Schmidtke, P. le Guilloux, V.; Maupetit, J.; Tuffery, P. (2010) fpocket: online tools for protein ensemble pocket detection and tracking. *Nucleic Acids Research*, **38**, Web Server issue.W582–W589.

64. Trott, O. and Olson, A.J. (2010) AutoDock Vina: Improving the speed and accuracy of docking with a new scoring function, efficient optimization, and multithreading. *J. Comp. Chem*. **31**(2): 455-461.

65. Lu, C.-H.;Lin, Y.-F, Lin, J.-J.; Yu, C.-S. (2012) Prediction of metal ion-binding sites in proteins using the fragment transformation method. *PLoS One* **7**(6):e39252.

66. Levine, Ira N. *Quantum Chemistry*. Englewood Cliffs, New Jersey: Prentice Hall. 455–544.

67. Lengauer, T.; Rarey, M. (1996) Computational methods for biomolecular docking. *Curr. Opin. Struct. Biol.* **6**(3): 402–406.

68. Gamo, F.J.; Sanz, L.M.; Vidal, J.; de Cozar, C.; Alvarez, E.; Lavandera, J.L.; Vanderwall, D.E.; Green, D.V.; Kumar, V.; Hasan, S.; Brown, J.R.; Peishoff, C.E.; Cardon, L.R.; Garcia-Bustos, J.F. (2010) Thousands of chemical starting points for antimalarial lead identification. *Nature*. **465**(7296): 305-310.

69. The malERA Consultative Group on Drugs. (2011) A Research Agenda for Malaria Eradication: Drugs. *PLoS Med*. **8**(1): 1000402.

70. Beale, G. (1993) The Discovery of Mustard Gas Mutagenesis by Auerbach and Robson in 1941. *Genetics* **134**(2): 393–399.

71. Muller, H. J. (1927) Artificial Transmutation of the Gene. *Science* **66** (1699): 84–87.

72. Shortle, D.; Dimaio, D.; Nathans, D. (1981) Directed Mutagenesis. Annual Review of *Genetics* **15**: 265–294.

73. Bromberg, Y.; Yachdav, G.; Rost, B. (2008) SNAP predicts effect of mutations on protein function. *Bioinformatics* **24**(20): 2397-2398.

74. Cui, L.; Wang, Z.; Jiang, H.; Parker, D.; Wang, H.; Su, X.Z. (2012) Lack of association of the S769N mutation in *Plasmodium falciparum* SERCA (PfATP6) with resistance to artemisinins. *Antimicrob. Agents Chemother.* **56**(5): 2546-52.

75. Rester, U. (2008) From virtuality to reality - Virtual screening in lead discovery and lead optimization: A medicinal chemistry perspective. *Curr Opin Drug Discov Devel* **11**(4): 559–568.

76. Sun, H. (2008) Pharmacophore-based virtual screening. *Curr Med Chem* **15**(10): 1018–1024.

77. Kroemer, R.T. (2007) Structure-based drug design: docking and scoring. *Curr Protein Pept Sci* **8**(4): 312–328.

78. "Illustrated Glossary of Organic Chemistry". http://www.chem.ucla.edu/harding/IGOC/S/structure_activity_relationship.html

79. Sims, G. (1986) Biodegradation of pyridine derivatives in soil suspensions. *Environ. Toxicol. Chem*. **5**: 503-509.

80. Bhisutthibhan, J.; Philbert, M.A.; Fujioka, H.; Aikawa, M.; Meshnick, S.R. (1999) The *Plasmodium falciparum* translationally controlled tumor protein: subcellular localization and calcium binding. *Eur. J. Cell. Biol.* **78**: 665-670.

81. Eichhorn, T.; Winter, D.; Buchele, B.; Dirdjaja, N.; Frank, M.; Lehmann, W.-D.; Mertens, R.; Krauth-Siegel, L.; Simmet, T. Granzin, J.; Efferth, T. (2013) Molecular interaction of artemisinin with translationally controlled tumor protein (TCTP) of *Plasmodium falciparum. Biochemical Pharmacology*. **85**: 38-45.

82. Avery, M.A.; Gao, F.; Chong, W.K.M.; Hendrickson, T.F.; Inman, W.D.; Crews, P. (1994) Synthesis, conformational analysis, and antimalarial activity of tricyclic analogs of artemisinin. *Tetrahedron* **50**: 957-972.

VITA

Shuneize E. Slater
617 Saddle Creek Drive
Oxford, MS 38655
selowe@go.olemiss.edu

Academic Track Record

University of Mississippi Ph. D in Pharmaceutical Sciences August 2009 – May 2015

University of Arkansas- Monticello B.S. Chemistry August 2004 – May 2009

Teaching Experience

University of Mississippi- 2011 to 2014- Teaching Assistant for:

MEDC 416. Medicinal Chemistry of Therapeutic Agents I. Professional pharmacy course.

MEDC 501. Advanced Medicinal Chemistry I. Graduate course.

MEDC 417. Medicinal Chemistry of Therapeutic Agents II. Professional pharmacy course.

MEDC 502. Advanced Medicinal Chemistry II. Graduate course.

MEDC 319. Computer-Aided Drug Design. Professional pharmacy course.

University of Arkansas at Monticello- 2005-2009- Teaching Assistant for:

Intro to Chemistry lecture.

Intro to Chemistry lab.

Organic Chemistry lecture.

Meteorology lecture and lab.

Tutor for any college student in all college mathematics courses, all literature and composition courses, all chemistry courses, and all physics courses.

Second Baptist Church, Oxford, MS- 2012- Tutor for elementary, middle school, and high school students in all subjects

.**Other Experience**

2012-present- Computer Administrator, Department of Medicinal Chemistry.

2014- Session presider in Computers in Chemistry Division, 248th ACS National Meeting and Exposition. San Francisco, California

Research Experience

University of Mississippi- Synthesis of four potential inhibitors of glycogen synthase kinase 3-beta; performing all synthetic work using various equipment and techniques such as refluxing, running reactions under argon/nitrogen, flash column chromatography, gradient flash column chromatography, high vacuum pumps, TLC plates, preparatory TLC plates, rotary evaporation, pipetting, IR analysis, LCMS, HPLC, and NMR.

University of Mississippi- Performing a study of the mechanism of action of artemisinin on the inhibition of *Plasmodium falciparum* and proposing alternate plausible mechanisms. This was done using Maestro in Schrödinger 2013 Suite, Pymol Molecular Graphics System, Modeller program, fpocket software, and AutoDock Vina suite.

University of Mississippi- Researching different ways to synthesize omeprazole derivatives; performing all synthetic work using various equipment such as flash column chromatography, gradient flash column chromatography, high vacuum pumps, TLC plates, preparatory TLC plates, rotary evaporation, pipetting, IR analysis, LCMS, HPLC, and NMR.

University of Mississippi- Performed optimization of a lead glycogen synthase kinase-3-beta inhibitor using computational methods such as minimization and docking. These processes were done using Maestro which is included in the Schrödinger 2014 Suite. Also researched the current proteins that similar compounds are targeting using the Protein DataBank.

University of Arkansas Monticello- assisted in performing assays testing the ability of some peptidomimetic inhibitors against certain tumors using pipetting, centrifuging, heating, and obtaining absorbances using the UV-Vis spectrometer.

Awards, Fellowships, & Memberships

2004-2009- Dean's List and Chancellor's List

2005- Inducted into Sigma Zeta National Honor Society for Math and Sciences

2008- Inducted into Epsilon Zeta National Honor Society for Foreign Languages (Spanish)

2009- present- University of Mississippi Graduate School Minority Fellowship

2010- Inducted into Phi Kappa Phi Honor Society

2011- Center for Biomedical Research Excellence (COBRE) in Neurodegenerative Diseases Grant Recipient

2014- Second Place Winner in the Graduate School Forum Annual Poster Session

2014- Second Place Winner in the Annual Malaria Day Poster Session

2014- Judge for the Oxford Elementary Science Fair

2014- Inducted into Rho Chi National Honor Society for Pharmacy

2014- Member of the American Chemical Society

2015- First Place Winner in the MidSouth Computational Biology and Bioinformatics Society Meeting Poster Session

Publications

In preparation to be published.

Conference Presentations

Poster Presentations

2014- University of Mississippi Graduate Student Council Research Forum. University, Mississippi. Second Place Winner. The Development of Novel Phthalimide Inhibitors of GSK-3β. Shuneize E. Slater, Gang Fu, Manal Nael, Mitchell A. Avery, Robert J. Doerksen.

2014- University of Mississippi Malaria Day Symposium. Second Place Winner**.** University, Mississippi. The artemisinin argument: Basis for questioning the accepted mechanism. Shuneize E. Slater, Jakub Kollar, Kuldeep K. Roy, Robert J. Doerksen, Mitchell A. Avery.

2014- University of Mississippi Malaria Day Symposium. University, Mississippi. Possible Mechanism of Action of Artemisinin: SERCA Hypothesis Expanded. Jakub Kollar, Shuneize E. Slater, Kuldeep K. Roy, Robert J. Doerksen, Mitchell A. Avery.

2014- 41st Annual MALTO Medicinal Chemistry and Pharmacognosy Meeting. Memphis, Tennessee. Identification of Novel Phthalimide Inhibitors of GSK-3B: A Computational Study. Shuneize E. Slater, Gang Fu, Manal Nael, Mitchell A. Avery, Robert J. Doerksen.

2014- 248th ACS National Meeting and Exposition. San Francisco, California. Ferrous ion/PfATP6 Dual Requirement for Anti-Malarial Activity: Making Strides Towards Understanding the MOA of Artemisinin. Shuneize E. Slater, Jakub Kollar, Kuldeep K. Roy, Chih-Hao Lu, Sanjeev Krishna, Robert J. Doerksen, Mitchell A. Avery.

2014- SERMACS 2014 (Southeast Regional Meeting of the American Chemical Society). Nashville, Tennessee. Analysis of Water Molecules in the Active Site of the Protein Kinase RNA-like Endoplasmic Reticulum Kinase (PERK): Insights for Lead Optimization. Manal A. Nael, Shuneize E. Slater, Robert J. Doerksen.

2015- MidSouth Computational Biology and Bioinformatics Society XII Meeting. Little Rock, Arkansas. Determining Alternative Artemisinin Binding Sites in PfSERCA. Shuneize E. Slater, Kuldeep K. Roy, Jakub Kollar, Manal Nael, Khaled M. Elokely, Robert J. Doerksen, Mitchell A. Avery.

Podium Presentations

2014- Zing Drug Discovery Conference. Malaga, Spain. Molecular Details of the PfATP6 SERCA Hypothesis: Progress Towards Understanding the MOA of Artemisinin. Mitchell A. Avery, Shuneize E. Slater, Jakub Kollar, Kuldeep K. Roy, Sanjeev Krishna.

2014- 41st Annual MALTO Medicinal Chemistry and Pharmacognosy Meeting. Memphis, Tennessee. Finding A More Feasible Mechanism of Action For Artemisinin. Shuneize E. Slater, Jakub Kollar, Kuldeep K. Roy, Khaled M. Elokely, Chih-Hao Lu, Sanjeev Krishna, Robert J. Doerksen, Mitchell A. Avery.

2014- 248th ACS National Meeting and Exposition. San Francisco, California. Structure-Based Lead Optimization of a Novel Glycogen Synthase Kinase 3 Beta Inhibitor. Shuneize E. Slater, Gang Fu, Manal Nael, Mitchell A. Avery, Robert J. Doerksen.